MULTIPHASE MICROFLUIDIC FABRICATION OF POLYMERIC MICRO-CONTAINERS FOR BIO-ENCAPSULATION

CHAITANYA KANTAK

(B. ENG (DIST.), UNIVERSITY OF MUMBAI)

A THESIS SUBMITTED

FOR THE DEGREE OF DOCTOR OF PHILOSOPHY

DEPARTMENT OF BIOENGINEERING

NATIONAL UNIVERSITY OF SINGAPORE

2012

ACKNOWLEDGEMENTS

I am very grateful to my supervisor, Assistant Professor Dr. Dieter Trau for his invaluable guidance and mentoring during my PhD candidature. I will always cherish the memories of thought-provoking, creative discussions in the past four years and constructive feedback offered on a regular basis. I am thankful to Dr. Tushar Bansal for his co-supervision, understanding and patience during my PhD candidature. I am also thankful to Assistant Professor, Dr. Levent Yobas for introducing me to Microfluidics, for his external supervision, and sharing hands-on techniques with me.

I am grateful to my labmate Sebastian Beyer for his help during the past three years. I am very thankful to my former and current lab mates from the NanoBioanalytics Laboratory for their support: Zhu Qingdi, Jiang Jie, Wang Chen, Bai Jianhao, Matthew Pan, Dr. Chris Ochs and Nurhuda Ishak. I would also like to give special thanks to Ramesh Ramji and Wu Liqun from the Biofluids Laboratory, and Naveen Balla from the Optical Bioimaging Laboratory for their kind assistance. I also convey my special thanks to Dr. Darren Tan, Shashi Ranjan, and Patrick Tan Say Hwa for useful discussions.

I am very thankful to the staff of Institute of Microelectronics: I thank Dr. Chen Yu for generously letting me use the Biolab facilities in the Institute of Microelectronics. Dr Julien Reboud for his valuable suggestions; Siti Rafeah, Timothy Kok and Karen Wang for providing laboratory support; Jack Sheng, Wong Chee Chung, Tang Kum Cheong and Geoffrey Bo for sharing their experience; Zul Abdullah, Lawson Kor and Li Yong Hean for microfabrication support.

I give my sincere thanks to all my friends for their consistent support. I would like to give my warmest regards to my family for providing me unconditional support and love. Without you, this would not have been possible!

Finally, I will place my heartfelt gratitude to the Almighty for helping me out in this journey. I will be always indebted to you! Thank you.

Chaitanya S. Kantak

PUBLICATIONS, CONFERENCES AND AWARDS

Publications

1. Kantak C., Beyer S., Yobas L., Bansal T. and Trau D., " A Microfluidic Pinball for Generation of Layer-by-layer Microcapsules", ***Lab Chip***, 11, 1030-1035, (2011).

(Featured in RSC Chemistry World News)

2. Kantak C., Zhu Q., Beyer S., Bansal T. and Trau D., " Utilizing Microfluidics to Fabricate Polyethylene glycol Microbeads for FRET based Glucose Sensing" , ***Biomicrofluidics***, 6, 022006, (2012).

(Featured in American Institute of Physics News Room)

International Conferences

1. Kantak C., Beyer S., Yobas L., Bansal T., Trau D., A 'microfluidic pinball' for continuous generation of layer-by-layer polyelectrolyte microcapsules, MicroTAS, Groningen, Netherlands, October 2010.

2. Kantak C., Beyer S., Yobas L., Bansal T., Trau D., A 'microfluidic pinball' for continuous generation of polymeric layer-by-layer microcapsules, The 10th Asia-Pacific International Symposium on Microscale Separations and Analysis (APCE2010), Hong Kong, December 2010.

3. Kantak C., Beyer S., Yobas L., Bansal T., Trau D., A novel microfluidic approach for continuous layer-by-layer encapsulation of mineral oil droplets, 4th East Asia

Pacific Student Symposium on Nanobiomedical Engineering, Singapore, December 2010.

4. Kantak C., Beyer S., Yobas L., Bansal T., Trau D., A 'microfluidic pinball' for continuous generation of polymeric layer-by-layer microcapsules, Particles, Berlin, July 2011.

5. Kantak C., Beyer S., Yobas L., Bansal T., Trau D., Pinball Microfluidics: A novel approach for continuous generation of layer-by-Layer polymer microcapsules, International Conference on Materials for Advanced Technologies (ICMAT), Singapore, June 2011.

Awards

1. Best oral presentation award, 4th East Asia Pacific Student Symposium on Nanobiomedical Engineering, December 2010.

2. Best poster presentation award, The 10th Asia-Pacific International Symposium on Microscale Separations and Analysis, December 2010.

SUMMARY

Micro-containers can be defined as colloidal particles having a size range from sub-micrometers to several hundreds of micrometers fabricated for encapsulating the material of interest. Such micro-containers have been explored by the research community and industry for almost half a century due to their versatility, ability to tailor their properties (size, composition, porosity, stability, surface functionality etc.) and vast number of applications. The conventional fabrication of micro-containers is generally performed in batch processes suffering from the limitations of wide size distribution, aggregation of particles and loss of encapsulated material. These problems can be circumvented with the help from microfluidics, an important enabling technology. A branch of microfluidics, "multiphase microfluidics" can be used to generate continuous stream of droplets which are highly monodisperse and is capable of fabricating particles with an acute control on shape and morphology. The objective of this thesis was to develop microfluidic techniques for encapsulation of different template materials to fabricate polymeric micro-containers. The microfluidic techniques proposed in this thesis were able to encapsulate microdroplets of different carrier liquids such as hydrogel, organic phase and water for fabrication of micro-containers.

In the first work, a microfluidic encapsulation technique for fabricating polymeric micro-containers prepared from the hydrogel material is presented. The microdroplets generated at the T-junction were cross-linked *in-situ* by ultraviolet light to form hydrogel microbeads. A microfluidic device was fabricated in PDMS. The PEG based microbeads encapsulated a pair of biomacromolecules, FITC-dextran and TRITC-

ConA which work on the principle of Förster Resonance Energy Transfer (FRET). The monodisperse microbeads were fabricated with size of 72 µm, and showed the capability of glucose sensing in the physiological range of 1-10 mM.

In the second work, a microfluidic encapsulation technique for fabricating polymeric micro-containers with coating of six layers of polymers on the template of mineral oil microdroplets was demonstrated. In this work, higher complexity of droplet manipulation was achieved which is necessary for multilayered structure of LbL microcapsules. The encapsulation of oil microdroplets was achieved by generating droplets at the T-junction; followed by guiding them through laminar streams of polymer and wash solution in a single microchannel by zigzag like oriented rows of micropillars termed 'microfluidic pinball.' The microfluidic design was realized in PDMS. The polyelectrolyte microcapsules with 3 bi-layers of (PAA/PVPON) and average size of 45 µm were fabricated by this technique.

In the final work, a microfluidic encapsulation approach based on Reverse Phase layer-by-layer (RP-LbL) principle to directly encapsulate template of water microdroplets containing biomolecules was presented. In this study, the microdroplets were generated at the T-junction, and were subsequently transferred through laminar streams of polymers and wash solution in three parallel channels by high- resistance microstructures so as to encapsulate protein loaded aqueous droplets. This novel design based on the high resistance microstructures was prototyped in PDMS. The preliminary experiments demonstrated fabrication of (PSS/PEI) microcapsules encapsulating BSA loaded aqueous droplets having size of 95 µm.

TABLE OF CONTENTS **PAGE NUMBER**

ACKNOWLEDGEMENTS…….i

PUBLICATIONS, CONFERENCES, AWARDS…….iii

SUMMARY……..v

LIST OF SCHEMES…….x

LIST OF FIGURES...…….xi

ABBREVIATIONS…….xiv

CHAPTER 1- INTRODUCTION……1

1.1 BACKGROUND ……2

1.2 OBJECTIVE AND SCOPE OF THE THESIS ……4

CHAPTER 2- LITERATURE REVIEW……7

2.1 INTRODUCTION TO MICRO-CONTAINERS ……8

2.2 CONVENTIONAL TECHNIQUES FOR FABRICATION OF MICRO-CONTAINERS.10
2.2.1Liposomes or Self assembled Phospholipids Bilayers……10
2.2.2 Hydrogel Microparticles or Microbeads……11
2.2.2.1 Ionotropic Crosslinking Techniques for Hydrogels……12
2.2.2.2 Complex Coacervation Techniques for Hydrogels……12
2.2.2.3 Thermal Crosslinking Techniques for Hydrogels……13
2.2.3 Layer-by-Layer Polymer Assembly Technique……15
2.2.3.1 Principle of LbL Deposition Technique……15
2.2.3.2 Approaches for Polyelectrolyte Deposition on the Colloidal Particles……17
2.2.3.3 Encapsulation strategies for LbL Microcapsules……18

2.3 INTRODUCTION TO MICROFLUIDICS……22
2.3.1 Introduction to Continuous and Multiphase Microfluidics……22
2.3.2 Materials Used for Fabrication of Microfluidic Devices……25
2.3.2.1 Silicon……25
2.3.2.2 Glass……26
2.3.2.3 Poly (methylmethacrylate) (PMMA)……26
2.3.2.4 Polydimethylsiloxane (PDMS)……27
2.3.3 Droplet Manipulation Techniques……28
2.3.3.1 Droplet Generation…… 29
2.3.3.2 Droplet Fusion…… 31
2.3.3.3 Droplet Fission…… 32
2.3.3.4 Mixing in Droplets …… 33
2.3.3.5 Sorting of Droplets…… 34
2.3.4 Applications of Droplet Microfluidics…… 35
2.3.4.1 Biological and Chemical Analysis…… 35
2.3.4.2 Encapsulation of Biological Cells…… 36

2.3.4.3 Synthesis of Nanoparticles……..……..37
2.3.4.4 Synthesis of Microparticles ……..……37

2.4 THE INTERFACE ASPECTS OF MICRO-CONTAINERS AND MICROFLUIDICS ...38
2.4.1 Advantages of Fabrication of Micro-containers in the Device……38
2.4.2 Limitations of Fabrication of Micro-containers in the Device……..……39

CHAPTER 3 - MICROFLUIDIC FABRICATION OF POLYETHYLENE GLYCOL (PEG) BASED BEADS FOR BIOMOLECULAR ENCAPSULATION AND GLUCOSE SENSING……..41

3.1 INTRODUCTION…..……..……41

3.2 MATERIALS AND METHODS ……..44
3.2.1 Materials……..……..44
3.2.2 Mould Fabrication in SU8……..45
3.2.3 Soft Lithography ……..45
3.2.4 Preparation of Reagents……..46
3.2.5 Experimental Setup……..46
3.2.6 Characterization of PEG Microbeads and Glucose Sensing……..46

3.3 RESULTS AND DISCUSSION……..47
3.3.1 Device Design and Fabrication……47
3.3.2 Characterization of Droplet Generation……..49
3.3.3 Characterization of PEG Microbeads……..53
3.3.3.1 Size Distribution of PEG-DA Microbeads……..53
3.3.3.2 Scanning Electron Microscopy of PEG-DA Microbeads……54
3.3.4 Encapsulation of Biomolecules within PEG Microbeads ……54
3.3.5 PEG Microbeads for Glucose Sensing ……..56

3.4 CONCLUSION……..57

CHAPTER 4 - MICROFLUIDIC FABRICATION OF POLYELECTROLYTE MICROCAPSULES FOR ENCAPSULATING OIL MICRODROPLETS……..59

4.1 INTRODUCTION…..……59

4.2 MATERIALS AND METHODS……..62
4.2.1 Materials……62
4.2.2 Mould Fabrication ……62
4.2.3 Soft Lithography ……..63
4.2.4 Preparation of Reagents ……64
4.2.5 Experimental Setup ……..64
4.2.6 Sample Preparation for AFM Measurements……65

4.3 RESULTS AND DISCUSSION ……..65
4.3.1 Device Design and Fabrication……65
4.3.2 Proof-of-Concept Colour Dye Experiments……..68
4.3.3 Generation of Layer-by-Layer (PAA/PVPON)$_3$ Microcapsules……..72
4.3.4 Proof of Layer-by-Layer Polyelectrolyte Deposition……..74
4.3.5 Characterization of PEM Microcapsule by AFM……..75

4.4 CONCLUSION……78

CHAPTER 5- MICROFLUIDIC FABRICATION OF POLYMERIC CAPSULES USING REVERSE-PHASE LAYER-BY-LAYER APPROACH FOR BIOMOLECULAR ENCAPSULATION……79

5.1 INTRODUCTION……79

5.2 MATERIALS AND METHODS ……82
5.2.1 Materials……82
5.2.2 Mould Fabrication in SU8……83
5.2.3 Soft Lithography ……83
5.2.4 Preparation of Reagents ……84
5.2.5 Layer-by-Layer Deposition on Polystyrene Particles……84
5.2.6 Experimental Setup for Microfluidic Experiments……84

5.3 RESULTS AND DISCUSSION……85
5.3.1 Selection of Organic Phase and Polyelectrolytes……85
5.3.2 Device Design and Fabrication for RP-LbL Deposition……89
3.3.3 Working of the Microfluidic Device……93
5.3.4 Observation of Layer-by-Layer (PSS/PEI) Coated BSA Capsules……96

5.4 CONCLUSION……98

CHAPTER 6- CONCLUSION AND FUTURE WORKS……99

6.1 CONCLUSION……100

6.2 FUTURE WORKS……102
6.2.1 Encapsulation of Hydrogel Beads……102
6.2.2 Encapsulation of Oil Microdroplets……103
6.2.3 Encapsulation of Water Microdroplets……105

REFERENCES……106

APPENDIX……121

A. DROPLET SIZE VS FLOW RATE FOR PEG-DA MICRO-CONTAINERS (WITH STANDARD DEVIATION)……121

B. TARGETED BLOOD GLUCOSE LEVEL RANGES BY INTERNATIONAL DIABETES FOUNDATION……122

C. A COMPARISION OF SURFACE PROPERTIES OF PDMS FOR MICROFLUIDIC DEVICES……123

LIST OF SCHEMES

Scheme 3.1. Working mechanism of Förster Resonance Energy Transfer (FRET) based glucose assay. Concanavalin A, a sugar binding protein, has a higher affinity for glucose than dextran. The small Förster radius between FITC-dextran and TRITC-ConA quenches the fluorescence signal emitted by FITC molecules. The increase in glucose concentration releases more FITC-dextran from ConA and thereby resulting in a proportional increase in the fluorescence signal (Kantak et al., 2012)……..42

Scheme 3.2. Schematic for the generation of PEG based glucose sensing microbeads showing two inlets at the T-junction to form droplets encapsulating PEG-DA and biomolecules in an aqueous phase. The droplets were photopolymerized by UV light illuminated from a 20X microscope lens to form PEG microbeads……47

Scheme 4.1. Showing the dimensions of the device (Angle 20^{o}) for depositing six layers of polyelectrolytes. (Dimensions of pillars: 20 µm diameter, 80 µm height separated by 20 µm, 20 degree angle)……63

Scheme 4.2. Overview of the device for continuous generation of polyelectrolyte microcapsules by Layer-by-Layer (LbL) deposition of polyelectrolytes. Schematic view (not to scale) is shown with the required inputs and outputs for the deposition of six layers of polyelectrolytes. Expanded view of a single unit of pillars in zigzag arrangement (Kantak et al., 2011)……66

Scheme 4.3. Schematic shows the incubation of microcapsule in a solvent to dissolve the oil core. After removal of oil core, Atomic Force Microscopy (AFM) was performed to measure the thickness of the polymeric shell……..76

Scheme 5.1. (A) The schematic of the device consisting of a T-junction (T-j) for producing discrete droplets and connected to three parallel microchannels which are arranged in a serpentine manner. (B) Showing zoomed-in schematic view of the device with capsules being assisted to divert into adjacent channel due to less hydrodynamic resistance. (C) Depicting the experimental setup for generating layer-by-layer polyelectrolyte capsules encapsulating biomolecules using RP-LbL method……..91

LIST OF FIGURES

Figure 2.1. The semipermeable membrane for avoiding immunorejection of the transplanted cells by immune system molecules and allowing nutrients to flow inside the capsules (Li, 1998)……..10

Figure 2.2. Extrusion method explained with different kinds nozzle types on the left (a) dripping mode (b) electrostatic mode and (c) co-extrusion mode(Rabnel et al., 2009).……14

Figure 2.3. Schematic showing the principle of layer-by-layer technique. The substrate having initial positive charge was deposited with the first layer of a polyanion, poly(styrene sulfonate) (PSS) and a polycation, poly(allylamine hydrochloride) (PAH) alternatively to form polyelectrolyte multilayers of nanoscale thickness. The intermediate washing step is important for LbL technique to remove non-adsorbed polyelectrolyte from the surface (Decher, 1997)…….16

Figure 2.4. Schematic representation of the procedure for encapsulating biomoleules in PEM using porous microparticles as templates(SiO_2 and $CaCo_3$). (I)The immobilization of biomolecules into the pores (II) Assembly of polyelectrolyte multilayers (III) Dissolution of sacrificial template by HF or EDTA respectivly (IV) Retention of Biomolecules, in this case enzymes, within PEM. (V) Application of capsules for enzyme delivery (De Koker et al., 2011)...……19

Figure 2.5. (A)The mechanisms by which the permeability of capsules could be changed to load the molecules of interest viz. temperature, pH, ionic strength and solvent. Confocal micrographs of loading of (B) FITC-dextran (10 KDa) in $(PDADMAC/PSS)_4$ capsules by temperature (C)PAH-FITC (70 KDa) in $(PSS/PAH)_4$ capsules by changing ionic strength of the medium reversibly (D) FITC-dextran (2000 kDa) in) (TA/PAH)5 capsules by pH changes (E)FITC-urease into $(PSS/PAH)_4$ capsules by varying solvent polarity (De Cock et al., 2010)...……21

Figure 2.6. The effect of capillary number on the flow pattern of oil and water. The capillary number was tweaked by changing the interfacial tension by means of surfactant, and keeping other parameters flow rate ratio, viscocity ratio same. Droplet flow pattern on the left at Ca ~ 10^{-3} and stratified flow pattern at Ca~1 on the right can be observed (Shui et al., 2008)..……25

Figure 2.7. Microchannels in PDMS are fabricated by a technique of micromoulding – Soft lithography (McDonald et al., 2002)…….27

Figure 2.8. Droplet generation. (A) The first demonstration of T-junction to produce water in oil droplets (Thorsen et al., 2001). (B) A high performance flow focussing geometry with the circular orifice is capable of producing droplets with the frequency of 10^4 droplets per second (Yobas et al., 2006)……30

Figure 2.9. (A) Passive, serial droplet fission at T-junctions (Link et al., 2004) (B) Passive fusion of alternate droplets (Hung et al., 2006)……32

Figure 2.10. Mixing within droplets can be seen due to chaotic advection within droplets of different geometries. Mixing was found to be more efficient in smaller plugs in (b) (Bringer et al., 2004)……33

Figure 2.11. Dielectrophoretic sorting of droplets for collecting them through five different microchannels (Wang et al., 2007)… ……35

Figure 3.1. (A) Photomicrograph of T-junction exhibiting two inlets for droplet generation (Scale bar = 200 µm). (B) Generation of unpolymerized PEG-DA droplets at the T-junction. (C) Photopolymerized PEG-DA microbeads collected outside the microdevice (Scale bar = 100 µm)……..48

Figure 3.2. Droplet generation at the T-junction was characterized to determine an appropriate range of flow rates for generation of PEG microbeads. (A) The flow rate of continuous phase (Q_c) was varied by keeping the flow rate of discontinuous phase constant (Q_d) constant at 0.002 ml/hr. (Inset) shows a linear response of droplet size at lower values of Q_c. (B) Droplet sizes decreased as Q_c was increased from 0.02 to 1.0 ml/hr, for constant Q_d = 0.004 ml/hr (Kantak et al., 2012)...……50

Figure 3.3. (A) The droplets generated at the T-junction were having plug shape for Q_d >0.05 ml/hr at the constant Q_c = 0.1 ml/hr. (B) The graph plotted Q_d/Q_c ratio against droplet diameter of PEG-DA droplets. For the same values of Q_d/Q_c ratio, diameter of the droplet increased as Q_d decreased (Kantak et al., 2012)...……52

Figure 3.4. (A) PEG-DA microbeads observed in hexadecane (10X) in dark field. The size was measured to be 62.8 $\pm$ 3 µm (Scale Bar = 100 µm). (B) Size distribution of PEG-DA microbeads suspended in an aqueous phase of 1X PBS showing high levels of monodispersity and an average size of 72 µm (Scale bar = 100 µm) (Kantak et al., 2012) ..……53

Figure 3.5. SEM image of microbeads revealing multiple folds. Due to preparation steps for SEM, de-swelling of PEG leads to a smaller microbead size (~60 µm) (Kantak et al., 2012)……54

Figure 3.6. Confocal microscopic studies of PEG microbeads encapsulating FITC-dextran and TRITC-ConA observed in 1X PBS. (A) Observation of localization of FITC-dextran through FITC filter (Ex. = 490 nm, Em.= 525 nm for FITC) (B) Observation of localization of TRITC-ConA through TRITC filter images (Ex. = 557 nm, Em. = 576 nm for TRITC). (C) Brightfield image of microbeads with approximate size of 72 µm (Scale bars = 50 µm) (Kantak et al., 2012)...……55

Figure 3.7. Fluorescence intensity response to glucose concentrations varied from 0 to 10 mM. The steady proportional intensity increase in the fluorescence levels of FITC-dextran molecules with respect to increase in the glucose concentrations showed the sensing abilities of the PEG microbeads (Kantak et al., 2012)..……..56

Figure 4.1. (a) Actual PDMS device for generation of microcapsules for 6 layers of polyelectrolytes primed with blue dye. (b) Experimental setup where the microfluidic device mounted on the inverted microscope, connected to five individual syringe pumps (Kantak et al., 2011)……67

Figure 4.2. SEM images of the PDMS microdevice showing micropillars (80 µm height, 20 µm diameter) in a microchannel. The relative smooth surface of micropillars offers uninterrupted travel of microcapsules (Kantak et al., 2011)……..68

Figure 4.3. Colour dye system to visualise the 3 liquid streams - Micrographs of droplet getting incubated in the first polyelectrolyte (PE) and changing the PDMS ladder within the same PE [(1)-(2)]; Droplet entering the washing solution which removes the non-adsorbed polyelectrolyte [(3)-(4)]; Droplet entering into the second PE for deposition after the wash solution [(5)-(6)]; Deposition of second PE on droplet surface and droplet changing the PDMS ladder within the second PE [(7)-(8)] Scale Bar = 200 µm (Kantak et al., 2011).……69

Figure 4.4. Four frames showing 1-4 number of droplets per ladder during colour dye experiments representing solutions of PAA (blue stream), washing solution (colorless) and PVPON (red stream) (Kantak et al., 2011)…….71

Figure 4.5. (a) Generation of an oil droplet in PAA stream at the T-junction. (b) Movement of droplets guided with micropillars (80 µm height, 20 µm diameter) (c) Droplets undergo a final rinse solution and are collected through the middle stream d) The generated capsules (45 ±2 µm). Scale bar 50 µm (Kantak et al., 2011)…….72

Figure 4.6. The narrow size distribution of microcapsules with SD of ±2 µm (Kantak et al., 2011)……...73

Figure 4.7. PEM-coated oil droplets (a) Bright field image (b) Fluorescence image. PAA was conjugated with Rhodamine and the fluorescence serves as an indicator of polyelectrolyte adsorption. The droplets were collected through the middle stream and analyzed under the microscope. (c) Fluorescent intensity increased linearly as the number of PEMs increased. Scale bar 100 µm (Kantak et al., 2011)……..74

Figure 4.8. (a) AFM image of a collapsed microcapsule after oil core removal. Three bi-layers of (PAA/PVPON) (Z-scale Bar= 1000 nm) (b) 3-D reconstructed view of the same collapsed microcapsule (c) Measured thickness of PEMs after the removal of the oil core for 2, 4 and 6 layer capsules. (Kantak et al., 2011)……77

Figure 5.1. The polymer solutions of PEI (a) and PSS-FITC (b) were prepared in 1-undecanol in the concentration of 1 mg/ml and were mixed in the ratio of 1:1. The precipitation of insoluble polyelectrolyte complex could be observed in bright field (c) and fluorescent (d) images……87

Figure 5.2. The deposition of PSS-FITC on the surface of BSA droplets could be observed without (a) and with surfactant Tween 20 (b)……88

Figure 5.3. The RP-LbL deposition of PSS and PEI on the polystyrene microparticles for 4 layers each in 1-undecanol. The linear increase in the fluorescence intensity confirms the deposition of 8 layers……..89

Figure 5.4. Experiments to roll the BSA microdroplets along the micropillars in PSS-FITC dissolved in 1-undecanol stream did not exhibit rolling of droplets. Arrows are showing the leaking streaks of BSA from the ruptured microdroplets…… 89

Figure 5.5. (A) Microfluidic device fabricated in PDMS for deposition of 2 LbL layers. (B) showing the scanning electron microscopy image of PDMS device with the microstructures for diverting capsules into adjacent stream (Scale Bar = 100 µm)…….92

Figure 5.6. Frames (a)-(b) showing generation of microdroplets at the T-junction. The PSS-FITC in 1-undecanol (continuous phase) sheering the BSA (discontinuous stream) stream into microdroplets which were directed in the stream of PSS-FITC (Scale Bar = 200 µm)…….93

Figure 5.7. (a)-(b) shows four sequential frames of droplet manipulation by the microstructures placed in the microchannel for PSS-FITC to deflect the capsules into adjacent washing stream (Scale Bar = 200 µm)……..95

Figure 5.8. Bright field and fluorescence images of the (PSS/PEI) capsules observed under the microscope at 4X (Scale bar = 200 µm)……96

Figure 5.9. The microcapsules observed at 20X under the microscope after 2 hours. The wrinkled nature of capsules could be observed……..97

ABBREVIATIONS

AFM	Atomic Force Microscopy
Aq-LbL	Aqueous LbL
BSA	Bovine Serum Albumin
Ca	Capillary Number
ConA	Concanavalin A
CVD	Chemical Vapour Deposition
d.d.	Double distilled
DMPA	2, 2-dimethoxy-2-phenylacetophenone
DMSO	Dimethyl sulfoxide
DNA	Deoxyribonucleic acid
EDC	N-(3-dimethylaminopropyl)-N-ethylcarbodiimide
EDTA	Ethylenediaminetetraacetic acid
EHD	Electrohydrodynamic
FITC	Fluorescein isothiocyanate
FOTES	Fluoroctyltriethoxysilane
FRET	Förster resonance energy transfer
LbL	Layer-by-Layer
LUV	Large Unilamellar Vesicles
MAC	Matrix-assisted colloidosome
MI	Material of interest
MLV	Multilamellar vesicles
Mw	Molecular weight
NHS	N-hydroxysuccinimide
PA	Poly(allylamine)
PAA	Poly(acrylic acid)
PAH	Poly(allylamine hydrochloride)
PBS	Phosphate buffer saline
PDMS	Poly(dimethylsiloxane)
PE	Polyelectrolyte
PEI	Poly(ethyleneimine)
PEG	Poly(ethylene glycol)
PEM	Polyelectrolyte multilayers
PLL	Poly(L-Lysine)
PMA	Polymethacrylic acid
PS	Polystyrene
PSS	Poly(sodium 4-styrene-sulphonate)
PVPON	Polyvinylpyrrolidone
RP-LbL	Reverse-Phase Layer-by-Layer
SEM	Scanning Electron Microscope
SUV	Small Unilamellar Vesicles
TRITC	Tetramethylrhodamine isothiocyanate
UV	Ultraviolet

Chapter 1 - Introduction

Chapter 1

Introduction

1.1 Background

Micro-containers can be defined as colloidal particles ranging in size from sub-micrometers to several hundreds of micrometers, fabricated for encapsulating the material of interest. Such micro-containers have been explored by research community for almost half a century due to their versatility, ability to tailor their properties (size, composition, porosity, stability, surface functionality etc.); and numerous applications in encapsulating drugs, biomolecules, biological cells, and other organic and inorganic substances (Johnston et al., 2006; Fenske et al., 2008; Orive et al., 2003; Petrov et al., 2005). The different examples of micro-containers include, but not limited to multilamellar liposomes with sub-micron size range; Layer-by-layer (LbL) polymeric capsules with submicron to tens of micron size range; hydrogel microparticles with a micron to hundreds of micron size range (Taylor et al., 2005; Rabnel et al., 2009). These micro-containers have plethora of applications such as drug delivery (Fenske et al., 2008; Kalshetti et al., 2012), cell therapy (Orive et al., 2003; Li, 1998), biosensing (Zhou et al., 2012) and drug encapsulation (Johnston et al., 2006).

The conventional fabrication of micro-containers is generally performed in batch processes suffering from the limitations of wide size distribution, aggregation of particles and loss of encapsulated material. (Rossier-miranda et al., 2009; Engl et al.,

2008). Firstly, the processes are carried out by top-down approaches like emulsification or extrusion methods which tend to form particles with wide size distribution (Refer to literature review of this thesis). This is undesirable in the applications where stringent control on size or amount of encapsulated material is necessary. Secondly, the process of fabrication of micro-containers is a batch process. Let us herein consider an example of layer-by-layer process. The conventional layer-by-layer method involves repetitive steps of incubation, centrifugation, washing and re-suspension of particles making it a laborious, batch process. Lastly, the current encapsulation methods suffer from aggregation of particles creating unstable particles, and thus wasting the precious encapsulation material (Voigt et al., 1999).

These abovementioned problems can be addressed with the help from microfluidics. Microfluidics is considerably a nascent field in comparison with micro-containers and is an important enabling technology. Microfluidics has seen a surge in research efforts over the past fifteen years which can be attributed to its potential to impact various fields like point-of-care diagnostics (Yager, 2006), chemical and biomolecular synthesis (Janasek et al., 2006; DeMello, 2006), optofluidics (Psaltis et al., 2006) and tissue engineering (El-Ali et al., 2006). A branch of microfluidics 'multiphase microfluidics' has already proven potential to generate stable, discrete microdroplets in an immiscible continuous phase. Due to the 'bottom-up approach' of multiphase microfluidic devices, microdroplets generated within the microdevices are highly monodisperse with coefficient of variation less than 5%. The shape, size and morphology of the micro-containers can be precisely controlled by using microfluidic techniques. Additionally, the fabrication process can be transformed into a continuous process, in contrast to the conventional techniques involving microtubes or macroscale

reactors. The process of fabrication of micro-containers can even become faster due to microscale length scale and economical due to smaller reagent volumes.

With this in hindsight, various techniques of fabrication of micro-containers using multiphase microfluidics were explored in this thesis. In addition to this, passive droplet handling techniques were utilized deliberately for their simplicity, ease of device fabrication, in contrast to active devices which require electric actuation; and possibilities of higher droplet generation frequencies (Refer to the literature review).

1.2 Objective and Scope of the Thesis

The **objective** of this thesis is to develop microfluidic techniques for encapsulation of different template materials to fabricate polymeric micro-containers. The microfluidic techniques proposed in this thesis were able to encapsulate microdroplets of different carrier liquids such as hydrogel, organic phase and water for fabrication of micro-containers.

For this thesis work, three **Specific Aims** were defined:

1. To develop continuous type microfluidic techniques to generate uniform size micro-containers.
2. To explore microfluidic methods for various types of template materials.
3. To successfully encapsulate biomolecules within the micro-containers.

The entire thesis has been strictly scoped to the development of microfluidic systems, with due respect to the consideration of the template material of polymeric micro-

containers. The developed methods are kept most generic and can be extended to fabricate micro-containers of the same genre but with the different composition.

Such micro-containers fabricated from the microfluidic devices exhibit: high levels of monodispersity; integration of the conventional encapsulation processes onto a single chip; faster fabrication of micro-containers; economical use of reagents.

This work aims to bring along two fields of research: Micro-containers and Microfluidics. Following along those lines, the **literature review** gives the brief introduction to the micro-containers, various types of micro-containers; and their preparation techniques such as hydrogel beads, layer-by-layer capsules etc. The remaining part of the literature review introduces brief concepts of microfluidics and multiphase microfluidics primarily, droplet handling/manipulation techniques, and applications of multiphase microfluidics.

In **chapter 3**, a microfluidic encapsulation technique for fabrication of polymeric micro-containers prepared from a template of hydrogel material was presented. The PEG-DA droplets encapsulating proteins were generated at the T-junction and were cross linked by UV exposure. The ability of microbeads to perform glucose assay was further explored.

In this work, droplet manipulation within single microchannel was achieved using a T-junction.

In **chapter 4**, a microfluidic encapsulation technique for fabrication of polymeric micro-containers with a template of organic phase was demonstrated. A novel droplet manipulation approach using micropillars termed as "Microfluidic Pinball" was presented to fabricate layer-by-layer microcapsules encapsulating mineral oil microdroplets.

In this work, the droplets were generated in a T-junction in the first channel and were further manipulated in the second microchannel through parallel laminar streams.

In **Chapter 5**, a microfluidic encapsulation approach to directly encapsulate the template of water droplets containing biomolecules using Reverse Phase layer-by-layer (RP-LbL) principle was demonstrated. The microdroplets of model protein system of BSA were encapsulated with two layers of polyelectrolytes using the novel design. The preliminary experiments showed the potential of the technique to generate RP-LbL microcapsules.

In this work, the droplets were generated in a T-junction in a single channel and were further manipulated through three parallel microchannels, connected to each other with high resistance microstructures.

In **chapter 6**, the thesis is concluded along with suggested future works.

Chapter 2 - Literature Review

Chapter 2

Literature Review

This literature review surveys several cutting-edge research works as well as the fundamentals. The relevant research papers have been cited, categorised and reviewed in this chapter. This literature review gives information on the following four sections: The first section explains about the concept of micro-containers. The second section focuses on conventional encapsulation technologies for fabrication of micro-containers. The third section equips the readers with the basics of microfluidics, multiphase microfluidics, and droplet manipulation techniques. The last section discusses, in brief, the overlap between these two fields and the possible advantages.

2.1 Introduction to Micro-containers

The term “micro-containers” can be widely used to describe colloidal particles having size range from the sub-micrometers to several hundreds of micrometers for encapsulating material of interest. The material of interest could be a therapeutical drug, biological cells, biomolecules or other inorganic/organic substances.

The purpose of micro-containers:

1. To successfully encapsulate the material of interest (MI) by the least harmful methods.

2. To provide structural integrity and material compatibility for retaining the functionality of the MI over time sustainably.

3. To protect the MI from degradation from environmental/surrounding factors such as pH, light, temperature, ionic strengths, microbes, biomolecular agents such antibodies, enzymes etc.

4. To tune the surface properties of the material of micro-container to impart it with the specificity for its target (e. g. targeted organ or tumour). This is a secondary purpose.

One such practical example of the micro-containers was proposed as early as in 1964 by Chang (Chang, 1964) to encapsulate cells within a polymer membrane. This work was the first step towards immuno-protection of transplanted cells inside human body, commonaly termed as "Cell Therapy". The idea of cell therapy (Figure 2.1) is to protect transplanted cells from immune cells and antibodies for avoiding immunorejection; but at the same time to allow nutrients, oxygen and stimuli to flow across the membrane in the inward direction, and therapeutic molecules secreted by the cells to flow outwardly (Orive et al., 2003).

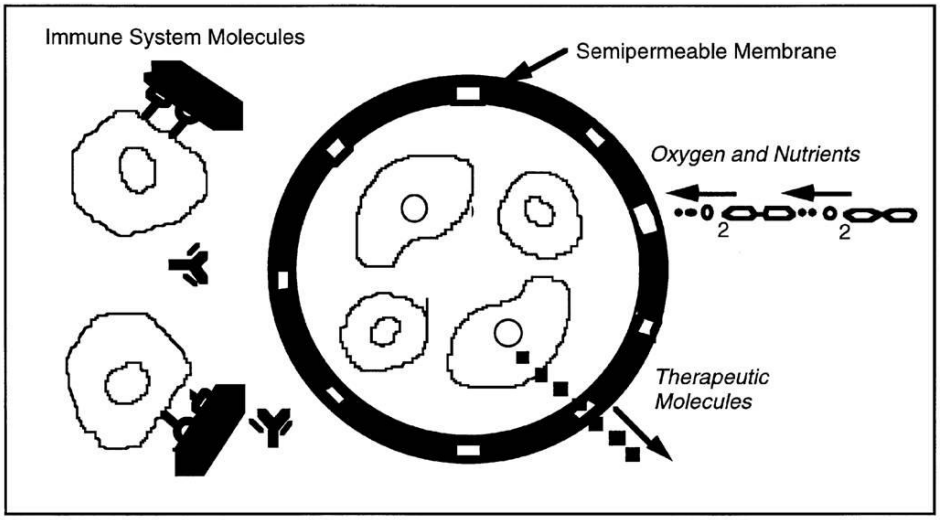

Figure 2.1. The semipermeable membrane for avoiding immunorejection of the transplanted cells by immune system molecules and allowing nutrients to flow inside the capsules (Li, 1998).

2.2 Conventional Techniques for Fabrication of Micro-containers

2.2.1 Liposomes or Self assembled Phospholipids Bilayers

Liposomes have been studied extensively in the literature for their versatility, and have been demonstrated in the applications of a drug or a nutrient career. Consisting of bilayer phospholipids with spherical nature, liposomes can vary in size from nanometres to sub-micrometers. Liposomes were first described by Bangham and co-workers in 1964, however their utility as a tool for drug delivery vehicles was proposed by Gregoriadis et al. in 1974. The capabilities of liposomes for delivering drugs (Fenske et al., 2008), enzymes (Chaize et al., 2004), nutrients (Banville et al.,

2000; Taylor et al., 2005), plasmids (Wheeler et al., 1999) have been demonstrated in the literature previously. The liposomes are generally fabricated by mechanical methods such as high intensity ultrasonication (Bangham et al., 1974), extrusion (Hope et al., 1985) and membrane homogenization (Barnadas-Rodraguez et al., 2001). The techniques for liposome fabrication are up-scalable which is desired for the industry scale applications. The liposomes are divided into three types, based on number of bilayer membrane and size: Liposomes with a single bilayer membrane are either called Small Unilamellar Vesicles (SUV) with diameter less than 30nm or Large Unilamellar Vesicles (LUV) with diameter less than 30-100 nm. The liposomes that contain more than one single bilayer which are arranged in concentric manner are called multilamellar vesicles (MLV). The liposomes of MLV type could be treated like micro-containers with their diameter in sub-micrometer ranges. The liposomes tend to be unstable sometimes and exhibit coalescence.

The double emulsions too have been studied in the literature (Garti et al., 1998), which have dispersed phase containing even smaller dispersed droplets of another phase. The double emulsions are mostly of types such oil/water/oil (O/W/O) and water/oil/water (W/O/W), which have oil droplets emulsified in aqueous phase droplets in continuous organic solution; and water droplets emulsified in the organic phase droplets in continuous aqueous solution.

2.2.2 Hydrogel Microparticles or Microbeads

Hydrogels are one of the most common gel systems utilised for diverse applications as scaffolds for tissue engineering (Geckil et al., 2010), encapsulation material for cell therapy (Rabnel et al., 2009), biosensing agents (Zhou et al., 2012) and drug delivery systems (Kalshetti et al., 2012). The hydrogel is a network of polymeric chains,

containing large proportions of water. The focus of this sub-section is primarily on the preparation of hydrogel microparticles/microbeads. The preparation methods of hydrogel microbeads mainly include ionotropic crosslinking techniques, polyelectrolyte complex crosslinking techniques, and natural/synthetic thermal crosslinking techniques.

2.2.2.1 Ionotropic Crosslinking Techniques for Hydrogels

Polyelectrolytes form ionotropic gels when put in contact with divalent cations or anions. The structure of the gel primarily depends on the molecular weight, charge and density of polyelectrolyte. A common example of such hydrogels is a natural polymer like alginates. Alginates belong to the family of unbranched anionic polysaccharides composed of 1-4-linked α-L-guluronate and β-D-mannuronate arranged in homopolymeric (GGG-blocks and MMM-blocks) or heteropolymeric block structures (MGM-blocks) (H. Zimmermann et al., 2007). The gelling of low-viscosity alginates by calcium, barium or strontium is based on the guluronate blocks, which selectively and instantaneously bind to the divalent cations.

2.2.2.2 Complex Coacervation Techniques for Hydrogels

This method involves fabrication of polymeric particles by forming a complex between oppositely charged polyelectrolytes. In the complex coacervation technique, drops of polyanionic polymer are added to the bulk solution of polycationic polymer, leading to the formation polymeric complex at the interface. The commonly used anionic polymers are alginate, K-carrageenan, chondroitin sulphate, carboxymethyl-cellulose dextran sulphate, gellan, heparin, pectin and xanthan whereas cationic polymers are poly (L-Lysine) (PLL) or Chitosan (Polk et al., 1994; Berger et al., 2004;

Baruch et al., 2006). The naturally occurring polymers have been preferred over synthetic polymers because of high biocompatibility. The pair Alginate/PLL beads have been used widely studied for cell encapsulation applications. Another typically used cationic polymer, chitosan, which structurally resembles components of extracellular matrix such as glycoaminoglycan, is being considered more preferable choice than Alginate due to its less cytotoxicity. An extensive study by Prokop et al. (Prokop et al., 1998 a; Prokop et al., 1998 b) has evaluated 75 synthetic, semi-synthetic and natural polyelectrolytes, and their over 1000 complex coacervates. The polymers were investigated in the systematic manner for their cytotoxicity, gel strength, capsules resistance, permeability and physical characteristics.

2.2.2.3 Thermal Crosslinking Techniques for Hydrogels

The temperature dependent hydrogels have shown to be useful in the applications of cell encapsulation, drug delivery and tissue engineering because of their non-tedious preparation, fast gelation reactions in aqueous environments, and excellent control on mechanical properties and controlled porosity (Bellamkonda et al., 1995). The common examples of the materials used for preparing beads by thermal crosslinking are natural polymers like agarose and synthetic thermotropic polymers like poly(propylene glycol)-bl-poly(ethylene glycol)- bl- poly(propylene glycol), and poly(*N*-isopropyl acrylamide) homo polymer (PNIPAAm).

All of the above-mentioned techniques for hydrogel bead production could be achieved by the following physical preparation methods:

1. Emulsification method by dispersing aqueous solution in an immiscible organic phase stabilised by surfactants. The gelation process is initiated by introduction of

gelation agent or cooling etc. The beads have approximate size range of hundreds of micrometers to millimetres and have large size distribution.

2. Extrusion method by extruding crosslinkable polymer solution through a small tube or a needle and letting it fall into a gelation bath providing divalent cations, polyelectrolytes or cooling (Figure 2.2). The beads produced could vary in size from 0.5 to 3 mm. The size of hydrogel beads could be further reduced by applying electrostatic potential (size in between 0.2 to 2 mm) at the nozzle or by using vibrating nozzle (size of about 0.3 mm).

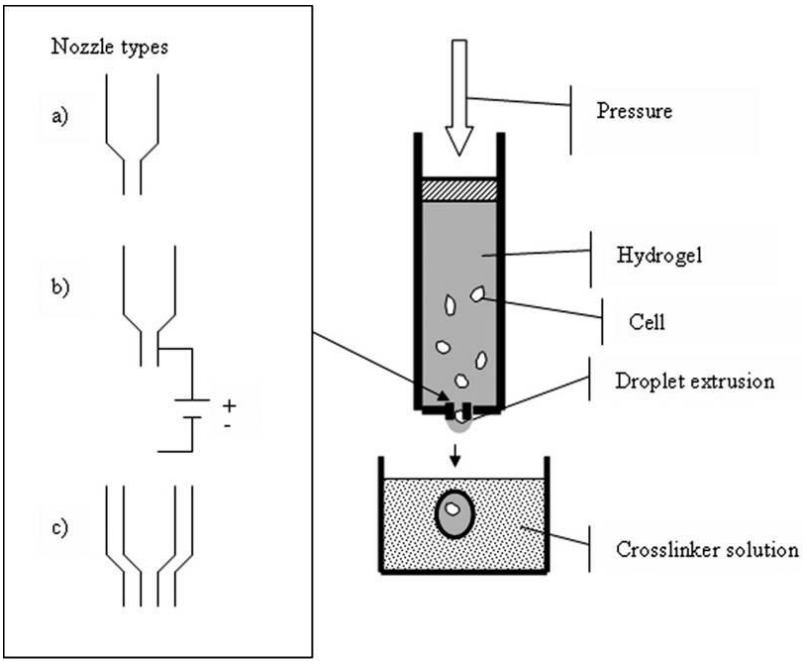

Figure 2.2. Extrusion method explained with different kinds of nozzle types on the left (a) dripping mode (b) electrostatic mode and (c) co-extrusion mode (Rabnel et al., 2009).

Extrusion method suffers from two disadvantages: The minimum size that can be achieved is controlled by nozzle diameter and viscosity of the polymeric solution. Therefore, microbeads with less than 500 µm diameter are difficult to produce. The

microdrops tend to possess teardrop shape due to drag forces after impacting the liquid in the gelation bath.

2.2.3 Layer-by-Layer Polymer Assembly Technique

Decher et al. proposed the Layer-by-Layer (LbL) technique in 1991 for depositing charged polymers onto solid surfaces by electrostatic interaction (Decher et al., 1992). Since then the field of LbL technique has witnessed tremendous research efforts to exploit the technique for applications of biosensors, microreactors, encapsulation, and drug delivery and so on. This sub-chapter discusses the principle of LbL technique, approaches for LbL deposition in the literature, versatility of the chemistries used and finally the strategies of encapsulation.

2.2.3.1 Principle of LbL Deposition Technique

The LbL deposition technique works on the electrostatic deposition of charged polyelectrolyte molecules from the solution to oppositely charged surfaces. Consider a pair of polyions, poly(styrene sulfonate) (PSS) and poly(allylamine hydrochloride) (PAH) for explaining the phenomenon of LbL deposition. A substrate surface with initial positive charge was introduced to the anionic polymer, poly(styrene sulfonate), leading to a formation of PSS layer on the surface (Figure 2.3). The total number of charges on the adsorbed molecules of PSS is greater than that needed to neutralise the oppositely charged surface, and therefore charge reversal occurs. This overcompensation of polyelectrolyte charges has two consequences. Firstly, the charged polyelectrolyte molecules of PSS form a monolayer on the surface as the electrostatic repulsion between the saturated surface and non-adsorbed molecules of polyelectrolyte prevents any further adsorption. Secondly, the charge reversal allows

the subsequent deposition of oppositely charged polyelectrolyte, in this case a cationic polymer, PAH. The alternate addition of polyelectrolytes to the surface develops a well defined, stable multilayered polyelectrolyte film. The deposition of the polyelectrolyte could be achieved on solid surfaces as well as on colloidal materials.

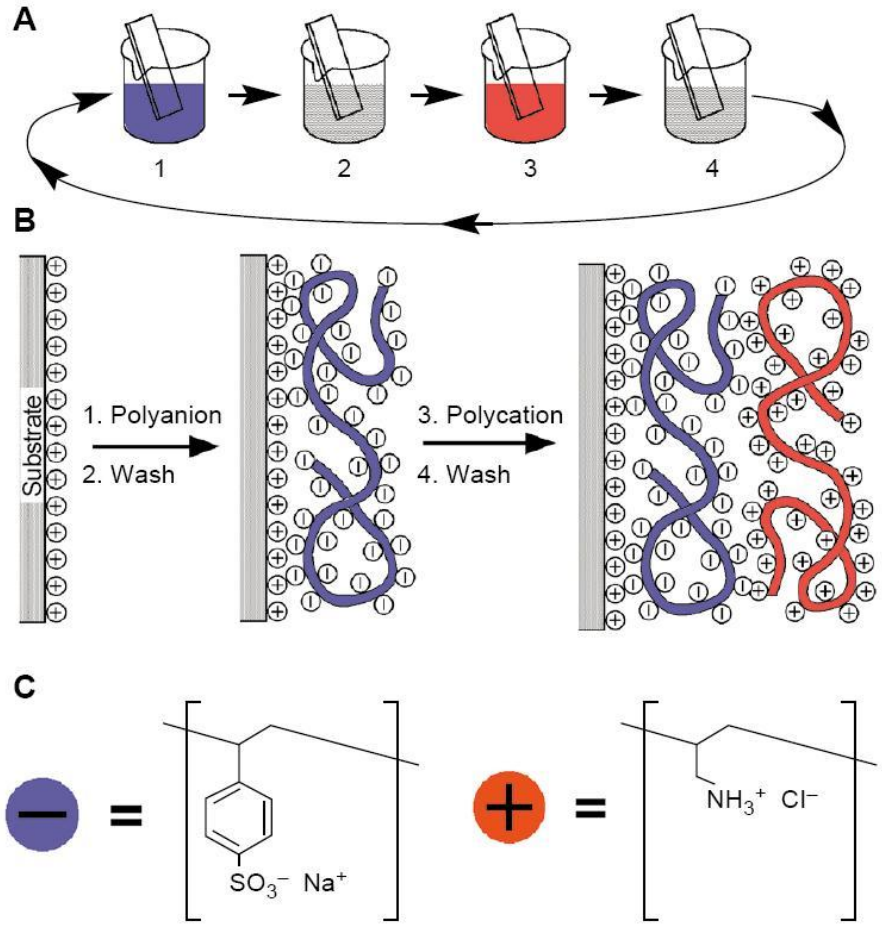

Figure 2.3. Schematic showing the principle of LbL technique. The substrate having initial positive charge was deposited with the first layer of a polyanion, poly(styrene sulfonate) (PSS); and a polycation, poly(allylamine hydrochloride) (PAH) alternatively to form polyelectrolyte multilayers of nanoscale thickness. The intermediate washing step is important for LbL technique to remove non-adsorbed polyelectrolyte from the surface (Decher, 1997).

2.2.3.2 Approaches for Polyelectrolyte Deposition on the Colloidal Particles

Three different approaches for depositing polyelectrolytes on the colloidal templates are enlisted which can yield stable polyelectrolyte multilayers:

1. Saturation method: It involves addition of just enough amount of polyelectrolyte to template material so as to sufficiently coat the template and ensuring that very little traces of free polyelectrolyte remain in the solution phase. The saturation concentration is calculated empirically by determining zeta potential. This approach is difficult to implement and can often lead to bridging or depletion flocculation respectively due to very less or more polyelectrolyte concentration (Guzey et al., 2006).

2. Filtration method. This method involves removal of excessive and non-adsorbed polyelectrolyte through membrane filter while withholding colloidal particles simultaneously. The process is carried under pressure gradient while adding buffer solution continuously. This method is up-scalable and could be used in industry applications. However, it generally suffers from the aggregation of particles (Voigt et al., 1999).

3. Centrifugation method. In this method, more than an adequate amount of polyelectrolyte is added to a colloidal suspension in order to saturate the surface of particles. To remove excessive polyelectrolyte in the suspension, following steps are performed several times: centrifugation, removal of supernatant and resuspension of particles. This has been the most commonly method used in literature; however it does suffer from the inefficiency due to loss of template material and aggregation (Sukhorukov et al., 1998).

The LbL capsules can be even fabricated by mechanism other than electrostatic deposition. This has helped to overcome the limitations possessed by capsules fabricated using electrostatic interactions viz. limitations in using only charged species, inability to work in the extreme pH conditions, high ionic strengths and strong polar solvents. Such new mechanisms include covalent bonding (Feng et al., 2006; Zhang et al., 2003), base pair interaction (Johnston et al., 2007), hydrogen bonding (Yang et al., 2002; Kozlovskaya et al., 2006), click chemistry (Such et al., 2006), host-guest interactions (Crespo-Biel et al., 2005) and Van der Waals interaction (Kida et al., 2006).

2.2.3.3 Encapsulation Strategies for LbL Microcapsules

The encapsulation strategies within LbL capsules can be classified into two types depending on the instance of loading of material of interest: Pre-loading and post-loading.

Pre-loading strategies:

The sacrificial template contains molecules of interest. The strategy involves loading of encapsulation material into the template material which is followed by subsequent LbL coating on the template material (Figure 2.4). The various materials have been explored so far to be used as template material. The hydrophobic compounds were mixed in organic phase, emulsified and followed by coating of polyelectrolyte multilayer film (Sivakumar et al., 2009; Teng et al., 2008). However, the technique is limited to hydrophobic molecules and thus use of other template materials have been sought such as mesoporous silica (SiO_2) and calcium carbonate ($CaCO_3$) microparticles. These materials are capable of encapsulating hydrophobic and

hydrophilic molecules within their pores and can withstand pH of wide range (e .g. acidic pH). Mesoporous silica particles have been used so far for encapsulating proteins (Wang et al., 2006), enzymes (Wang et al., 2005) and DNA (Price et al., 2009). The advantages of silica particles are: (i) The higher monodispersity of template particles than other methods; (ii) the ability to remain stable over wide pH range, and especially during lower pH range which is necessary for hydrogen bonding based LbL deposition (Yang et al., 2002). However, essentiality of using hydrofluoric acid (HF) to dissolve the silica core is the major drawback of such systems, due to the toxic nature of HF. Another method for preloading of molecules is by co-precipitating within calcium carbonate ($CaCO_3$) crystals, which are formed by mixing calcium chloride and sodium carbonate; followed by subsequent PEM deposition. The $CaCO_3$ particles can be easily dissolved in aqueous ethylenediaminetetraacetic acid (EDTA) solution, making the process of encapsulation much gentler than in case of mesoporous silica systems. The approach is found to have better encapsulation efficiency than physical adsorption techniques (Petrov et al., 2005; Sukhorukov et al., 2004).

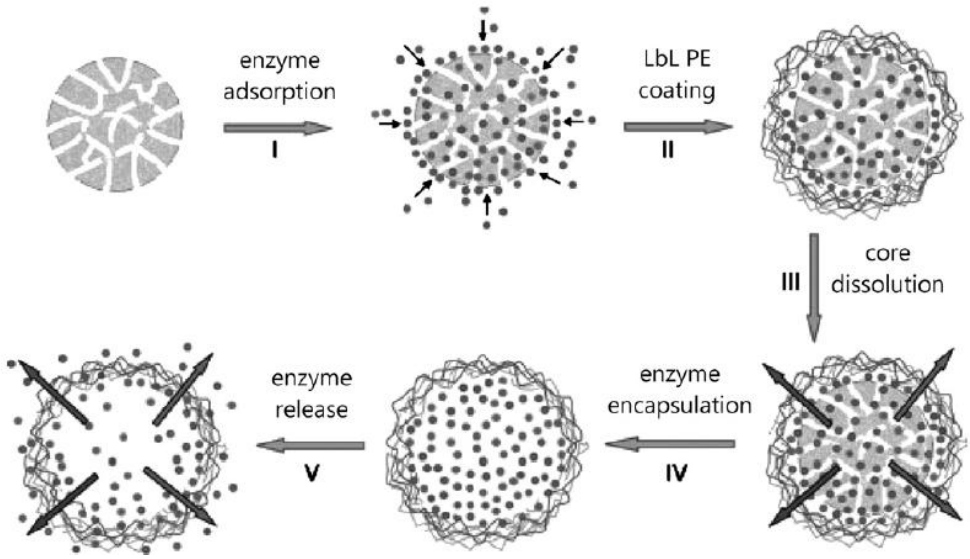

Figure 2.4. Schematic representation of the procedure for encapsulating biomoleules in PEM using porous microparticles as templates (SiO_2 and $CaCo_3$) (I)The immobilization of biomolecules into the pores (II) Assembly of polyelectrolyte

multilayers (III) Dissolution of sacrificial template by HF or EDTA respectively (IV) Retention of Biomolecules, in this case enzymes, within PEM. (V) Application of capsules for enzyme delivery (De Koker et al., 2011).

Other pre-loading strategies involve encapsulation of molecules of interest within hydrogel network, followed by PEM deposition on the hydrogel template. The hydrogel network offers well hydrated, stable 3D network capable of preservation of bioactivity of biomolecules and biotherapeutical substances (De Koker et al., 2011). Some of the works demonstrated by Srivastava et al. (Srivastava et al., 2005) for encapsulation of glucose oxidase within alginate beads; and Mak et al. (Mak et al., 2008) for encapsulating DNA and polymerase within agarose beads for polymerase chain reaction (PCR) constitute so-called 'Matrix assisted LbL Encapsulation Techniques.'

The recently proposed Reverse-Phase Layer-by-Layer (RP-LbL) method from the Trau group (Beyer et al., 2007; Beyer et al., 2012) is capable of directly encapsulating highly water soluble crystals such as glucose and ascorbic acid within PEM by depositing polyelectrolytes on the template through organic phase (e.g. aliphatic alcohols such as 1-Butanol).

Post-loading strategies:

In the post-loading approach, the molecules of interest are loaded in the pre-fabricated capsules, primarily hollow capsules fabricated by sacrificial template removal technique described in the above section. This can be achieved either by changing the semi-permeability of the microcapsule shell reversibly (Figure 2.5). The semi-permeability of capsules' wall was tuned by "opening" the capsules, during which capsules were loaded with the molecules of interest, followed by "closing" of capsules

for entrapping the molecules (De Koker et al., 2011). The semi-permeability of walls of hollow capsules can be modified reversibly by changing temperature (Köhler et al., 2007), ionic strengths (Ibarz et al., 2001; Georgieva et al., 2002), pH (Ghan et al., 2004; Shutava et al., 2005), solvent polarity (Lvov et al., 2001) and drying (Kreft et al., 2006).

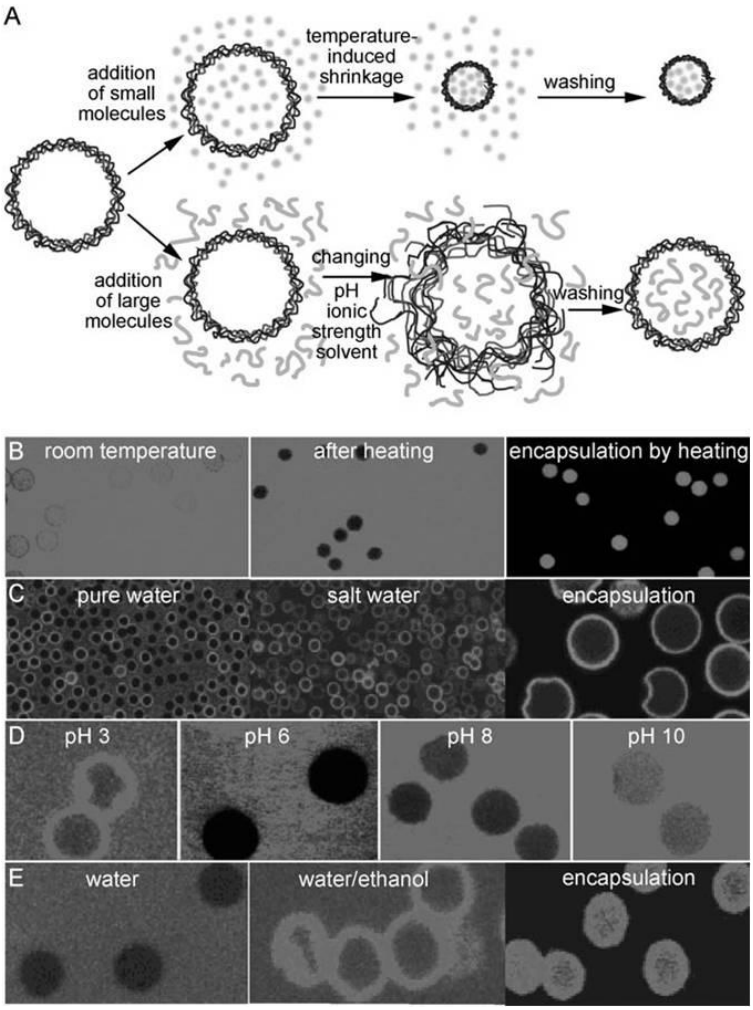

Figure 2.5. (A) The mechanisms by which the permeability of capsules could be changed to load the molecules of interest viz. temperature, pH, ionic strength and solvent. Confocal micrographs of loading of (B) FITC-dextran (10 kDa) in $(PDADMAC/PSS)_4$ capsules by temperature (C) PAH-FITC (70 kDa) in $(PSS/PAH)_4$ capsules by changing ionic strength of the medium reversibly (D) FITC-dextran (2000 kDa) in $(TA/PAH)_5$ capsules by pH changes (E) FITC-urease into $(PSS/PAH)_4$ capsules by varying solvent polarity (De Cock et al., 2010).

The post-loading method suffers from the low encapsulation efficiencies (total amount of material encapsulated within capsules/ amount of material added X 100%), which can be economically detrimental while loading expensive biomolecules such as enzymes, drugs into the capsules. Additionally, the harsh conditions used to tune the permeability of capsules could lead to loss of bioactivity and reduced integrity of therapeutic molecules.

Due to above-mentioned reasons pre-loading techniques of molecules within LbL capsules have been studied and applied more extensively than post-loading techniques.

2.3 Introduction to Microfluidics

This sub-chapter aims to give essential background of microfluidics and related fields. This section provides a brief summary of some of the important parameters/ratios involved in microfluidics, basics of continuous and multiphase microfluidics, materials used for the fabrication of microfluidic devices and droplet handling or manipulation techniques, and applications of droplet microfluidics.

2.3.1 Introduction to Continuous and Multiphase Microfluidics

Microfluidics involves handling of fluids within microchannels having length scale less than a millimetre. Some of the theoretical studies have been presented as early as in 1965 by Happel and Brenner in the book of "Low Reynolds Number Hydrodynamics" whereas practical applications were witnessed as micro nozzles of inkjet printers in 1980s; however the field received a real research thrust in the past 15 years (Stone et al., 2004). The reasons could be attributed to the (i) development of

microfabrication methods capable of fabricating flow channels with the length scale of a micron to sub-millimetre range with the extensive control on feature size (ii) the necessity of investigations on the cellular scale and manipulation of small volumes for the fields of biology and biotechnology and (iii) the need for development of economical devices for point-of-care analytical applications.

Microfluidics is a vast field, and it is indeed difficult to give the accounts of all theories in this literature review. The detailed theoretical aspects of microfluidics can be further referred by readers in some of the excellent reviews from Squires et al. (Squires et al., 2005), Stone et al. (Stone et al., 2004) and in the book "Theoretical Microfluidics" by Henrik Bruus (H. Bruus, 2008). In this section, some of the very basis microfluidic concepts are discussed to lay the foundation for understanding of rest of the sub-chapter.

In 'continuous microfluidics' a flow of fluids having the same phase is established in the microchannel actuated by passive or active pumping. At such length scale, surface forces become dominant over the inertial forces. The Reynolds number (R), a dimensionless number, is used in fluid dynamics to determine the nature of flow. The Reynolds number decides the mode of operation for the microdevice: Laminar or turbulent or transient. The microfluidic devices usually operate in the laminar flow region at lower Reynolds number.

The Reynolds number is defined as,

$$R = \frac{\rho v h}{\mu}$$

Where ρ is the density of the fluid, v is the mean velocity of the fluid, h is the characteristic linear length and μ is the dynamic viscosity of the fluid. A flow within a cylindrical pipe having value of Reynolds number less than 2300 is considered to be laminar. The observed values of Reynolds number for the flow within the microfluidic devices are usually less than one.

'Multiphase microfluidics' involves the flow of immiscible fluids within microfluidic devices. Such flow of immiscible fluids has an interface between different phases implying the presence of intermolecular forces acting on the interface. The dominant forces at the interface are viscous forces and interfacial forces, which are represented by a dimensionless parameter, capillary number (Ca).

The capillary number, Ca is often used in determining droplet dynamics in multiphase microfluidics. The capillary number is defined as

$$\mathrm{Ca} = \frac{\mu v}{\gamma}$$

Where μ is the viscosity of continuous phase, v is the velocity of the continuous phase and γ is the interfacial tension between continuous and discontinuous phase. The viscous forces act tangentially to the phase boundary, so that it elongates the boundary whereas interfacial forces act normal to the boundary surface so as to minimise the interfacial area. The critical capillary number decides a number above which droplet breaks from the stream of discontinuous phase. The lower capillary numbers signify the domination of interfacial forces, and thus droplet based flows are observed whereas the higher capillary numbers signify the dominance of viscous forces, leading to elongated phase boundaries leading to stratified flow (Figure 2.6).

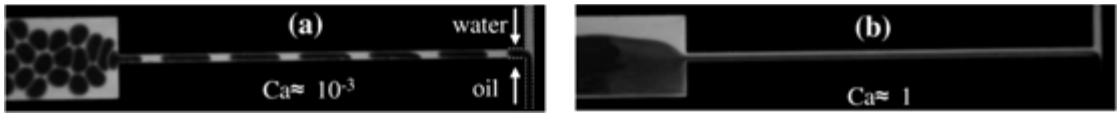

Figure 2.6. The effect of capillary number on the flow pattern of oil and water phase. The capillary number was tweaked by changing the interfacial tension by means of surfactant and keeping other parameters flow rate ratio, viscosity ratio constant. Droplet flow pattern on the left at Ca ~10^{-3} and stratified flow pattern at Ca ~1 on the right can be observed (Shui et al., 2008).

Flow rate, viscosity and geometry of the microchannels decide nature of the flow and whether it is segmented or stratified (Shui et al., 2008; Squires et al., 2005). The value of capillary numbers usually vary between 10^{-3} to 10^{-2} for oil-water interface with the surface tension γ ~30 gm/sec^2, viscosity of water μ_{water} ~ 10^{-2} g/cm/sec and velocity range ~1–10 cm/sec.

2.3.2 Materials Used for Fabrication of the Microfluidic Devices

The microchannels are conventionally fabricated using silicon and glass. The recent developments in the usage of polymeric materials have surged the interests for using microfluidic devices for point-of-care applications.

2.3.2.1 Silicon

Silicon has been reported to be used as a material for microfluidic devices as early as in 1980s for development of micronozzle ink-jet printers and pressure sensors. As an ideal material for microelectromechanical system (MEMS), it has proved its importance for microfluidic applications (Madou, 1997). Silicon has excellent mechanical strength, thermal and chemical stability and is supported by a plethora of well established micromachining methods developed by microelectronic industry. The various methods such as photolithography, thin film deposition techniques such as

chemical vapour deposition or plasma enhanced chemical vapour deposition; etching techniques like wet or dry etching have given suitable control on the features of microstructures. Furthermore, silicon devises can be easily integrated with metal electrodes which is crucial for various applications of electrophoresis as well as with optical components in case of optofluidic applications. Silicon devices can also be treated with various surface functionalization and passivation techniques. However, silicon devices require complex fabrication processes requiring clean room facilities and are inherently expensive. They lack optical transparency required for imaging in biology applications and have limitations on biological compatibility.

2.3.2.2 Glass

In contrast to silicon, glass has an excellent optical transmitivity. It has been traditionally used in chemistry applications for carrying out reactions, and is compatible with a wide range of chemical systems. Glass surface can be also easily modified to immobilize DNA/proteins. However, fabrication of glass microchannels suffers from the dependence on expensive cleanroom facilities (Madou, 1997) and lack of permeability to gases that are crucial for cell culture applications.

2.3.2.3 Poly (methylmethacrylate) (PMMA)

PMMA is a polymer with mechanical rigidity, optical transparency, solvent compatibility and capability to mass produce the chips at a large scale. PMMA chips can be fabricated by various techniques of microfabrication such as hot embossing, microcontact printing, X-ray lithography (LIGA) and injection moulding (Becker et al., 2002). The techniques like microcontact printing can yield structures with lateral dimensions as small as 100 nm in PMMA (Gale et al., 2008). PMMA has been used in

many point-of-care diagnostic applications because it is a low cost material and can be easily disposed (Becker et al., 2002).

2.3.2.4 Polydimethylsiloxane (PDMS)

Polydimethylsiloxane (PDMS) has been able to replace conventional materials like silicon and glass for various microfluidic applications (McDonald et al., 2000). It is economical, easy to fabricate and does not require sophisticated microfabrication cleanroom facilities. Unlike silicon, it is optically transparent upto wavelength of 240 nm (McDonald et al., 2002) and has permeability to gases like oxygen, carbon dioxide making it useful in cell culture applications (Sia et al., 2003). Non-toxicity, biocompatibility and availability of different surface modification techniques (Makamba et al., 2003) make PDMS an important material for biological analysis (Sia et al., 2003).

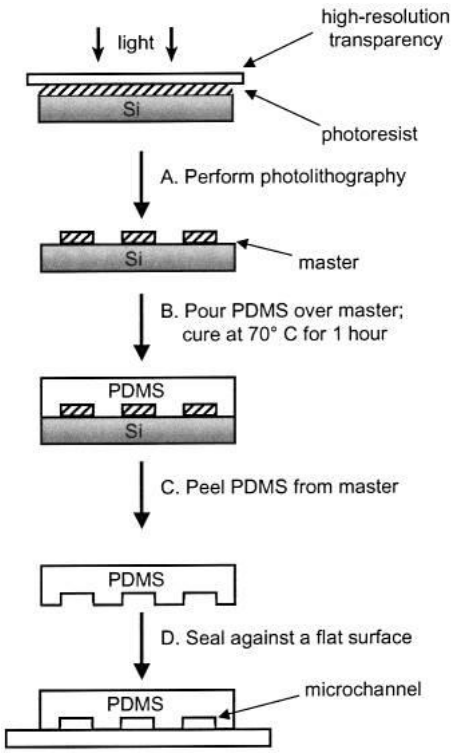

Figure 2.7. Microchannels in PDMS are fabricated by a technique of micromoulding – Soft lithography (McDonald et al., 2002).

Microchannels in PDMS are fabricated by a micromoulding technique called Soft Lithography (Figure 2.7) involving preparation of a PDMS replica from the master mould (Duffy et al., 1998) fabricated usually by patterning photoresist on a silicon wafer to create positive relief structures. The PDMS is provided in two components: Base and curing agent. Silicon hydride groups from the curing agent react with vinyl groups present in the base forming elastomeric solid. The liquid pre-polymer conforms to the shape of the master with the fidelity of 10s of nanometre and replicates the fine features of the master. The PDMS replica can be sealed with silicon, glass or PDMS surface reversibly or irreversibly. The reversible bonding can be achieved by Van der Waals forces or the irreversible bonding can be achieved by condensation of hydroxyl groups between the PDMS and substrate after treatment with oxygen plasma or corona discharge (Makamba et al., 2003; Zhou et al., 2012). PDMS has a hydrophobic surface and is poorly wettable. This nature of the surface can be changed by either plasma treatment, corona discharge or UV/ozone treatment (Makamba et al., 2003; Zhou et al., 2012). PDMS cannot be swollen by aqueous solution and has limited compatibility with organic solvents (Lee et al., 2003).

2.3.3 Droplet Manipulation Techniques

Droplet microfluidics involves generation and manipulation of discrete droplets within microfluidic devices. The range of droplet diameter produced varies from sub-micrometer to few hundreds of micrometer with the generation frequency up to twenty thousand per second (Kobayashi et al., 2007). In contrast to continuous microfluidic systems, droplet based microfluidics can offer control on an individual droplet. This provides the ability of treating individual droplet as an individual microreactor system, which can be processed and analysed. In the droplet systems, heat and mass transfer time are shorter which speeds up the reaction. The droplet microfluidic systems allow

parallel processing and high throughput analysis. This sub-topic gives brief introduction to different droplet manipulation methods: generation, fusion, fission, mixing, sorting.

2.3.3.1 Droplet Generation

The two most commonly used microfluidic droplet generation methods are T-junction and flow focusing geometry. The T-junction was first proposed by Thorsen et al. (Thorsen et al., 2001) which involves sheering of discontinuous phase by continuous phase oriented in perpendicular manner (Figure 2.8 A). The competition of shear force (which elongates the discontinuous stream) and surface tension (which breaks off the stream) at the T-junction results in the droplet formation. The size of the droplet is decided by various parameters like flow rates of discontinuous and continuous stream, interfacial tension between the two phases and respective viscosities. Some other variations of the T-junction were presented in the past few years: Adding a step in the T-junction to create monodisperse droplets with coefficient of variation (CV) less than 1.5 % (Priest et al., 2006), oppositely facing T-junctions to create alternate streams of droplets (Zheng et al., 2004), and 2-stage T-junctions to create double emulsions (Okushima et al., 2004).

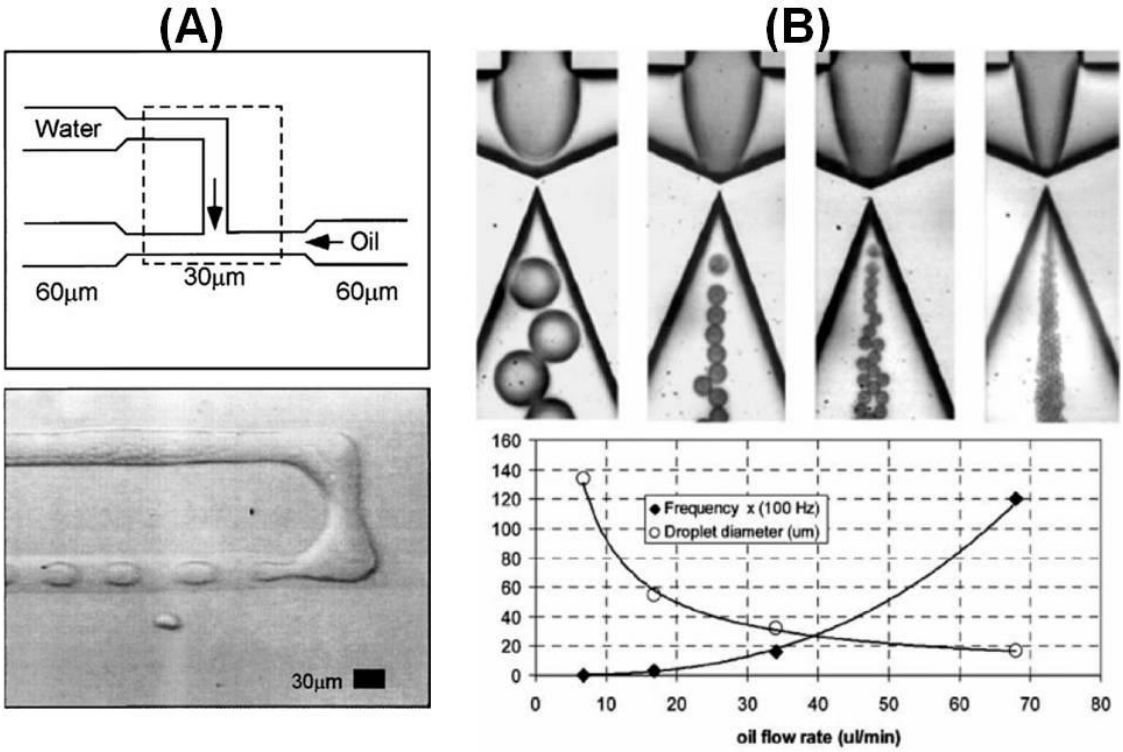

Figure 2.8. Droplet generation. (A) The first demonstration of T-junction to produce water in oil droplets (Thorsen et al., 2001). (B) A high performance flow focussing geometry with the circular orifice is capable of producing droplets with the frequency of 10^4 droplets per second (Yobas et al., 2006).

Another frequently used droplet generation mechanism is a flow focussing geometry which works on the squeezing/pinching of discontinuous, middle stream by two co-flowing continuous streams (Anna et al, 2003). The droplet size is usually governed by flow rates of two phases, the ratio of flow rates and cross section of the focusing geometry. A high performance flow focussing geometry was demonstrated by Yobas et al. (Yobas et al., 2006) having an orifice of circular size so to exert concentric ring-shaped pressure on the discontinuous stream which made droplet generation possible as high as 10^4 droplets per second (Figure 2.8 B).

T-junction and flow focussing geometry are passive ways of generating droplets which heavily rely on the channel geometry, whereas electrohydrodynamic (EHD) methods allow electrical control on the droplet formation by integrating electrodes into

microfluidic chips. Such active or EHD droplet generation methods have been demonstrated in the literature by using principles of dielectrophoresis (DEP) (Ahmed et al., 2006; Jones et al., 2001) and Electrowetting on dielectric (EWOD) (Cho et al., 2003, Lee et al., 2002).

2.3.3.2 Droplet Fusion

Fusion or coalescence of droplets in microfluidic chips is useful for carrying out various applications such as synthesis of materials and biomolecules, fabrication of microparticles as well as kinetic studies (Teh et al., 2008). The process of droplet fusion is a microfluidic equivalent of adding new reagent/substances to the previous reaction. The droplet fusion is usually achieved by active (electrode based) or passive (channel geometry based) means.

Passive fusion has shown to be done by synchronizing droplet generation frequency of two droplet generators and causing the droplet fusion at the junction of two channels. The droplet fusion can also be achieved by passing droplets through a channel obstruction offering channel resistance enough to pass coalesced droplet (Köhler et al., 2004). Another method of droplet fusion is by removal of the continuous phase between two subsequent droplets, either by expanding channel width or by integrating microchannel structures to divert continuous phase (Tan et al., 2004; Liu et al., 2007). The passive methods require stringent control on flow parameters and sometimes are stochastic.

Various active droplet fusion methods have been demonstrated by the principles of dielectrophoresis (DEP) (Schwartz et al., 2004), Electrowetting on dielectric (EWOD) (Ahn et al., 2006) and optical tweezers (Lorenz et al., 2006).

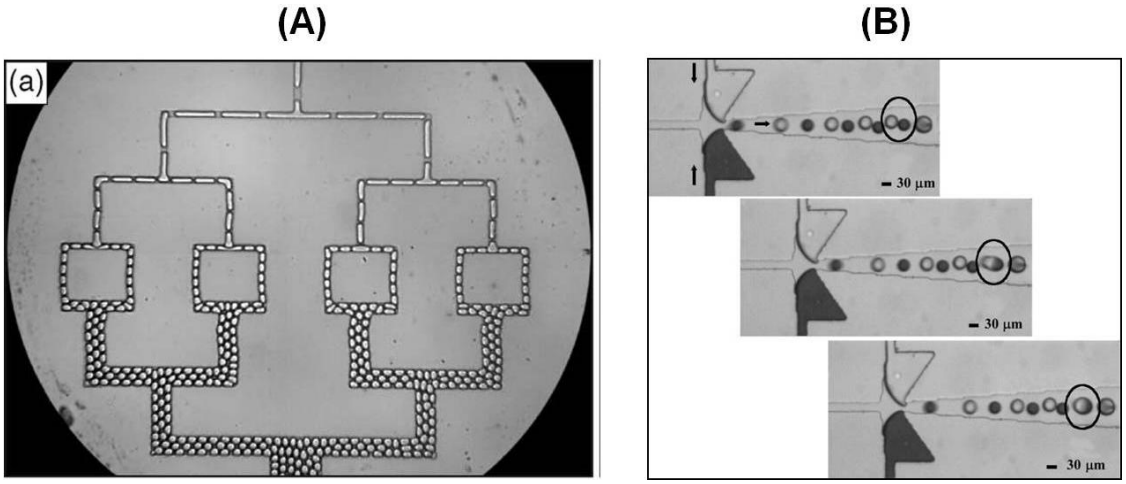

Figure 2.9. (A) Passive, serial droplet fission at T-junctions (Link et al., 2004) (B) Passive fusion of alternate droplets (Hung et al., 2006).

2.3.3.3 Droplet Fission

Microdroplet fission or splitting is required to reduce the volume of droplets, or to reduce the concentration of the substance dissolved in the droplets or to produce the arrays of droplets to increase the experimental throughput (Teh et al., 2008; Yang et al., 2009). The droplet fission could be achieved in two ways by passive or active ways. The passive fission relies on the sheer force created accurately by channel geometry such as T-junction (Tan et al., 2004; Link et al., 2004) or branch channels (Menetrier-Deremble et al., 2006) or obstruction structures placed in the microchannel such as blocks or pillars (Link et al., 2004). The active fission of droplets is realised by EWOD techniques by the authors (Cho et al., 2004) who demonstrated the droplet fission in two equal parts.

2.3.3.4 Mixing in Droplets

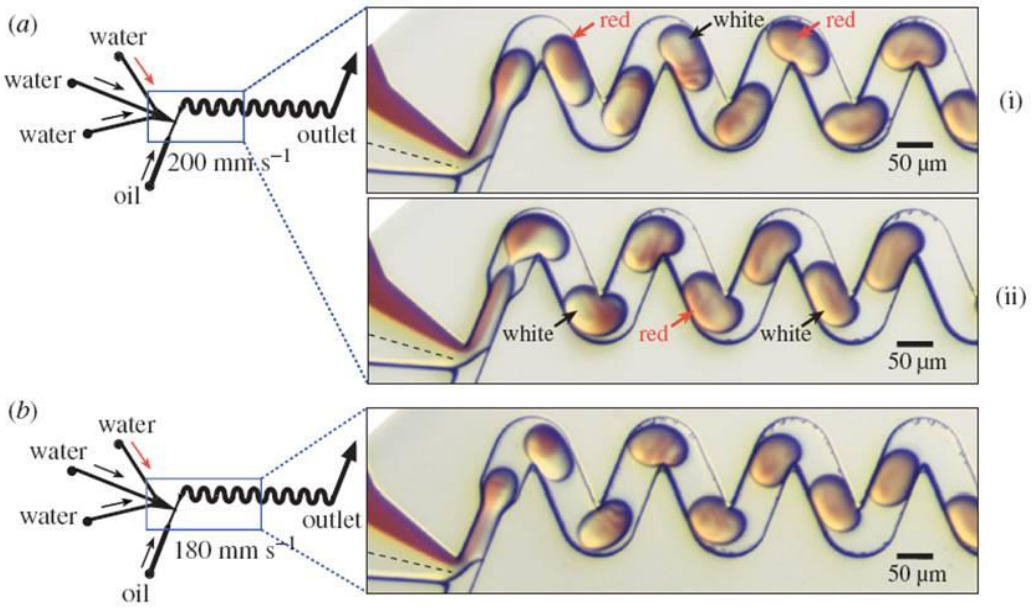

Figure 2.10. Mixing within droplets can be seen due to chaotic advection within droplets of different geometries. Mixing was found to be more efficient in smaller plugs in (b) (Bringer et al., 2004).

Mixing of reagents within droplets is important in studying kinetics for biological and chemical reactions. Similar to continuous microfluidic systems, mixing within droplets is limited by diffusive behaviour, wherein convective/turbulent mixing is absent due to the laminar nature of microflow. Mixing has been achieved either by channel geometry (passive) or by various strategies used in electrowetting devices (active). Passive mixing technique relies on the creation of unequal recirculating flows within the droplets, which results in asymmetrical vortices in two halves, leading to chaotic mixing within droplets (Bringer et al., 2004). Such mixing can be created by serpentine microchannel by incorporating bends and turns in microchannels which stretch, reorient and fold droplets (Figure 2.10). Liau et al. (Liau et al., 2005) showed some improvement in mixing by adding protruding structures in the microchannel to introduce oscillating interfacial shear within droplets. Droplet mixing has also been

demonstrated by active means by moving the droplet in back and forth direction by linearly placed electrodes in the EWOD device (Paik et al., 2003). Such active devices can work in small, confined places in contrast to their passive mixer counterparts which require long winding serpentine channels and specific range of flow rates.

2.3.3.5 Sorting of Droplets

Sorting of microdroplets of different sizes has been achieved by passive and active means. Microchannel geometry with main channel and side channel was demonstrated for filtering out the satellite droplets produced through the side channel and collecting the bigger primary droplets at the outlet of the main channel (Tan et al., 2004). By 'utilizing microfluidic sorting device with hydrodynamic separation amplification' (μSOHSA), heavier droplets were sorted out from the lighter droplets by the difference in their sedimentation velocity (Huh et al., 2007). The active methods for sorting of droplets offer substantial improvement over their passive counterparts which heavily rely on channel geometry and hydrodynamic forces. The active techniques discussed before have also been extended for the sorting of droplets as demonstrated by Cho et al. (Cho et al., 2007), who demonstrated serial operations of splitting the droplet, incubation and sorting the droplet. Dielectrophoresis has also been utilised for sorting the droplets, wherein (Wang et al., 2007) a train of droplets was routed through five different outlets by dielectrophoretic forces (Figure 2.11).

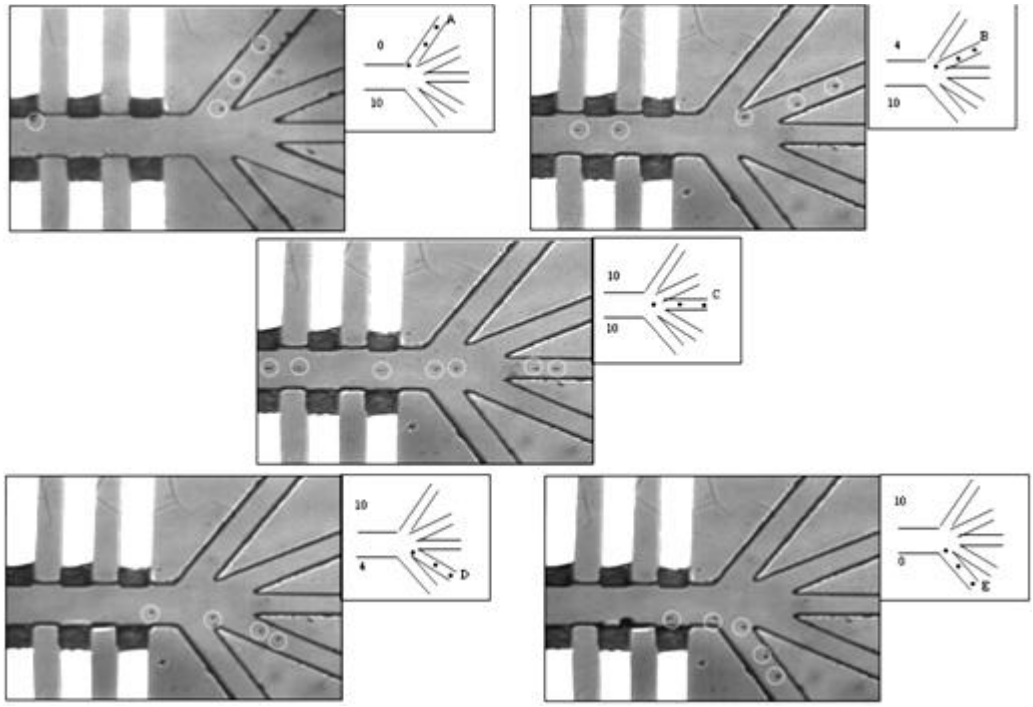

Figure 2.11. Dielectrophoretic sorting of droplets for collecting them through five different microchannels (Wang et al., 2007).

2.3.4 Applications of Droplet Microfluidics

It will be difficult here to give accounts of all applications of microfluidic droplet technology. Perhaps, the readers should refer to some of the latest reviews for (Teh et al., 2008; Leng et al., 2008; Yang et al., 2009; Elizarov, 2009; Hartman et al., 2009; Theberge et al., 2010; Abou-Hassan., 2010 ; Helgeson et al., 2011; Wang et al., 2011 Chung et al., 2012) in-depth information on the applications of microdroplets and their versatility. This subsection only serves to give the overview of applications of droplet microfluidic techniques along with some of the representative examples.

2.3.4.1 Biological and Chemical Analysis

The droplet technology has enabled high throughput analysis for biological and chemical systems. Zheng et al. demonstrated screening of protein crystallisation

conditions within droplets of several nanolitres volume with more than thousand conditions (Zheng et al., 2003). Polymerase chain reaction for amplification of nucleic acids (PCR) has also been demonstrated within droplets by moving droplets through a temperature gradient to achieve PCR (Ohashi et al., 2008; Mazutis et al., 2009). Various enzymatic assays (Li et al., 2007) as well as chemical kinetic studies (Song et al., 2003) have been performed within the microdroplets on-chip. Li et al. studied the enzymatic activity of thrombin, a blood clotting protein to find out the coagulation time for human blood. Song et al. studied the rate of chemical reaction of binding of Ca^{2+} to Fluoro-4 on a millisecond timescale.

2.3.4.2 Encapsulation of Biological Cells

There have been substantial efforts to encapsulate living cells within microbeads fabricated using droplet technology. HepG2 cells were encapsulated by Um et al. (Um et al., 2008) into alginate beads of diameter of 100 µm by using special double t-junction geometry and MEL cells into alginate beads by Shintaku et al. (Shintaku et al., 2007) using flow focussing geometry. Yeast cells expressing green fluorescent protein were encapsulated into alginate microbeads using a t-junction microfluidic geometry by Choi et al. (Choi et al., 2007). A detailed study of encapsulation of various cell lines HEK293, U-2 OS and PC12 within alginate beads having size in the range of 80 µm to 400 µm was presented by Workman et al. (Workman et al., 2007 ; Workman et al., 2008). By using novel geometry, authors were able to encapsulate large number of cells within each capsule which were found to be viable for more than 14 days. Apart from alginate microbeads, cells were also encapsulated within beads of polyethyelene glycol and Triproplylene glycol diacrylate (TPGDA) and acrylic acid

(AA) copolymer. The encapsulation of single cell within each droplet has also been achieved in the literature (Edd et al., 2008).

2.3.4.3 Synthesis of Nanoparticles

The droplet microfluidic devices have been shown to obtain nanoparticles with different size and anisotropy (Abou-Hassan., 2010). In droplet/plug microreactors, reactants are compartmentalized into small droplets which reduce the residence time distribution. The examples of nanoparticles include semiconductor nanoparticles, such as quantum dots made of binary compounds CdS and CdS/CdSe (Chan et al., 2005; Shestopalov et al., 2004). Oxide nanoparticles such as SiO_2 have been also reported by Khan et al. (Khan et al., 2004).

2.3.4.4 Synthesis of Microparticles

The microfluidic techniques for synthesis of hydrogel particles have been studied in the literature which can be referred in some of the excellent reviews (Helgeson et al., 2011; Wang et al., 2011). For preparation of hydrogel microparticles, various approaches have been reported for crosslinking the hydrogel pre-polymer such as ionotropic (Zhang et al., 2007), thermal (Luo et al., 2007) or photo-crosslinking techniques (Seo et al., 2005). In particular, the developments of microfluidic fabrication techniques of photo-crosslinking hydrogel have given an unprecedented control on the particle shape (Seo et al., 2005), anisotropy (Nie et al., 2006) and spatial functionality (Hwang et al., 2008). By combining lithography and microfluidic principles, various microfluidic flow lithographic techniques have been proposed by Doyle group from MIT; which include continuous flow lithography (CFL), stop flow lithography (SFL) and stop flow interference lithography (SFIL). These techniques

have enabled the fabrication of 2D, 3D or encoded PEG non-spherical microparticles. (Dendukuri et al., 2006; Dendukuri et al., 2007; Jang et al., 2007)

2.4 The Interface Aspects of Micro-containers and Microfluidics

In the section 2.2 of this review, the field of micro-containers was reviewed. In the previous section 2.3, the field of microfluidics was reviewed. This section will shortly discuss various overlapping aspects of two fields: microfluidic fabrication of micro-containers.

2.4.1. Advantages of Fabrication of Micro-containers in the Device

The major advantages of multiphase microfluidic techniques for fabrication of micro-containers are enumerated here:

1. The micro-containers fabricated within microfluidic device are highly monodisperse *i.e.* micro-containers produced from the microdevices usually have coefficient of variation of size lower than 5%. This allows user to control the total volume of encapsulated material of interest, which can be important for drug delivery.

2. Due to the bottom-up approach in microfluidic devices; shape, size and morphology of micro-containers can be precisely controlled. (Helgeson et al., 2011)

3. The entire fabrication process can be made continuous and miniaturised on the small device. For example, to conventionally produce alginate beads, solution of sodium alginate is released drop-wise through a circular nozzle fixed at certain height into a bath containing free calcium ions ($CaCl_2$, CaI_2 etc). This entire process can be performed within microdevice with a better control on the size of alginate beads produced. (Zhang et al., 2007)

4. High throughput generation of micro-containers can be achieved in microdevice due to very fast droplet generation speed. (Yobas et al., 2006; Kobayashi et al., 2007)

5. Due to the microfluidic length-scale, the process of fabrication of micro-containers can be sped up ensuring faster fabrication.

6. After fabrication of micro-containers within the microdevice, micro-containers can be further handled within the device in a controlled, enclosed environment. For example, after generating alginate beads within the microdevice, they were trapped in the downstream of the device, coated with the external layer of poly-l-lysine (PLL) to form microcages and to observe movement of *Chlamydomonas* (Morimoto et al., 2009).

7. The entire process becomes economical due to handling of small liquids.

2.4.2. Limitations of Fabrication of Micro-containers in the Device

1. The total quantity of micro-containers fabricated by microfluidic chips has always been a concern with comparison to their industrial or even microtube counterparts. The smaller outputs can be somewhat mitigated by using parallel microfluidic devices. The choice of fabrication of micro-containers using microfluidics in specific applications such as biosensors, encoding systems (Bai et al., 2010) is more pragmatic.

2. Microfluidic chips are often specific for preparation of certain micro-containers, and not generic. The microfluidic geometry for fabricating micro-containers correlates mostly with the structural and material properties of the micro-containers. Due to this, it becomes very difficult to use the same geometry for the different types of the micro-containers e. g. hydrogel based or layer-by-layer type of micro-containers may not be

suitable to fabricate in the same microdevice. In fact, for fabrication of single type of micro-container with similar material composition but different specifications (e.g. size, layer thickness, and shape) could require different channel geometry due to differential residence and reaction times.

Chapter 3 - Microfluidic Fabrication of Polyethylene glycol (PEG) Based Beads for Biomolecular Encapsulation and Glucose Sensing

Chapter 3

Microfluidic Fabrication of Polyethylene glycol (PEG) Based Beads for Biomolecular Encapsulation and Glucose Sensing

3.1 Introduction

Glucose is an important ingredient in cell culture media (CCM) and accurate glucose monitoring during cell growth is important because cells grown outside of normal physiological glucose conditions (0 - 10 mM) can get modified by the processes of glycation and glyoxidation causing unwanted secondary modification of produced proteins (Wells-Knecht et al., 1995; Luo et al., 2002). Standard protocols to monitor glucose or oxygen concentrations in CCM require invasive and tedious handling of the sample for sterile media removal and can be very time consuming (Rosario et al., 1990; Ksinantova et al., 2002). Optical glucose sensors integrated within miniaturized systems provide an attractive alternative because they enable glucose monitoring of sensitive samples with minimal disturbance. A fluorescein isothiocyanate dextran (FITC-dextran) and tetramethyl rhodamine isothiocyanate concanavalin A (TRITC-ConA) biomolecular system offers the potential to monitor glucose levels by relying on Förster Resonance Energy Transfer (FRET) based quenching mechanism. Briefly, when TRITC-ConA (quencher) is introduced in a solution of FITC-dextran (fluorescer), TRITC-ConA reversibly attaches to FITC-dextran resulting in a

sufficiently small (~5 nm) Förster radius (defined as a distance at which energy transfer is 50% efficient). The small molecular proximity leads to quenching of the fluorescence signal of FITC-dextran. Addition of glucose to this system results in competitive binding of glucose to ConA and releases FITC-dextran from TRITC-ConA. Once released, FITC-dextran starts to fluoresce again thereby creating a homogeneous glucose assay (Scheme 3.1).

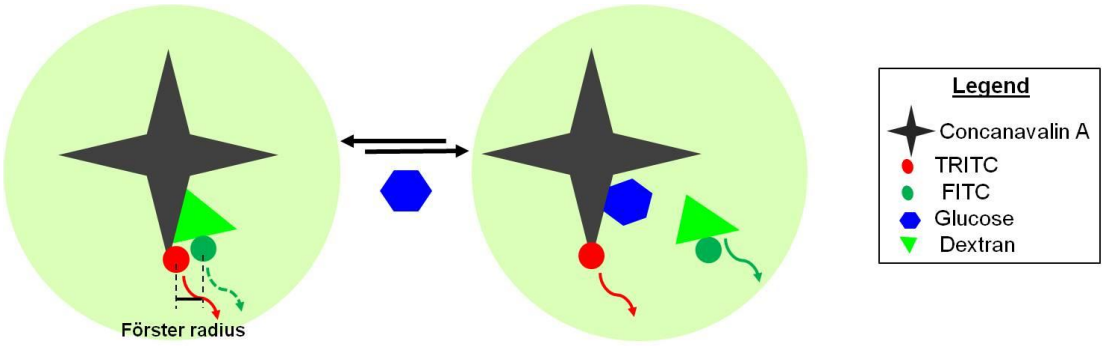

Scheme 3.1. Working mechanism of Förster Resonance Energy Transfer (FRET) based glucose assay. Concanavalin A, a sugar binding protein, has a higher affinity for glucose than dextran. The small Förster radius between FITC-dextran and TRITC-ConA quenches the fluorescence signal emitted by FITC molecules. The increase in glucose concentration releases more FITC-dextran from ConA and thereby resulting in a proportional increase in the fluorescence signal (Kantak et al., 2012).

Various fluorescence based assays have been developed in the past based on this principle. Meadows et al. (Meadows et al., 1988) were the first to develop a fluorescence assay in an aqueous system and use an optical biosensor to detect various glucose concentrations (Meadows et al., 1993). Encapsulation of these compounds within an alginate/poly-L-lysine microbead was conducted by Russell et al. (Russell et al., 1998) but suffered from leakage and structural rigidity problems.

The use of polymeric materials with encapsulated biological components has provided a promising platform for the development of new biotechnology applications such as

chemical sensing, cell encapsulation, drug delivery etc. (Johnston et al., 2006; Cho et al., 2009; DeGeest et al., 2009). Among various types of polymeric materials, polyethylene glycol (PEG) has stood out due to its non-toxic, inert and structurally rigid properties which enable it to be used *in vivo*. Also, due to its advantages over the alginate/poly-L-lysine based systems, various new techniques have been proposed to control the size and manipulation of PEG-based structures (Choi et al., 2008). Traditional methods for synthesizing PEG beads use a syringe based system to extrude droplets into a bath of heavy mineral oil followed by an ultraviolet exposure (Tanaka et al., 1984; West et al., 1995). Temenoff et al. (Temenoff et al., 2004) used a thermal radical initiation method to synthesize PEG and encapsulate marrow stromal cells. An et al. (An et al., 2009) developed a method to encapsulate PEG hydrogels inside the cavity of a liposome, extrude them through a membrane and photopolymerize the contents. These proposed methods, however, have difficulties and limitations in generating a uniform size and shape of the microbeads.

For polymer-based droplets, especially PEG, microfluidic devices with a T-junction or flow-focusing method can be combined with photopolymerization techniques (such as UV) to synthesize microbeads. Various groups have utilized different techniques to generate PEG particles (Seo et al., 2005; Choi et al., 2009; Wang et al., 2011). Especially, the Doyle group has developed various modifications to generate polymeric particles with customized geometries using PEG (Dendukuri et al., 2006; Dendukuri et al., 2007; Helgeson et al., 2011). Their approach offers a high throughput method to generate these particles with this different size and geometries. However, it requires an additional masking step to lithographically define the planar geometry. A

spherical microbead generated in a T-junction or flow focusing method offers simplicity and the added advantage of uniform sensing across its boundary.

In this chapter, a microfluidic T-junction was utilized to generate PEG microbeads encapsulating FITC-dextran and TRITC-ConA bioconjugates. Flow conditions were carefully characterized with various continuous and discontinuous flow rates to generate stable droplets. Generated droplets were photopolymerized *in-situ* with UV light (230 nm) resulting in highly monodisperse 72 $\pm$2 µm microbeads in aqueous environments. Encapsulation of biomolecules was confirmed with confocal microscopy and introduction of 1-10 mM glucose concentrations showed a proportional response in the system's fluorescence signal. We utilize physical entrapping as compared to currently existing chemical crosslinking methods which require additional reagents.

3.2 Materials and Methods

3.2.1 Materials

Polyethylene glycol diacrylate (PEG-DA) (MW 575 Da), 2, 2-dimethoxy-2-phenylacetophenone (DMPA) and hexadecane 99%, anhydrous, Fluorescein isothiocyanate dextran (FITC-dextran, MW 2,000 kDa), D-(+) glucose and Span 80 were purchased from Sigma-Aldrich. Tetramethyl rhodamine isothiocyanate concanavalin A (TRITC-ConA, MW 102 kDa) was obtained from Invitrogen (SU-8 2035 and SU-8 developers were purchased from MicroChem. Polydimethylsiloxane

(PDMS) SYLGARD® 184 Silicone Elastomer Kit was purchased from Dow Corning Inc.

3.2.2 Mould Fabrication

The mould pattern was drawn using Cadence® Virtuoso® software and printed on a plastic photomask for photolithography. Standard one-step photolithography was carried out to fabricate the mould using SU-8 2035, a negative photoresist. SU-8 2035 was spin-coated on top of an 8 inch silicon wafer, baked and patterned using UV photolithography. After the development, the mould was hard baked for 15 minutes at 200 °C and was treated with fluoroctyltriethoxysilane (FOTES) using chemical vapor deposition (CVD) to form a self assembled monolayer (SAM).

3.2.3 Soft Lithography

Polydimethylsiloxane (PDMS) was prepared by mixing the base and curing agent in a 10:1 ratio. The mixture was mixed thoroughly and degassed for 40 min to remove air bubbles. The mixture was poured on the SU-8 mould and cured at 65 °C for two hours. Through-holes having 1.5 mm diameter were punched using Harris Biopsy Needles at the inlet and outlet ports of the microdevice. This patterned piece of PDMS was bonded to a flat piece of PDMS by exposing them in oxygen plasma for 30 seconds at 200 W. The device was kept overnight in a curing oven at 65 °C to improve the bond and to make the channels hydrophobic.

3.2.4 Preparation of Reagents

PEG-DA solution was prepared by dissolving photocrosslinking agent (DMPA) at a concentration of 2% (w/v) in pure PEG-DA. The TRITC-ConA and FITC-dextran solutions were mixed in a ratio of 40:1 by mass in phosphate buffered saline (1X PBS) as mentioned previously. The PEG-DA solution and the above bioconjugate solutions (TRITC-ConA and FITC-dextran) were mixed in a ratio of 1:1 by volume. Hexadecane was mixed with a nonionic surfactant (Span 80) at 4% (v/v). The glucose solutions in the physiological range (1-10 mM) were prepared in 1X PBS.

3.2.5 Experimental Setup

The microfluidic PDMS device was mounted on an upright microscope, Olympus BX41, for observation and for UV exposure for photocrosslinking. The reagents for microbead generation were loaded into two plastic syringes of different sizes (1, 3 or 5 ml) from Braun/Nippro/Terumo Inc. and delivered through Fusion 200 syringe pumps from Chemyx Inc. The syringes were connected to the PDMS device with suitable plastic tubing. High speed images were acquired using a Rolera-XR camera from Qimaging Corp connected to an Olympus IX71 inverted microscope and saved using Image Pro Express software. Software NIH-ImageJ was used for image processing. The dimensions of the UV zone were 800 µm x 100 µm.

3.2.6 Characterization of PEG Microbeads and Biosensing

Once generated, the microbeads were transferred from hexadecane into PBS by rinsing with 1X PBS, followed by centrifugation (250 rpm for 5 min) and re-suspension (3 times). Low centrifuge speed was used to ensure that capsules are not damaged during

centrifugation. The microbeads were pipetted on a clean silicon wafer and dried for Scanning Electron Microscopy (SEM) imaging. For glucose sensing, microbeads were pipetted on glass slides and incubated with 50 µl of different glucose concentrations for 15 min each. Results were obtained via brightfield and fluorescence microscopy. Precautions were taken to keep experimental conditions constant (e.g. exposure times and dark room observations). FITC filter (Ex. = 490 nm, Em.= 525 nm) was used for FITC-dextran. TRITC filter (Ex. = 557 nm, Em. = 576 nm) was used for TRITC-ConA.

3.3 Results and Discussion

3.3.1 Device Design and Fabrication

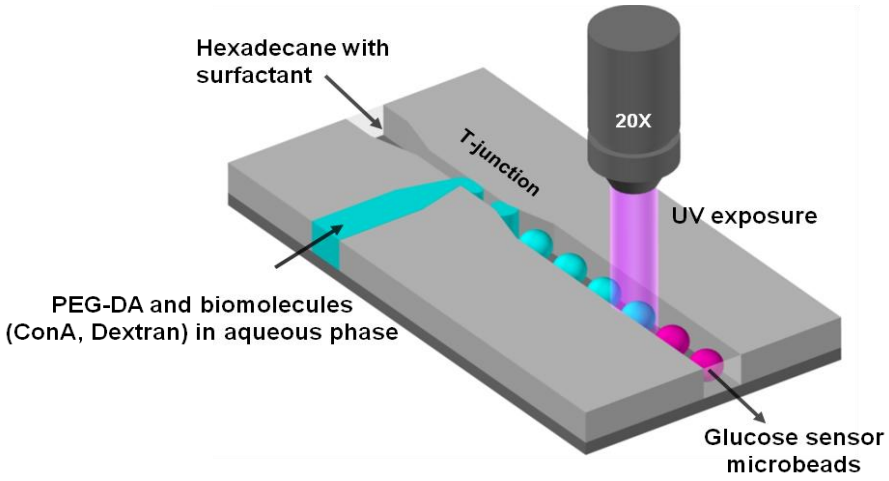

Scheme 3.2. Schematic for the generation of PEG based glucose sensing microbeads showing two inlets at the T-junction to form droplets encapsulating PEG-DA and biomolecules in an aqueous phase. The droplets were photopolymerized by UV light illuminated from a 20X microscope lens to form PEG microbeads (Kantak et al., 2012).

Scheme 3.2 represents a schematic overview of the microfluidic device for generating PEG microbeads for encapsulation of biomolecules. The simple design consisted of a T-junction and a 2 cm long channel (to avoid polymerization at the T-junction). The T-junction had two inputs: (i) a narrowing microchannel (50 µm wide x 100 µm deep) for injecting hexadecane mixed with Span 80 (ii) a nozzle shaped microchannel (30 µm wide x 100 µm deep) for injecting aqueous PEG-DA encapsulating ConA and FITC-dextran. The surfactant, Span 80 dissolved in hexadecane plays an important role as it wets the hydrophobic walls of the microchannels ensuring that droplets don't adhere to the walls. Additionally, it also helps in avoiding droplet coalescence, thereby improving monodispersity.

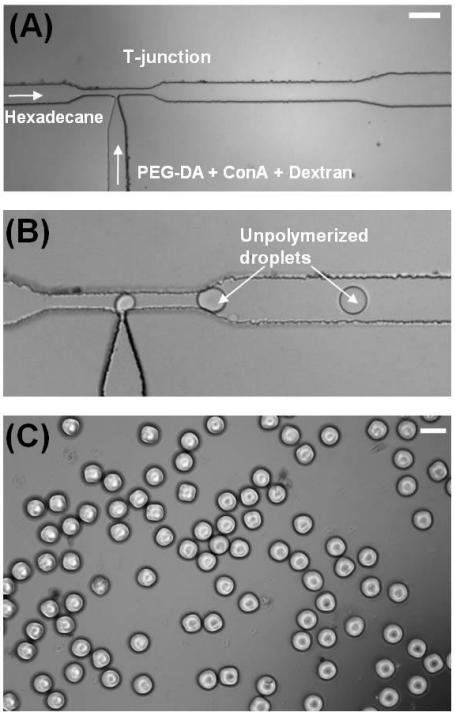

Figure 3.1. (A) Photomicrograph of T-junction exhibiting two inlets for droplet generation (Scale bar = 200 µm). (B) Generation of unpolymerized PEG-DA droplets at the T-junction. (C) Photopolymerized PEG-DA microbeads collected outside the microdevice (Scale bar = 100 µm).

Figures 3.1 (A) and (B) present photomicrographs of the T-junction and droplet generation respectively. Monodisperse droplets were generated by shearing PEG-DA discontinuous phase by a viscous, inert and continuous phase of hexadecane (density = 0.773 g/mL). The droplets travelled down the microchannel and were illuminated with a focused beam of UV light *in situ* which resulted in instant photoactivated polymerization of these droplets to form PEG hydrogel microbeads. The PEG-DA was crosslinked by using up to 2% DMPA crosslinker in the solution. The photomicrograph of PEG-DA microbeads collected in a hexadecane solution outside of the microdevice is shown in Figure 3.1 (C).

3.3.2 Characterization of Droplet Generation

Droplet generation/breakup mechanisms and parameters have been studied extensively in the past (Christopher et al., 2007; Garstecki et al., 2006). It has been shown that for a T-junction geometry involving 'confined' breakup of droplets, the size of the droplets is mostly dependent upon the flow rates of continuous and discontinuous phases rather than the capillary number, *Ca* (Christopher et al., 2007). In the microfluidic device, droplet generation was characterized by keeping parameters such as capillary pressure and channel geometry constant, while varying the flow rates of the continuous and discontinuous phases (Q_c and Q_d respectively). This characterization also helped in empirically identifying a suitable range of flow rates for (i) Uniform sized droplets and (ii) Determining the appropriate residence time of droplets in the UV zone for polymerization. It is necessary to ensure that PEG droplets are completely crosslinked in order to guarantee their mechanical stability and ability to retain biomolecules.

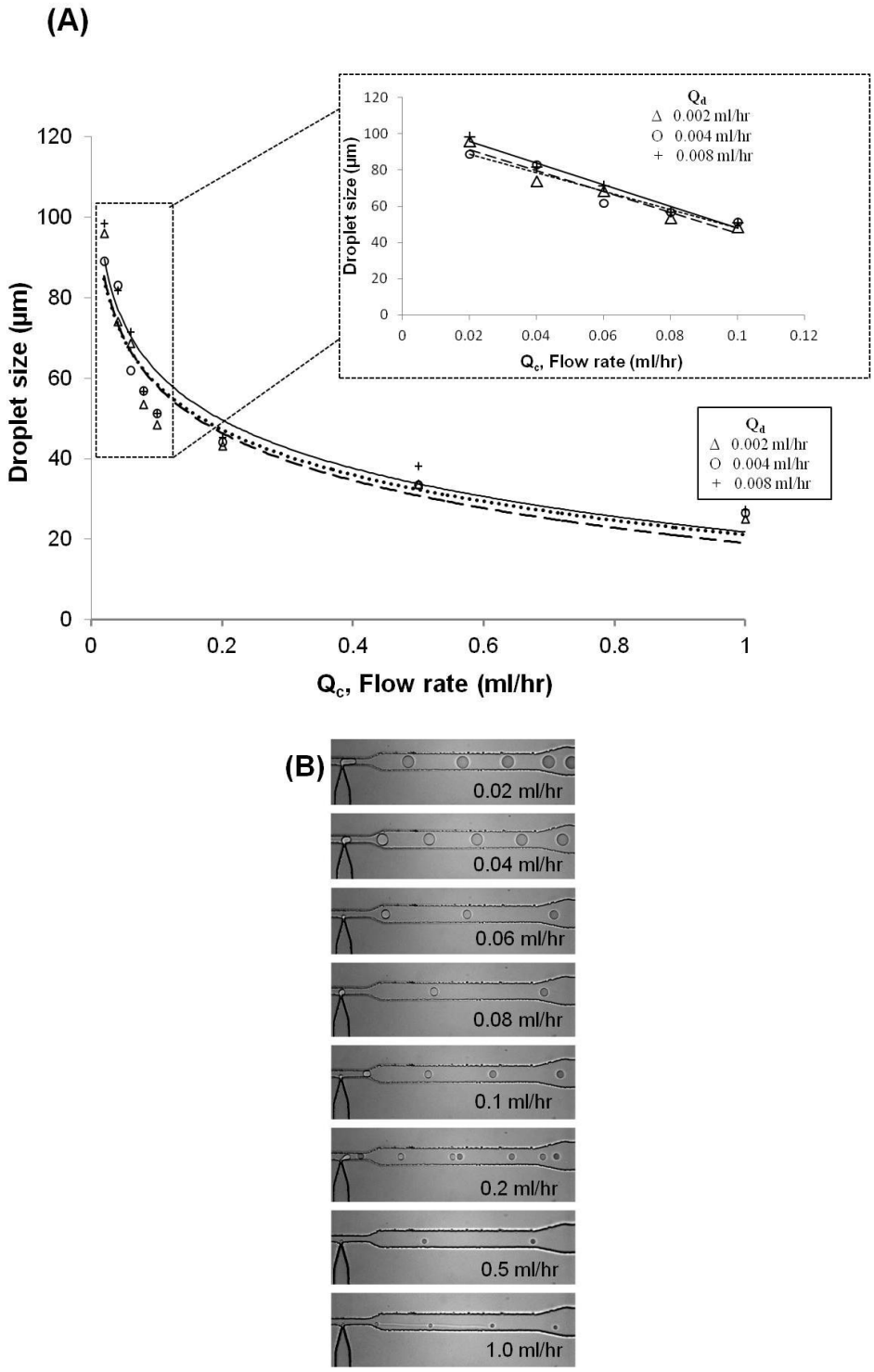

Figure 3.2. Droplet generation at the T-junction was characterized to determine an appropriate range of flow rates for generation of PEG microbeads. (A) The flow rate of continuous phase (Q_c) was varied by keeping the flow rate of discontinuous phase constant (Q_d) constant at 0.002 ml/hr. (Inset) shows a linear response of droplet size at lower values of Q_c. (Appendix A gives tabulated information about standard deviation for size) (B) Droplet sizes decreased as Q_c was increased from 0.02 to 1.0 ml/hr, for constant Q_d = 0.004 ml/hr (Kantak et al., 2012).

Figure 3.2 presents the results for droplet generation and characterization. Initially, Q_d of PEG-DA was held constant at 0.002 ml/hr, while Q_c of hexadecane was varied from 0.02 to 1.0 ml/hr. This process was repeated with Q_d at 0.004 ml/hr and 0.008 ml/hr as well. In the proposed microfluidic device, it was observed that the size of the PEG-DA droplets was inversely dependent on Q_c as can be observed in Figure 3.2 (A) and Figure 3.2 (B). For values of Q_c >1 ml/hr were not able to generate droplets in the range of Q_d (0.002 ml/hr, 0.004 ml/hr or 0.008 ml/hr). Additionally, the residence time of the droplets within the UV illumination area decreased from 540 ms to 55 ms as Q_c increased from 0.1 ml/hr to 1.0 ml/hr, which was not sufficient for crosslinking.

As a result, the microdevice was operated at the lower flow rates (0.04 ml/hr to 0.06 ml/hr) of Q_c where the droplet generation was stable and found to be linearly proportional to Q_c (Inset, Figure 3.2 A). The residence time of the droplets within the UV illumination beam was also found sufficient (900 ms to 1350 ms) for crosslinking of the PEG-DA microdroplets.

The T-junction was further characterized by keeping Q_c constant at 0.1 ml/hr and varying Q_d. The device operated in a jetting mode for $Q_d \geq 0.05$ ml/hr and the droplets formed were of plug-shaped (Figure 3.3 A). The operation of the device in such mode was not desirable, as droplets did not have a free shape in the channel and adhered to the sidewalls. Additionally, beads formed at these flow rates will not be spherical as the height of the channel was 100 µm. Lower flow rates such as Q_d >0.01 ml/hr were found to produce unstable droplets. Eventually, Q_d = 0.002 ml/hr and Q_c = 0.04 to 0.06 ml/hr were finalized for PEG microbead generation. Normally droplet generation at the T-junction is studied by plotting a graph of the droplet size against ratio of the flow

rates. A typical increase in the droplet size was also observed as the non-dimensional ratio (Q_d/Q_c) increases as can be seen in Figure 3. 3 B.

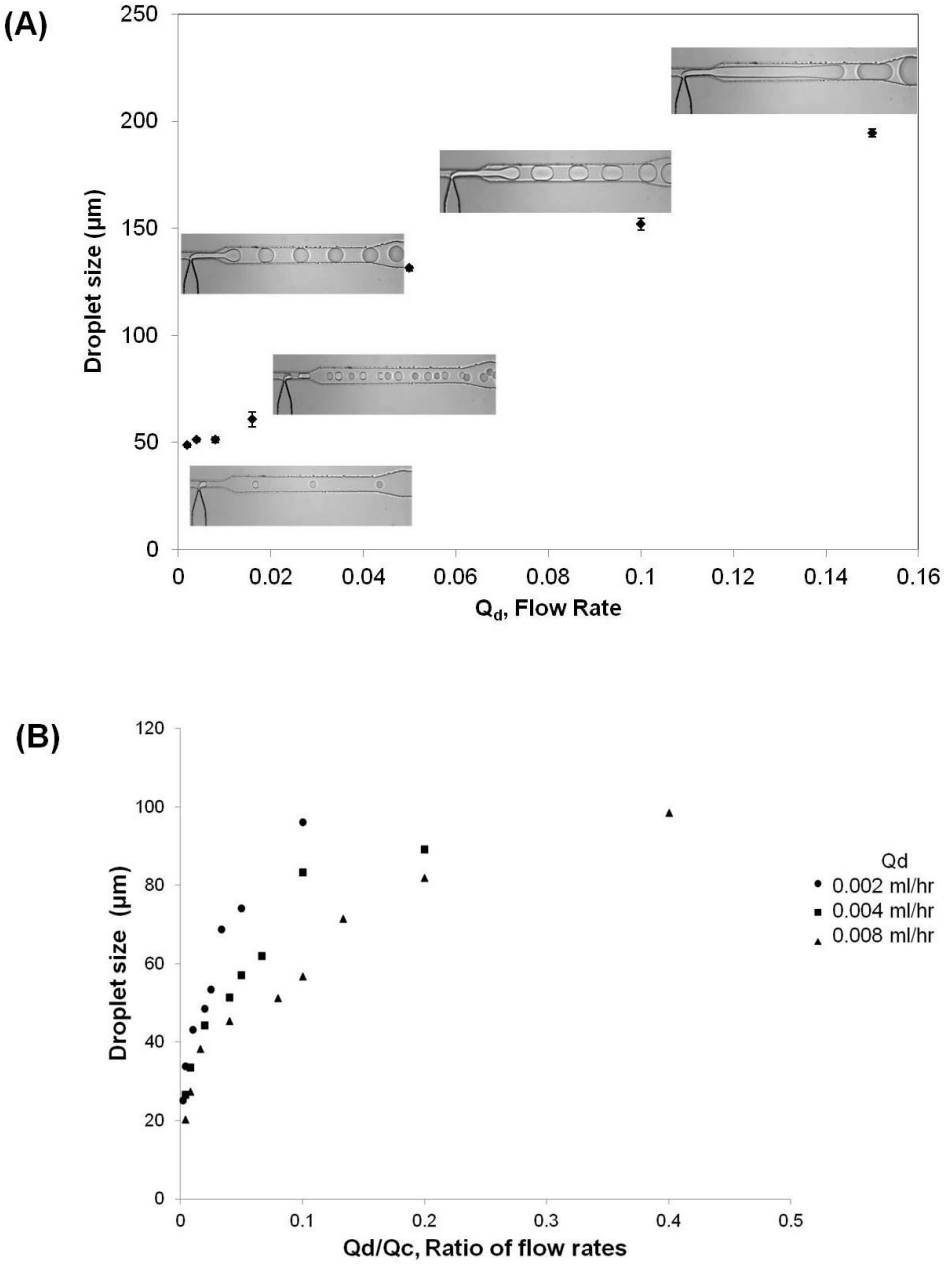

Figure 3.3. (A) The droplets generated at the T-junction were having plug shape for Q_d >0.05 ml/hr at the constant Q_c = 0.1 ml/hr. (B) The graph plotted Q_d/Q_c ratio against droplet diameter of PEG-DA droplets. For the same values of Q_d/Q_c ratio, diameter of the droplet increased as Q_d decreased (Kantak et al., 2012).

3.3.3 Characterization of PEG Microbeads

3.3.3.1 Size Distribution of PEG-DA Microbeads

PEG microbeads were collected outside the device within hexadecane and had mean diameter of 62.8 ±3 µm (Figure 3.4(A)). The microbeads were transferred into 1X PBS by centrifugation and resuspension. Figure 3.4 (B) shows the size distribution graph of the microbeads in 1X PBS. The microbeads were found to be monodisperse with an average diameter of 72 ±2 µm after transfer into PBS. The increase in the bead size can be explained as the typical swelling of a hydrogel in aqueous environments. It has been shown in the literature that swelling ratio of the PEG beads can be controlled (Mellot et al., 2001) by controlling the ratio of PEG-DA to aqueous phase. In this case, the ratio was kept 1:1. The concentration of aqueous phase can be increased to increase the swelling ratio of beads. While transferring from hexadecane to aqueous phase, the PEG beads were found to be mechanically stable after centrifugation and pipetting.

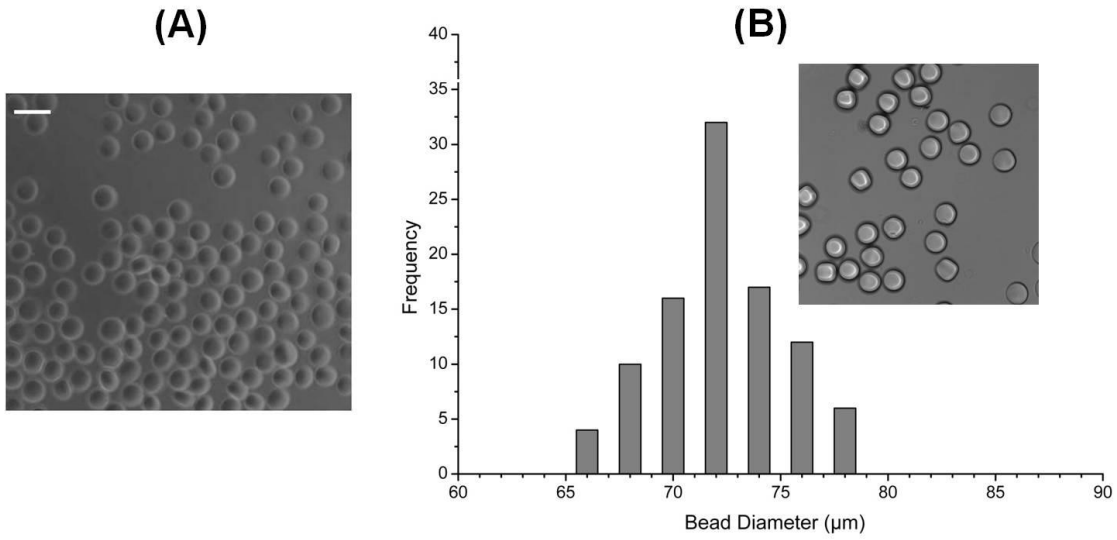

Figure 3.4. (A) PEG-DA microbeads observed in hexadecane (10X) in dark field. The size was measured to be 62.8 ± 3 µm (Scale Bar = 100 µm). (B) Size distribution of PEG-DA microbeads suspended in an aqueous phase of 1X PBS showing high levels of monodispersity and an average size of 72 µm (Scale bar = 100 µm).

(Kantak et al., 2012)

3.3.3.2 Scanning Electron Microscopy of PEG-DA Microbeads

For SEM characterization, the microbeads were first dried on a silicon surface and then observed under low acceleration potential. The approximate size of the microbeads was found to be about 60 µm due to de-swelling (Figure 3.5). The surface of the microbeads was found to consist of multiple folds and appeared wrinkled, which is due to removal of water phase as the beads were exposed to the electron beam and were heated up. The zoomed-in images show white residues on the surface, which are most likely to be salt crystals from the 1X buffer solution.

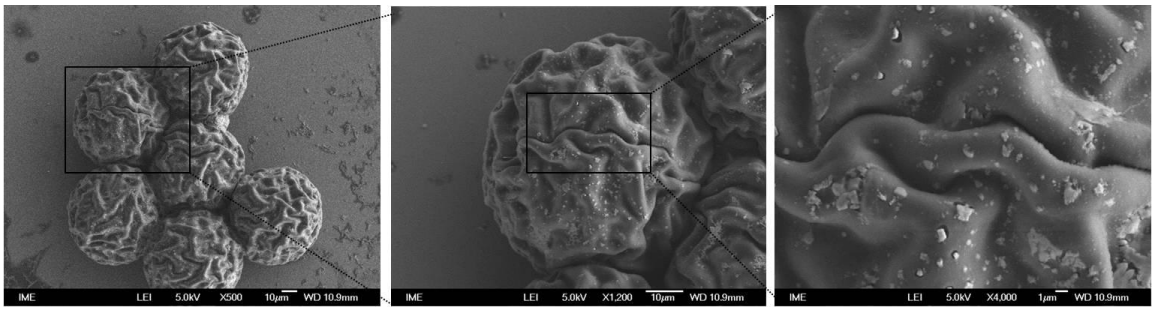

Figure 3.5. SEM image of microbeads revealing multiple folds. Due to preparation steps for SEM, de-swelling of PEG leads to a smaller microbead size (~60 µm) (Kantak et al., 2012).

3.3.4 Encapsulation of Biomolecules within PEG Microbeads

The PEG-DA microbeads encapsulating FITC-dextran (polysaccharide) and TRITC-ConA (protein) were observed using confocal microscopy by exciting with blue and yellow light filters. The images were further reconstructed using ImageJ software. The distribution of ConA and FITC-dextran was not uniform within the microbeads. ConA and FITC-dextran were found to be co-immobilized at the same location within the microbead (Figure 3.6) as observed previously (Russell et al., 1999). The PEG-DA and

PBS form a clear solution when mixed together, but have a tendency to separate gradually after 2 to 3 hours. This can be attributed to phase separation between the aqueous phase and the PEG phase. The PEG-DA is significantly more hydrophobic due to the introduced photo crosslinking system in comparison with the pure PEG that is fully water miscible. The physical entrapping method of biomolecules was used for the first time in the literature for such beads. The previous encapsulation approaches proposed by Russell et al. and by other researchers involved chemical crosslinking of ConA to the PEG molecules by NHS-EDC chemistry.

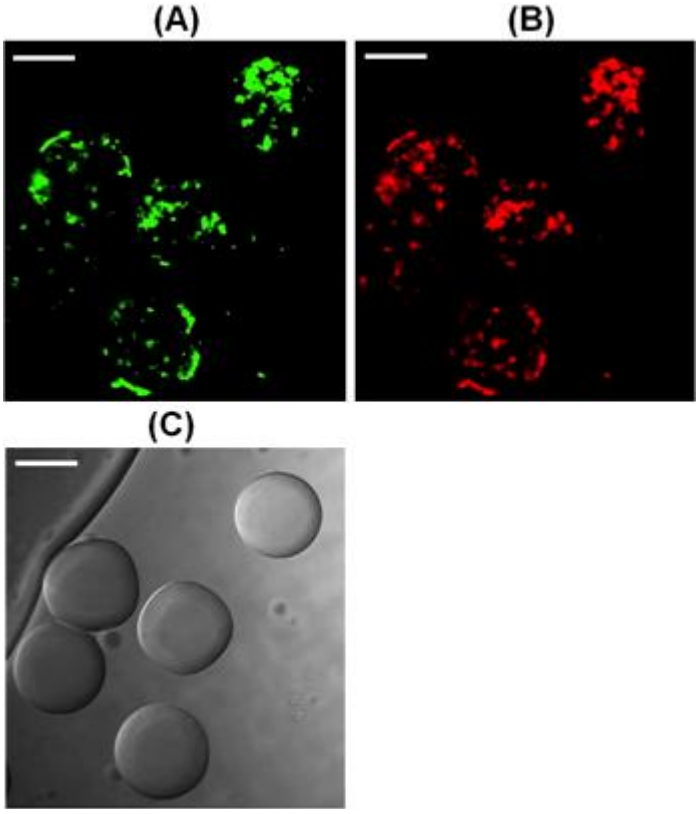

Figure 3.6. Confocal microscopic studies of PEG microbeads encapsulating FITC-dextran and TRITC-ConA observed in 1X PBS. (A) Observation of localization of FITC-dextran through FITC filter (Ex. = 490 nm, Em. = 525 nm for FITC) (B) Observation of localization of TRITC-ConA through TRITC filter images (Ex. = 557 nm, Em. = 576 nm for TRITC). (C) Brightfield image of microbeads with approximate size of 72 µm (Scale bars = 50 µm) (Kantak et al., 2012).

3.3.5 PEG Microbeads for Glucose Sensing

Figure 3.7 shows a normalized FITC-dextran and TRITC-ConA fluorescent intensity response to different glucose concentrations. PEG microbeads in 1X PBS were pipetted on a glass slide and incubated with glucose samples for 15 min. In the absence of glucose, dextran and ConA bind together. Introduction of glucose displaces dextran from ConA binding sites and increases the fluorescence signal. The calibration curve was obtained from 1 to 10 mM glucose concentrations showing a concentration proportional response.

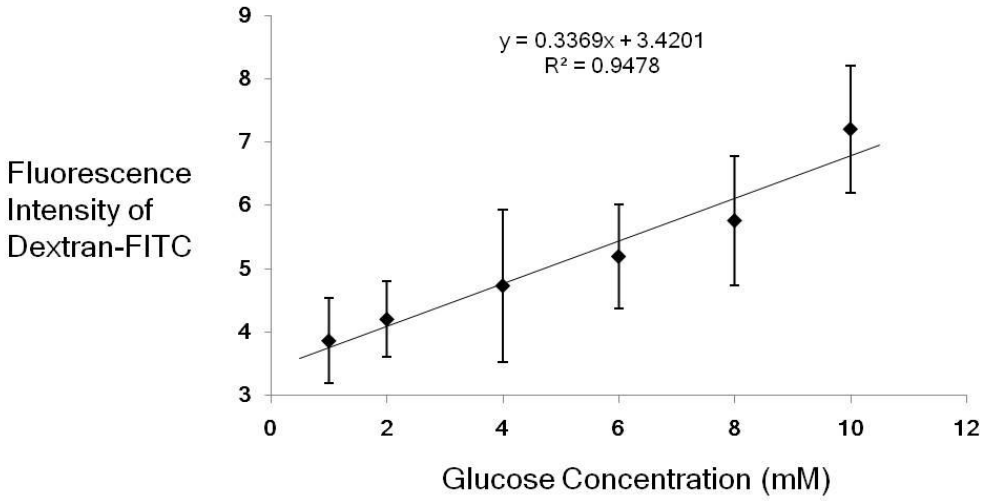

Figure 3.7. Fluorescence intensity response to glucose concentrations varied from 0 to 10 mM. The fluorescence values were re-calculated using blank readings (0 mM) to compensate for background fluorescence. The steady proportional intensity increase in the fluorescence levels of FITC-dextran molecules with respect to increase in the glucose concentrations showed the sensing abilities of the PEG microbeads (Kantak et al., 2012).

The linear increse (R^2 = 0.9478) in the fluorescence intensity with respect to glucose concentration can be seen in Figure 3.7. The normal and abnormal physiological range of glucose for humans (Appendix B) vary in between 4 to 9 mM. The proposed microbead based glucose sensing system comfortably covers this physiological range.

A study from Russell et al., 2001 experimentally calculated the pore size of 0.86 to 10.6 nm for a hydrogel having pure PEG composition. It can be estimated here that this distance range would be suitable to carry out the FRET assay (Förster radius= 5 nm), however, it could affect the sensitivity of the assay. Russell and co-workers (Russell et al., 1999) have noted the reduced biomolecule mobility impacting biosensor sensitivity. The PEG network needs to provide FITC-dextran and TRITC-Con A with the flexibility to rapidly associate or dissociate, while allowing glucose to diffuse into the hydrogel beads. Also Russel et al., 1999 remarked that PEG has a pore size just good enough to allow biomolecules to interact within its mesh, however the authors did suggest to utilize a bigger molecular weight PEG chain to increase sensitivity of the assay. Readjusting reagent ratios and mannose conjugation onto FITC-dextran can result in faster response times and increased linearity range for such sensors (Ballerstadt et al., 1997).

4.4 Conclusion

In this chapter, a microfluidic encapsulation technique for fabrication of polymeric micro-containers prepared from the hydrogel material is presented. A microfluidic device was demonstrated to fabricate highly monodisperse and structurally stable glucose sensing microbeads. The PEG hydrogel microbeads incorporated physically entrapped FITC-dextran and TRITC-ConA conjugates by employing a Förster resonance energy transfer principle. The glucose sensing microbeads had an average size of 72 µm in aqueous environments and were highly monodisperse. Glucose biosensing was conducted in the physiological glucose range (1-10 mM) and a

proportional fluorescent intensity response was observed confirming the technique's potential to create biosensing probes. The ultimate goal of these beads is to be used as glucose sensing probes in microfluidic cell culture systems, which will be discussed in the future works of this thesis.

Chapter 4 - Microfluidic Fabrication of Layer-by-Layer Polyelectrolyte Microcapsules for Encapsulating Oil Microdroplets

Chapter 4

Microfluidic Fabrication of Layer-by-Layer Polyelectrolyte Microcapsules for Encapsulating Oil Microdroplets

4.1 Introduction

In the classical Layer-by-Layer (LbL) technique, oppositely charged polyelectrolytes are alternatively deposited onto a bulk or colloidal template to form polyelectrolyte multilayers (PEMs). Adsorption of these polyelectrolytes is mainly a result of electrostatic interactions occurring between polycationic and polyanionic electrolytes on a charged colloidal template (Decher et al., 1997). Alternatively, LbL encapsulation can also be achieved by forming interpolymer complexes which rely on donation-acceptance of protons such as hydrogen bonding LbL (Wang et al., 1997). The encapsulation of various templates was reported, such as enzymes (Caruso et al., 2000), organic crystals (Trau et al., 2002), vitamins (Beyer et al., 2007), cells (Diaspro et al., 2002) or hydrogel beads (Mak et al., 2008). Nanometer sized films of polyelectrolytes can be obtained after dissolving the colloidal core (Mao et al., 2005) or core LbL shell constructs can be used for various applications in the biomedical industry (Johnston et al., 2006; DeGeest et al., 2009) or the food processing industry (Guzey et al., 2006; Faldt et al., 1993).

Current methods for the automation of LbL encapsulation process utilize conventional macro-scale reactors which are time consuming non-continuous processes requiring bulky and expensive equipment (Somasundaran et al., 1999; Voigt et al., 1999). These reactors not only extend the duration of the LbL process, but also impart problems such as non-uniformity and aggregation of microcapsules requiring further centrifugation, washing and re-suspension steps. For such conventional cases, an alternative method of membrane filtration was suggested by Voigt et al. to sequentially add polyelectrolytes and a washing solution to the colloidal particles while subjecting the container to continuous mechanical stirring. Although the authors reported a reduced severity of the aggregation problem, the method was still a batch process and required changing the membrane filter depending on the size of the colloidal particles. Attempts to form polyelectrolyte microcapsules with an oil core were made by Sivakumar et al. (Sivakumar et al., 2008) who achieved oil encapsulation and PEM release chemically by forming polyelectrolyte shells on silica particles, infiltrating oil through semipermeable walls of the PEM capsule and eventually disassembling the polyelectrolyte layers with exposure to the solutions with pH 7.5. Grigoriev et al. (Grigoriev et al., 2008) demonstrated the direct encapsulation of dodecane emulsion but the microcapsules formed were poorly monodispersed and showed flocculation. Moreover, both techniques still suffered from tedious and lengthy preparation procedures and depended upon hazardous chemicals in some cases (e.g. chloroform).

One could foresee here that properties of microfluidics such as fine control on the microenvironment and bottom-up approach for generating template particles can be extended to perform microfluidic generation of LbL microcapsules for its miniaturization and automation. Previously, Trau and coworkers have utilized

microfluidics to report the deposition of alternative layers of polyelectrolytes (PSS/PAH-FITC) on mineral oil droplets (Peng et al., 2007), where the droplets were generated by a flow focusing geometry and travelled through various bifurcation regions for actual deposition. Non-adsorbed polyelectrolytes were removed by exploiting the Zweifach-Fung effect (Fung et al., 1973) while the colloidal droplets remained in the main channel. More recently, this technique was refined by guiding the generated droplets through different streams of polyelectrolytes and bumping them on obstacle pillars (Zhang et al., 2008). Priest et al. (2008) reported the deposition of three layers of polymers PMA and PVPON on liquid crystal droplets using similar microfluidic techniques (Peng et al., 2007; Zhang et al., 2008). However, for all the above-mentioned literature, the system size and interface complexities are proportional to the number of polyelectrolytes being deposited, as each layer of polyelectrolyte requires its own microfluidic circuitry components (e.g. pumps and channels), thereby enlarging the overall system.

In this chapter, a novel LbL deposition method termed as "microfluidic pinball" which utilizes micropillars to guide discrete droplets is described. Similar to the game of pinball in which a metal ball rolling down a slope lands on ramps, rollovers and other guiding structures, the droplets generated in our microdevice were also guided and diverted to the downstream direction smoothly by repeated unit rows of fabricated micropillars. The microdevice was prototyped in PDMS. The device was initially tested using colour dyes to observe the working principle and then used along with the polymer solutions to create LbL polymer microcapsules. The microcapsules were collected outside the microdevice and were analysed using fluorescence microscopy for the proof of LbL deposition. Finally, the polymeric wall of the microcapsules was

observed using atomic force microscopy and quantified for its thickness. This is the first extensive demonstration of miniaturizing LbL technique for the deposition of 6 polymeric layers on the template material.

4.2 Materials and Methods

4.2.1 Materials

Polyacrylic acid (PAA) M_w 250 kDa and polyvinylpyrrolidone (PVPON) M_w 40 kDa were purchased from Aldrich. Mineral oil, Tween 20, Rhodamine 123, N'-ethylcarbodiimide hydrochloride (EDC), N-hydroxysuccinimide (NHS), tert-butyl methyl ether and fluoroctyltriethoxysilane (FOTES) were purchased from Sigma. Dimethyl sulfoxide (DMSO) was purchased from MP Biomedicals. SU-8 2100/2035 and SU-8 developers were purchased from MicroChem. Polydimethylsiloxane (PDMS) or SYLGARD® 184 Silicone Elastomer Kit was purchased from Dow Corning.

4.2.2 Mould Fabrication

The mould pattern was drawn using CAD software and printed on a plastic photomask for photolithography. Standard one step photolithography was used to fabricate the mould with soft lithography techniques using SU-8 2100/2035 (negative photoresist). SU-8 was spin-coated on top of a silicon wafer, baked and patterned using UV photolithography. The final mould was hard baked for 15 minutes at 200 °C to impart strength and was subjected to chemical vapour deposition (CVD) of fluoroctyltriethoxysilane (FOTES), a fluorosilane to form a self assembled monolayer. This coating reduces the surface energy of the SU-8

mould, making peeling of PDMS easier during the soft lithography process (Zhuang et al., 2007).

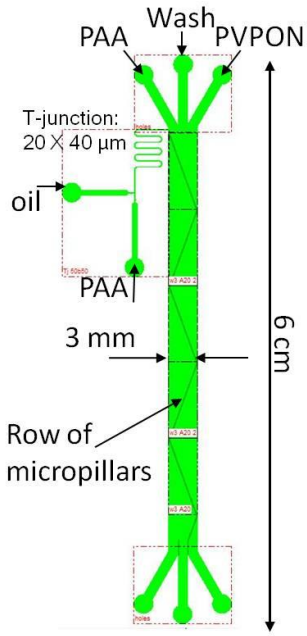

Scheme 4.1. Showing the dimensions of the device (Row of micropillars at an angle 20^{o}) for depositing six layers of polyelectrolytes. (Dimensions of micropillars: 20 µm diameter, 80 µm height, separated by 20 µm).

4.2.3 Soft Lithography

Polydimethylsiloxane (PDMS) was prepared by mixing the base and curing agent in a 10:1 ratio. The mixture was mixed thoroughly and degassed for 30 min to remove any remaining air bubbles. The final mixture was poured on the SU-8 mould and cured inside an oven at 80 °C for 2 hours. The mould was peeled off carefully to avoid damaging the micropillars. Through holes having 1 mm diameter were punched to serve as inlet and outlet ports. This patterned piece of PDMS was bonded to a flat piece of PDMS by treating them in oxygen plasma for 60 seconds at 70 W.

4.2.4 Preparation of Reagents

Colour dye solutions were prepared in distilled water by mixing them in 1% Tween 20 (V/V) surfactant. Polyacrylic acid (PAA) ($(C_3H_4O_2)_n$, 250 kDa) was used as a negative polyelectrolyte and polyvinylpyrrolidone (PVPON) ($(C_6H_9NO)_n$, 40 kDa) was used as a neutral polymer. PAA was labelled with Rhodamine 123 by a conjugation protocol as described (Hermanson, 1996). Mineral oil was chosen as the colloidal phase to form the template drops. All polyelectrolyte solutions were prepared in a sodium acetate buffer (20 mM, pH 4) and 0.05% Tween 20.

4.2.5 Experimental Setup

The microfluidic device was mounted under an inverted microscope (Olympus IX71). Liquid reagents were loaded into plastic syringes of various sizes (3, 5, 10 ml) from Becton Dickinson and delivered through syringe pumps from KD Scientific, Inc. The syringes connected to the microdevice with suitable plastic tubings. A total of five syringes were used. Additional polyelectrolyte layers can be added in our design without increasing the syringe count. Images were acquired using a Rolera-XR camera from Qimaging Corp. and saved using Image Pro Express software. Fluorescence images were captured with an Olympus BX61 microscope. The PDMS microdevice was subjected to oxygen plasma before the experiment in order to render the surface hydrophilic (60 seconds, 70W). Appendix C gives comparative information about the surface modification techniques used in the chapters 3, 4 and 5.

4.2.6 Sample Preparation for AFM Measurements

PEM microcapsules obtained from the device were pipetted onto a flat mica sheet (10 mm diameter) and dried at room temperature for 30 min. Once dried, the microcapsules were immersed in tert-butyl methyl ether for 24 hours to dissolve the oil core. Afterwards, the samples were subjected to AFM measurements in the tapping mode to determine the surface topology and thickness of PEM films using a machine from Nanonics Imaging limited.

4.3 Results and Discussion

4.3.1 Device Design and Fabrication

Scheme 4.1 gives the overview of working of the device. It consists of two main parts:

(i) A T-junction for the generation of oil droplets and

(ii) A main channel consisting of a single file of micropillars arranged in a zigzag configuration to guide the movement of oil droplets through various laminar streams as depicted in the blown out portion of Scheme 4.1.

The droplets travelled through a small side channel to enter the main channel. The main channel consisted of 3 inlet and 3 outlet ports for injecting three different solutions (positive polyelectrolyte, washing solution and negative polyelectrolyte). Due to the operation of the device in the lower range of Reynolds Number, the injected solutions flow as laminar streams within the microdevice without any convective mixing.

The device was fabricated in PDMS using soft lithography technique. Figure 4.1 (a) shows the PDMS device primed with blue dye. It consisted of PDMS micropillars for guiding the generated droplets into different reagent streams. The micropillar row angle was empirically determined to be 30° and 20° with the channel wall for achieving a smooth droplet transition. The device was mounted on an inverted microscope and was interfaced to the syringe pumps (Figure 4.1 (b)).

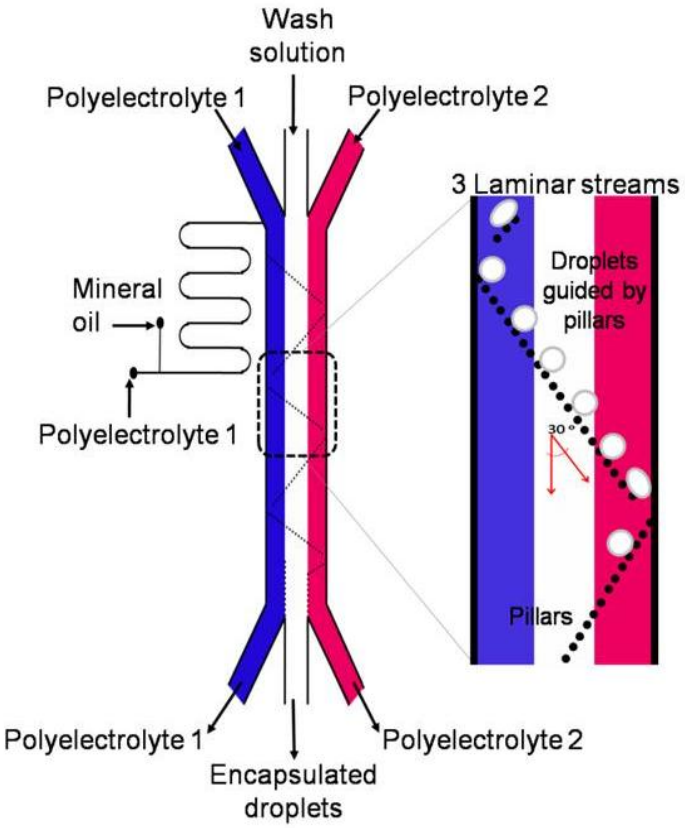

Scheme 4.2. Overview of the device for continuous generation of polyelectrolyte microcapsules by Layer-by-Layer (LbL) deposition of polyelectrolytes. Schematic view (not to scale) is shown with the required inputs and outputs for the deposition of six layers of polyelectrolytes. Expanded view of a single unit of pillars in zigzag arrangement (Kantak et al., 2011).

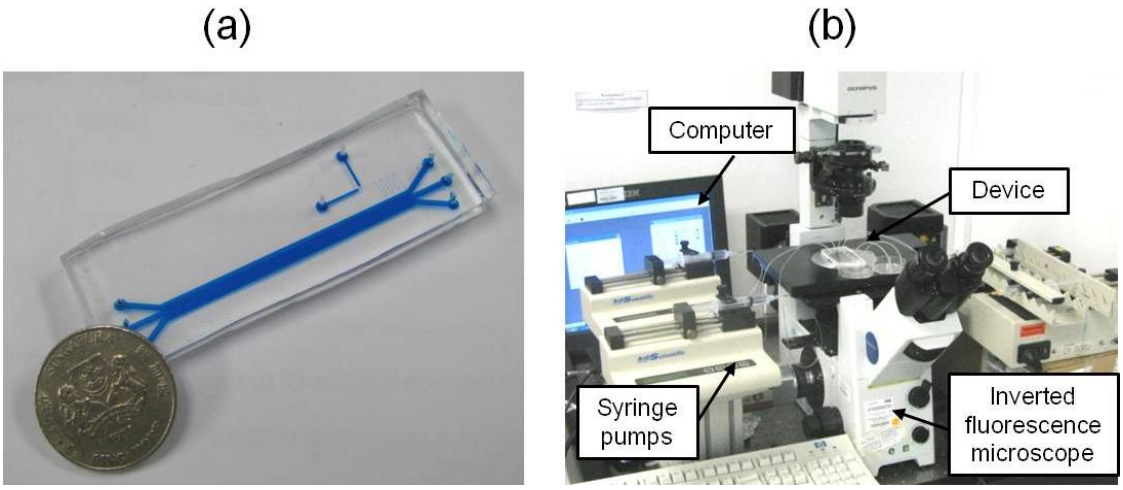

Figure 4.1. (a) Actual PDMS device for generation of microcapsules for 6 layers of polyelectrolytes primed with blue dye. (b) Experimental setup where the microfluidic device mounted on the inverted microscope, connected to five individual syringe pumps (Kantak et al., 2011).

PDMS micropillars were observed under the Scanning Electron Microscope to observe their surface texture and smoothness. The pillars were found relatively smooth and provided hindrance free guidance to the oil droplets as demonstrated in the next subsection. Figure 4.2 (a) shows the SEM image of the pillars along with the side channel from where the droplets enter into the main channel. The zoomed in image of micropillars however shows some irregularities in shapes, possibly because of high aspect ratio of variable depths the cavities in the SU-8 mould. As such moulded piece of PDMS will be bonded with the flat piece of PDMS, the irregular heads of the micropillars will attach to the PDMS bottom, thus minimizing the damage to the polyelectrolyte capsules.

The device was tested using colour dyes to observe the proof-of-concept and subsequently with the polymeric solutions to synthesize LbL microcapsules as explained in the subsections 4.3.2 and 4.3.3.

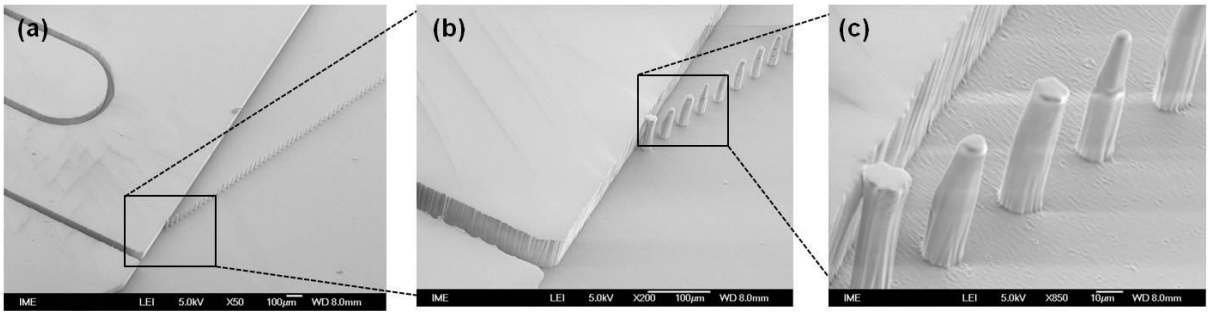

Figure 4.2. SEM images of the PDMS microdevice showing micropillars (80 µm height, 20 µm diameter) in a microchannel. The relative smooth surface of micropillars offers uninterrupted travel of microcapsules (Kantak et al., 2011).

4.3.2 Proof-of-Concept Color Dye Experiments

For proof-of-concept demonstration, colour dye experiments were initially performed to visualise the liquid streams and interaction of droplets with the micropillars. Blue and red dyes were used to represent two different polyelectrolytes, whereas plain water was used to represent the washing solution. As captured by a series of frames in time (Figure 4.3), an oil droplet flowed through the first stream of blue solution, guided with the help of micropillars and received its first coating (Frame 1). As the droplet reached the end of the row, it changed direction by changing onto the new downstream ladder smoothly (Frame 2) and stayed in the same solution stream until it finished the remaining half of its travel. To make the next layer deposition possible, it is important to remove the excess non-adsorbed solution which also helps in reducing coagulation of droplets. In this case, as the droplet crossed the boundary of the first solution

(Frame 3), it was made to pass through a washing solution (Frame 4). The droplet entered the second red dye laminar stream with very little perturbation which is essential to minimize mixing (Frame 5). Upon entering the second solution, the droplet repeated its initial movements and received a second coating (Frames 6–8). Afterwards, the droplet was once again guided into the washing solution to remove the excess non-absorbed second layer coating. This entire cycle (unit cycle) only allows

the deposition of two layers (single bi-layer) on the droplet surface and makes for one subunit of the whole device. Multiple bi-layers can be deposited in a similar manner by extending the length of the channel without introducing any extra interfacial complexities.

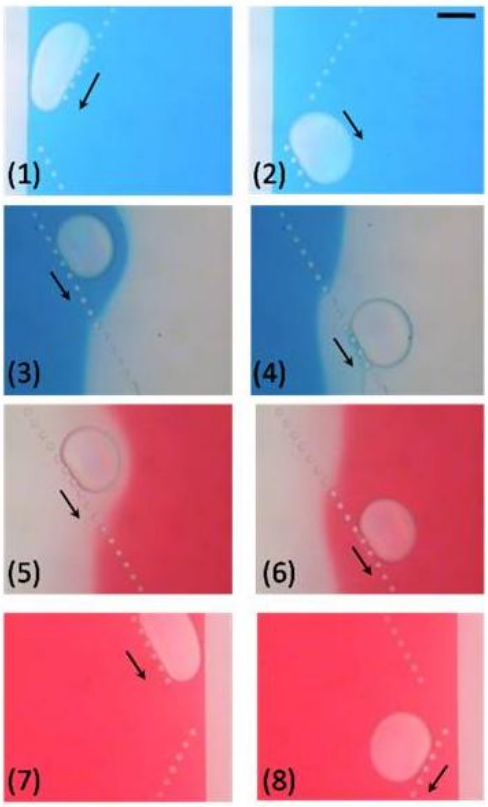

Figure 4.3. Colour dye system to visualise the 3 liquid streams - Micrographs of droplet getting incubated in the first polyelectrolyte (PE) and changing the PDMS ladder within the same PE [(1)-(2)]; Droplet entering the washing solution which removes the non-adsorbed polyelectrolyte [(3)-(4)]; Droplet entering into the second PE for deposition after the wash solution [(5)-(6)]; Deposition of second PE on droplet surface and droplet changing the PDMS ladder within the second PE [(7)-(8)]. Scale Bar = 200 µm (Kantak et al., 2011).

The design approach using micropillars has the following advantages: a) At the T-junction, if any small satellite droplets are generated, they pass through the gaps between the pillars (40 µm) and get screened out and are collected through the leftmost outlet port of the first polyelectrolyte. Thus, our design acts as an automatic filter to

sort out satellite droplets from the targeted size droplets which improves monodispersity b) The zigzag arrangement of the micropillars allows twice the incubation time for polyelectrolyte deposition as that of the washing step, which provides sufficient residence time for polyelectrolyte deposition and c) Since, the number of zigzag turns of the arrangement of micropillars decide the number of layers that get deposited on a droplet, input interface components remain constant irrespective of the number of polyelectrolyte layers to be encapsulated.

It is worth mentioning the importance of the washing step here, as it is an important technique in conventional LbL processing and consists of numerous sub-steps such as centrifugation, removal of unadsorbed polyelectrolyte supernatant and resuspension of particles. Droplet microfluidics offers unique advantages in manipulating individual droplets and constricting all sub-steps into a single step. The diffusion of polyelectrolyte molecules from the laminar stream of PAA to the laminar stream of PVPON, and vice versa could be considered negligible due to the laminar nature of three streams. The lower diffusivity of polyelectrolyte molecules, which are in the size range of 10 and 100s of kDa, also plays an important role in reducing diffusion and mixing of the laminar streams; thus helping the middle laminar stream to keep two polyelectrolyte streams separated. The polymeric molecules are continuously replenished in the laminar streams, after being deposited on surface of microcapsules – thus keeping the constant concentration of polyelectrolytes in the streams. All of the above factors are crucial for stable laminar streams. There is indeed presence of convective mixing, when the droplet transfer from the one stream to the adjacent stream as can be seen in the figure 4.3. However, this mixing does not create serious problems of contamination of liquid streams as it removes the unabsorbed

polyelectrolyte from the droplet surface due to linear drag forces. Secondly, it dilutes the polyelectrolyte streams by negligible amounts, when it enters from washing streams to polyelectrolyte streams.

For the microdevice, it was crucial to achieve suitable control on the number of droplets being generated and released into the main channel as uncontrollable generation of droplets led to droplet overcrowding, laminar stream blocking and change of flow profiles within the channel. In some case, the latter even resulted in convective mixing of the streams, adversely affecting the deposition process. To achieve suitable control, a second set of experiments was performed in the colour dye system where flow rates for droplet generation were optimized. As can be seen in Figure 4.4, a substantial control was achieved on the number of droplets per row of pillars. The flow rate of mineral oil were determined to be 0.010 ml/hr, 0.015 ml/hr, 0.020 ml/hr and 0.025 ml/hr for controlling the number of droplets to be one, two, three and four per ladder of PDMS micropillars. (Frames (a) to (d) respectively in figure 4.4)

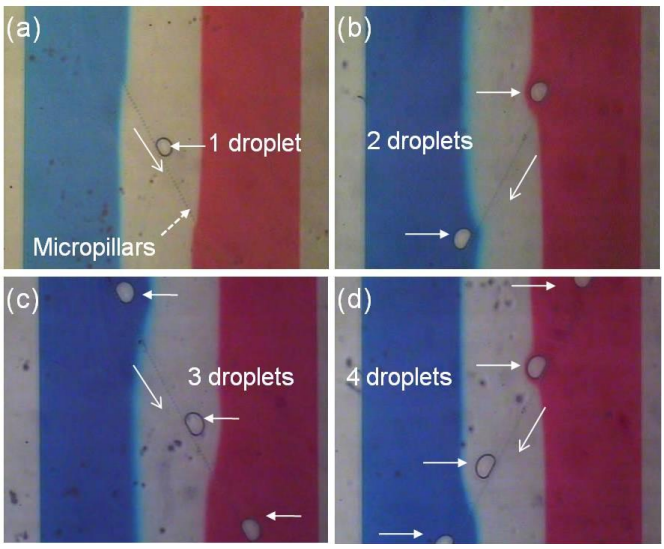

Figure 4.4. Four frames showing 1-4 number of droplets per ladder during colour dye experiments representing solutions of PAA (blue stream), washing solution (colorless) and PVPON (red stream). (Kantak et al., 2011)

4.3.3 Generation of Layer-by-Layer (PAA/PVPON)$_3$ Microcapsules

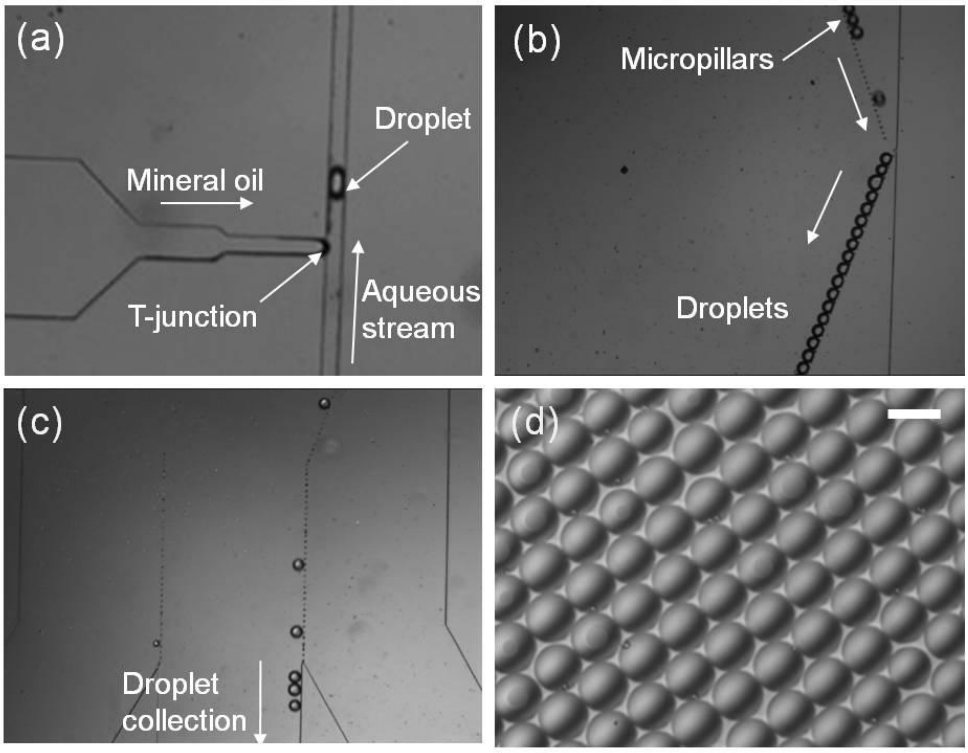

Figure 4.5. (a) Generation of an oil droplet in PAA stream at the T-junction. (b) Movement of droplets guided with micropillars (80 µm height, 20 µm diameter) (c) Droplets undergo a final rinse solution and are collected through the middle stream d) The generated capsules (45 $\pm$2 µm). Scale bar 50 µm. (Kantak et al., 2011)

The polyelectrolytes and wash solution were pumped in with the flow rates of 2 ml/hr from the inlet. Figure 4.5 (a) presents the actual generation of an oil droplet at the T-junction for polyelectrolyte deposition. The oil droplets were generated by shearing a mineral oil stream (9 µl/hr) with a continuous aqueous stream (0.15 ml/hr). Once generated, the droplets were introduced in the PAA stream of the main channel where they continuously adsorbed the negatively charged PAA until they were guided into

the sodium acetate washing buffer. The polyelectrolyte PAA was conjugated with Rhodamine (fluorescent dye) to optically confirm polyelectrolyte deposition on the droplet surface. At the end of the washing step, droplets entered the adjacent laminar stream of PVPON which got deposited on the PAA coated oil droplets because of a hydrogen bond formation between carboxyl group of PAA and the lactame group of PVPON (Subotic et al., 1989) (Figure 4.5 (b)). The microcapsules further travelled through the laminar streams of PAA, washing buffer and PVPON so as to coat total 3 LbL bi-layers of PAA/PVPON. The coated droplets were collected through the middle stream and subsequently analyzed (Figure 4.5 (c)). Highly monodispersed droplets of size 45 $\pm$2 µm were achieved as indicated by the tightly packed "array" in Figure 4.5 (d). The total duration of the capsule spent within the device was about 3 minutes, as observed by tracking individual capsules from entering into the main channel and leaving the outlet.

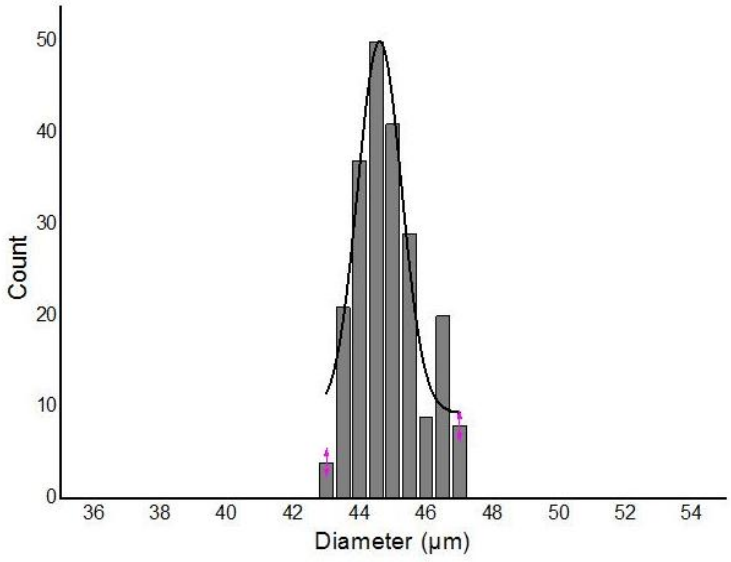

Figure 4.6. The narrow size distribution of microcapsules with SD of $\pm$2 µm (Kantak et al., 2011).

4.3.4 Proof of Layer-by-Layer Polyelectrolyte Deposition

The most common method used in the literature to study and visualise the LbL build-up of polymers is fluorescence labeled polymer technique. As the polymers are deposited on the template surface, a gradual linear increase in the fluorescent intensity is observed due to the deposition of fluorescently labeled thin film.

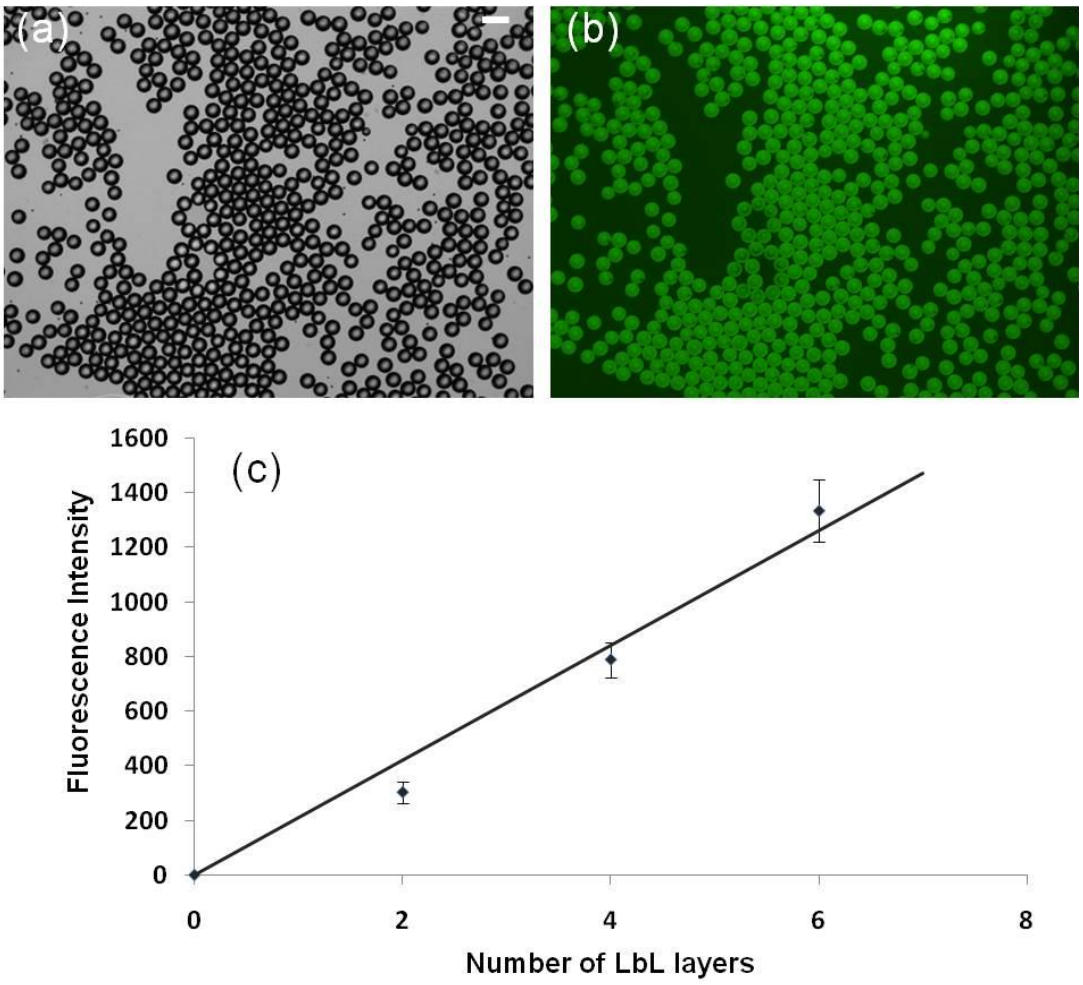

Figure 4.7. PEM-coated oil droplets (a) Bright field image (b) Fluorescence image. PAA was conjugated with Rhodamine and the fluorescence serves as an indicator of polyelectrolyte adsorption. The droplets were collected through the middle stream and analyzed under the microscope. (c) Fluorescent intensity increased linearly as the number of PEMs increased. Scale bar 100 µm (Kantak et al., 2011).

To confirm the deposition, one of the polyelectrolytes, PAA was conjugated with Rhodamine 123 fluorescence molecule. To confirm subsequent PEM adsorption, separate devices were fabricated to generate microcapsules having 2, 4 or 6 PEMs. The collected droplets exhibited uniform fluorescence indicating successful PAA deposition (Figure 4.7 (b)). Experimental conditions such as exposure time during microscopic imaging and polymer concentrations were kept consistent in all the devices. A linear increase in fluorescence intensity with increasing layer number confirmed the successful adsorption of PEMs (Figure 4.7 (c)).

The time duration for which the droplet/capsule resides in a laminar stream is important for sufficient deposition of polymers and for washing step (Combination of diffusion and partial convective mixing) to remove un-absorbed polymer molecules. The time duration mainly depends on two factors, with an assumption of suitable wettability of PDMS surface with the continuous phase: (1) The flow rate of continuous stream i.e. water in this case and (2) the angle at which micropillars are oriented in this device. Using high speed imaging videos, the time duration of every droplet within polymeric stream was calculated to be approximately 25.4 seconds, whereas the residence time within the washing buffer stream was found to be 16.2 seconds approximately. The average velocity of droplets travelling along the micropillar row (20^{o}) was 220 µm/s. The total time to get six coatings is approximately 3 minutes.

4.3.5 Characterization of PEM Microcapsule by AFM

Shell thickness of LbL microcapsules would give definite and important information about the deposition of polymeric layers. However, the characterization methods to

measure the shell thickness are limited. The scanning electron microscopy (SEM) has been used before by Grigoriev et al. (Grigoriev et al., 2008), which could only confirm the presence of capsule shell, however, could not measure the thickness of polymeric layers. Additionally, the technique requires absolutely dry samples without any water content, making it difficult to observe the surface properties of LbL shell. The common colloidal techniques such as dynamic light scattering and zeta potential measurements could not be performed because of the non-uniform distribution of microcapsules within the suspension and/or larger size of microcapsules. Ultimately, the surface characterization technique of atomic force microscopy was used as shown in the schematic 4.3.

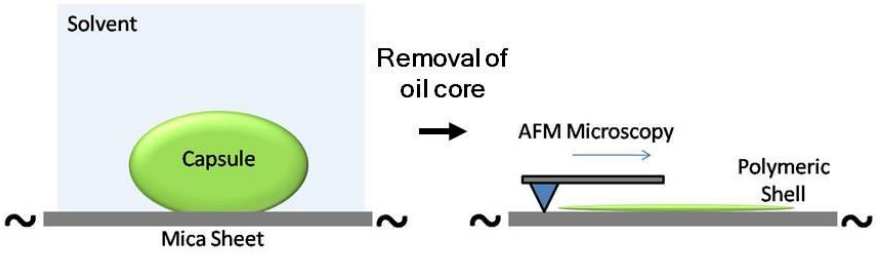

Scheme 4.3. Schematic shows the incubation of microcapsule in a solvent to dissolve the oil core. After removal of oil core, Atomic Force Microscopy (AFM) was performed to measure the thickness of the collapsed polymeric shell

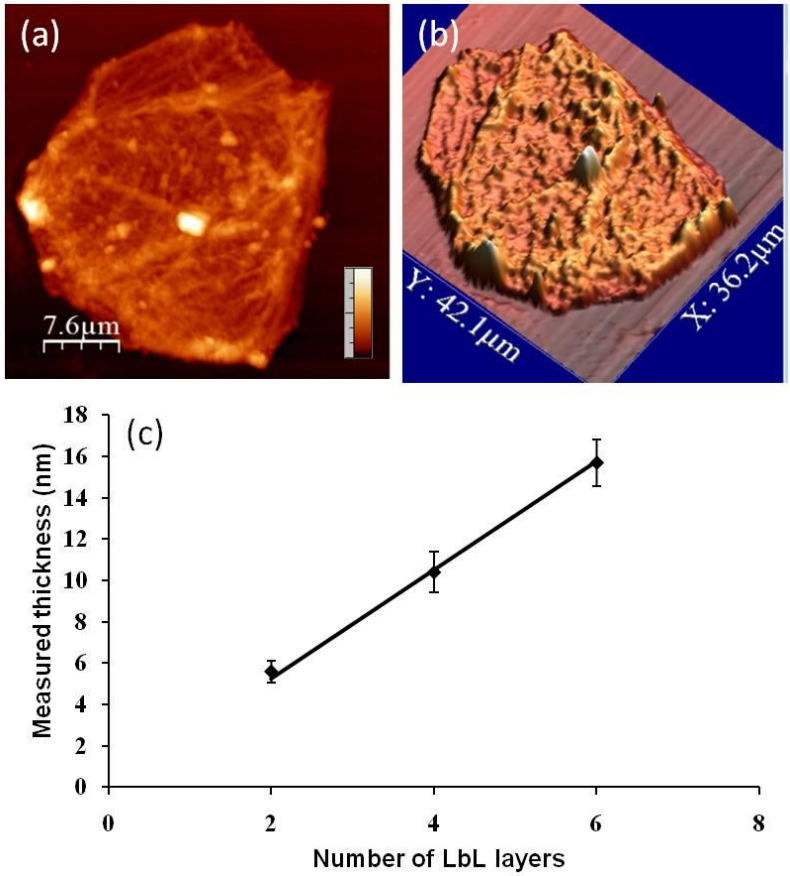

Figure 4.8. (a) AFM image of a collapsed microcapsule after oil core removal. Three bi-layers of (PAA/PVPON) (Z-scale Bar= 1000 nm) (b) 3-D reconstructed view of the same collapsed microcapsule (c) Measured thickness of PEMs after the removal of the oil core for 2, 4 and 6 layer capsules (Kantak et al., 2011).

To determine PEM thickness, collected microcapsules were analysed by atomic force microscopy (AFM) as shown in Figure 4.8. Oil capsules were placed on mica sheets and the mineral oil core was dissolved in tert-butyl methyl ether solvent. The microcapsules fell flat on the mica surface as the oil core dissolved in the solvent and was removed, predominantly due to diffusion (Leporatti et al., 2000). The microcapsule thicknesses were measured using AFM in tapping mode and were found to be approximately 11.2 $\pm$2.12 nm, 20.8 $\pm$3.93 nm and 31.4 $\pm$4.52 nm for 2, 4 and 6 layers respectively. For the collapsed microcapsule, these results represent double the true bi-layer thickness. The individual bi-layer thickness can be calculated as 5.6 $\pm$1.06

nm, 10.4 ±1.96 nm, 15.7 ±2.26 nm and the thickness of a single polymer layer can be calculated to be ~2.8 nm. This thickness is consistent with the average thickness obtained for single layer of conventional LbL polyelectrolyte capsule, which is reported to be 2 to 3 nm (Sivakumar et al., 2008). The linear increase of the microcapsule thickness shows the buildup of polymers on the droplet surface with each subsequent coating. The AFM 3D reconstructed view of the flat capsule (Figure 4.8 (b)) shows the membrane of the capsule after treatment with organic solvent. The rough domains and folds on the membrane surface have been previously recognised in conventional LbL approaches (Dong et al., 2005; Muller et al., 2001; Zuck et al., 2009) and are attributed to the reorganization of polymer complexes within LbL assembly due to the organic solvent treatment.

4.4 Conclusion

A microfluidic encapsulation technique for fabrication of polymeric micro-containers with the template of organic phase (mineral oil in this case) was demonstrated. A novel microfluidic approach termed ‘microfluidic pinball’ is presented in this chapter to generate LbL polyelectrolyte microcapsules in this chapter. The approach utilizes rows of micropillars arranged in a zigzag fashion to guide oil droplets through laminar streams of polymer and washing solution. The deposition of 3 bi-layers of polyelectrolytes PAA/PVPON was achieved in less than 3 minutes with a thickness of ~2.8 nm per layer. Higher number of PEMs can be achieved with our approach without adding any extra interfacial complexities which is a limitation in other devices. This

technique paves the way for a fast, continuous and automated microcapsule production process which is highly required in drug encapsulation fields.

Chapter 5 - Microfluidic Fabrication of Polymeric Capsules using Reverse Phase Layer-by-Layer Approach for Biomolecular Encapsulation

Chapter 5

Microfluidic Fabrication of Polymeric Capsules using Reverse Phase Layer-by-Layer Approach for Biomolecular Encapsulation

5.1 Introduction

The various methods for encapsulating biomolecules have been proposed by using Layer-by-Layer technique in aqueous solutions. These methods have been discussed in the literature review of this thesis in detail. Three methods have been primarily employed in the aqueous LbL (aq-LbL) for encapsulation of biomolecules (Beyer et al., 2012b):

1. Template based LbL encapsulation in aqueous phase

By reducing the solubility of microcrystals of biomolecules by utilising chilled and high salt aqueous solution which is followed by LbL assembly on the crystals (Caruso et al., 2000). Such techniques can be useful to achieve high encapsulation efficiencies; however they are limited to only few biomolecules.

2. Loading based LbL encapsulation in aqueous phase

Preloading of biomolecules within a template matrix which can be silica, carbonate or hydrogel material such as agarose followed by LbL deposition on the matrix (Yu et al., 2005; Volodkin et al., 2004). The quantity of biomolecules to be loaded in the matrix

could not be easily controlled as well as the preloading step of biomolecules in the matrix results in the low efficiency of biomolecules.

3. Diffusion based loading of biomolecules

By post-loading of biomolecules in the hollow LbL microcapsules under the concentration gradient of the biomolecules in the solution. The capsule wall could be "opened" by various parameters such as pH, temperature, solvent, ionic strength to allow in-flow of biomolecules and "closed" to retain the biomolecules within the capsules (Refer to literature review section 2.1.1.3 for more details). The diffusion based encapsulation of biomolecules results in low encapsulation efficiency, as the amount of material encapsulated within the capsules is dependent on the biomolecule concentration of the external solution.

All of the above LbL methods of depositing PEM using aqueous techniques suffer from relatively low encapsulation efficiency. Furthermore, the direct templating approach is inadequate to encapsulate water soluble biomolecules. Additionally, the aqueous LbL suffers from the limitation of encapsulating water-sensitive molecules such as sodium borohydride or rapidly hydrolysable biomolecules (Beyer et al., 2012b). In the case of diffusion based loading encapsulation approaches, harsh conditions are required to tune the permeability of walls for biomolecules which leads to loss of bioactivity and low integrity of biomolecules. (De Cock et al., 2010). The dependence of encapsulation yield on the isoelectric point for the proteins and difficulty in controlling the amount of substances adsorbed within the matrix template yearn for the technique which could circumvent the issues.

In order to overcome above limitations, Trau and co-workers have proposed the Reverse Phase Layer-by-Layer technique or RP-LbL technique (Beyer et al., 2007) which primarily utilises organic solvents as a deposition medium for polymers. The basis of interaction of polymers in the organic phase has been recently postulated by Brønsted acid base reaction (Beyer et al., 2012a), which is distinct from the electrostatic interactions or hydrogen bonded interactions observed in aqueous LbL techniques. The polymers were usually prepared in the polyamines or polyacids form dissolved in the aliphatic alcohols, which are relatively less toxic and biomolecular friendly compared to other solvent used such as dichloromethane, formamides and dimethyl sulfoxide. An initial encapsulation efficiency of 100% was achieved using RP-LbL technique due to insolubility of proteins in organic solvents (Beyer et al., 2007). The Trau group have already demonstrated the encapsulation of "highly water-soluble materials" which are difficult to encapsulate by traditional aqueous LbL techniques and have proposed the possible encapsulation of followings: proteins, saccharides, polysaccharides, nucleic acids, organic or inorganic salts, hydrophilic vitamins (Beyer et al., 2012b).

The RP-LbL technique offers the precise control on the concentration of material encapsulated within the capsules whereas multiphase microfluidics brings along the accurate control on the size of the microdroplets. The integration of RP-LbL technique within microfluidic devices can give unprecedented control on the amount of substance that can be encapsulated within the spherical capsules, which could be in particular important for water soluble materials. With this rationale in mind, RP-LbL based PEM deposition on water based droplets was initiated, which will be the last type of encapsulation material demonstrated in this thesis to fabricate micro-containers

using microdevices. This chapter discusses the selection of polymers and continuous phase for dissolving polymers for encapsulation of water based BSA droplets. The 1-undecanol was chosen as the continuous phase and PSS and PEI were chosen as the polyelectrolyte system. A novel generic design to deposit 2 layers of (PSS/PEI) on the aqueous based BSA droplets was proposed and prototyped in the PDMS. The preliminary experiments demonstrated the working of the device. The proof-of-concept experiments with polymers PSS and PEI were carried out to generate the droplets and to form 2 layered (PSS/PEI) microcapsules. The capsules were collected outside the microdevice and observed under bright field and fluorescence microscopy. The proposed system will be improved further by suggested future works.

5.2 Materials and Methods

5.2.1 Materials

Poly(sodium 4-styrene-sulphonate) (PSS) M_w 70 kDa and poly(ethyleneimine) (PEI) M_w 25 kDa, 1-undecanol 99% were purchased from Aldrich. Tween 20, Fluorescein isothiocyanate dextran (FITC), Bovine serum albumin (BSA), and fluoroctyltriethoxysilane (FOTES) were purchased from Sigma. Sodium Hydroxide (NaOH), Hydrochloric Acid (HCl), Span 80 and Tetramethyl rhodamine isothiocyanate (TRITC) were purchased from Fluka. Ethanol and 2-propanol were purchased from Fischer Scientific. Dimethyl sulfoxide (DMSO) was purchased from MP Biomedicals. Polystyrene microparticles with diameter of 20 µm were purchased from microParticles GmbH. SU-8 2035 and SU-8 developers were purchased from

MicroChem. Polydimethylsiloxane (PDMS) or SYLGARD® 184 Silicone Elastomer Kit was purchased from Dow Corning.

5.2.2 Mould Fabrication

The mould pattern was drawn using Cadence® Virtuoso® software and printed on a plastic photomask for photolithography. Standard one step photolithography was used to fabricate the mould with soft lithography techniques using SU-8 2035, a negative photoresist. SU-8 2035 was spin-coated on top of a 8 inch silicon wafer, baked and patterned using UV photolithography (Height = 100 μm). After the development, the mould was hard baked for 15 minutes at 200 °C and was treated with fluoroctyltriethoxysilane (FOTES) using chemical vapour deposition (CVD) to form a self assembled monolayer.

5.2.3 Soft Lithography

Polydimethylsiloxane (PDMS) was prepared by mixing the base and curing agent in a 10:1 ratio. The mixture was mixed thoroughly and degassed for 40 min to remove air bubbles. The mixture was poured on the SU-8 mould and cured inside an oven at 65 °C for two hours. Through-holes having 1.5 mm diameter were punched using Harris Biopsy Needles at the inlet and outlet ports of the microdevice. This patterned piece of PDMS was bonded to a flat piece of PDMS by exposing them in oxygen plasma for 30 seconds at 200 W. The device was kept overnight in an oven at 65 °C to improve the bond and to make the channels hydrophobic.

5.2.4 Preparation of Reagents

For preparing PSS-FITC, PSS in DI water and FITC in DMSO were mixed in the ratio of 50:1 ratio, conjugated by using ultraviolet light for 40 seconds and finally precipitating using iso-propanol. The final conjugated product of PSS-FITC was suspended in 1-undecanol at the concentration of 1 mg/ml. PEI and TRITC were suspended in DMSO in the weight ratio of 100:1, incubated for 30 minutes and finally dialysed against the DI water. The conjugated PEI-TRIC was suspended in 1-undecanol at the concentration of 1mg/ml. Polyelectrolyte solutions as well as wash solutions of 1-undecanol contain 0.5% (v/v) Span 80. The BSA was dissolved in the concentrations of 5 mg/ml, 50 mg/ml in 1X PBS.

5.2.5 Layer-by-Layer Deposition on Polystyrene Particles

The microparticles in water were first suspended in 1-undecanol. The microparticles were incubated in PSS-FITC in 1-undecanol for 15 minutes. This was followed by centrifugation at 3000 rpm for 5 minutes and re-suspension in 1-undecanol (3 times) to remove excessive polyelectrolyte. This was followed by depositing next polyelectrolyte PEI-TRITC on the microparticles. The fluorescence intensity of particles was captured by Olympus BX41 after each PEM deposition till $(PSS/PEI)_4$ achieved.

5.2.6 Experimental Setup for Microfluidic Experiments

The microfluidic device was mounted under on Olympus IX71 inverted microscope. Liquid reagents were loaded into three plastic syringes of various sizes (3, 5 ml) from Becton Dickinson and delivered through syringe pumps from KD Scientific. The

syringes were connected to the microdevice with suitable plastic tubings. High speed images were acquired using a Rolera-XR camera from Qimaging Corporation and saved using Image Pro Express software. Fluorescence images were captured with an Olympus BX61 microscope after obtaining capsules outside the microdevice. Software NIH-ImageJ was used for image processing.

5.3 Results and Discussion

5.3.1 Selection of Organic Phase and Polyelectrolytes

To achieve RP-LbL deposition in microfluidic devices, following criteria for polyelectrolytes and solvents needs to be satisfied.

1. The polyelectrolytes should be soluble in the solvent, preferably an aliphatic alcohol and should be able to interact with each other to form polymeric complexes. The ability of polyelectrolytes to form complexes with each other is the usual way of determining the extent of LbL deposition on the substrate material.

2. The solvent has to satisfy following three requirements:

(a) The solvent should be able to generate droplets, with the due consideration that it will be the continuous phase in the microfluidic device. It should have necessary viscosity to shear a discontinuous liquid stream at the T-junction in the microfluidic device. This can also be further facilitated using surfactants in the continuous phase.

(b) The solvent should be compatible with PDMS, which was envisioned as the material of the microdevice in this work. The solvent should not swell the PDMS microchannels or if it does so, should be within acceptable limits (Lee et al., 2003).

(c) The solvent should be immiscible with the water droplets which will be present as a discontinuous phase containing biomolecules.

To fulfil the above criteria, primarily aliphatic alcohols were considered, which are used generally for performing RP-LbL; whereas 1-butanol being the most commonly used alcohol (Beyer et al., 2007; Bai et al., 2009). Beyer et al. (Beyer et al., 2012a) have recently shown the possibility of dissolving polyelectrolytes polystyrenesulphonic acid (PSS) and polyallimine (PA) in 1-butanol, 1-pentanol, 1-hexanol, 1-heptanol and 1-octanol. However, these alcohols having lower number of carbon atoms (C4 to C8) are miscible with water in the descending order. Thus, aliphatic alcohol higher than 1-octanol (>C8) was intuitively chosen, which was 1-undecanol with eleven carbon atoms and with absolute immiscibility in water. Additionally, 1-undecanol has been used in microfluidic devices in the literature as a continuous phase previously (Zhang et al., 2007; Zhang et al., 2006), and is well known to be suitable along with the biological cells (Tumarkin et al., 2009).

However, the hydrophobic nature of 1-undecanol makes a very few polyelectrolytes to be miscible in 1-undecanol. Various polyelectrolytes like polyallimine (PA), Polyacrylic acid (PAA), polystyrenesulphonic acid (PSS), polyvinylpyrrolidone (PVPON), Poly (ethyleneimine) (PEI) were tested for solubility. The polyelectrolytes PA, PVPON and PAA were found not to be soluble in 1-undecanol. The polyelectrolytes PSS (negative polyelectrolyte) and PEI (positive polyelectrolyte) were found to be soluble in 1-undecanol and were selected for further investigations (figure 5.1 (a) and (b)). The ability of these polyelectrolytes to form polyelectrolyte complex was observed by mixing the polyelectrolyte solutions (1 mg/ml in concentration) in 1-

undecanol in the volume ratio of 1:1. The PSS and PEI formed instant complex which was observed on a glass slide under the microscope in the form of a precipitate. (Figure 5.1 (c) and (d))

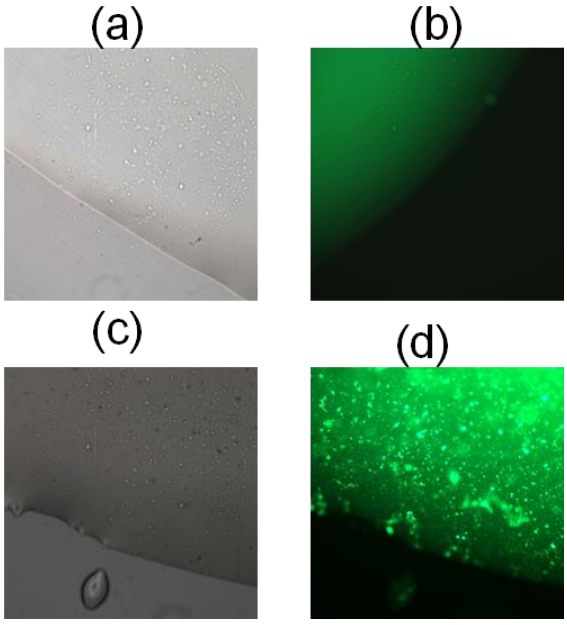

Figure 5.1. The polymer solutions of PEI (a) and PSS-FITC (b) were prepared in 1-undecanol in the concentration of 1 mg/ml and were mixed in the ratio of 1:1. The precipitation of insoluble polyelectrolyte complex could be observed in bright field (c) and fluorescent (d) images.

Bovine serum albumin (BSA) is one of the most commonly used protein model systems and was chosen for further experiments for observing the formation of droplets in PSS-FITC. BSA dissolved in water was emulsified by shaking the microtube without any surfactant, and by exploiting the amphiphilic nature of BSA molecules. The fluorescence observed on the droplet surface indicated the formation of PSS coating on the BSA droplets as can be observed in the figure 5.2(a). The PSS coated BSA droplets were found to be relatively stable, though found to be coalescing under the vigorous mechanical movement in the microtube. The addition of surfactant plays an important role, as in excessive amounts it could shield the PSS molecules to interact with BSA molecules. The addition of non-ionic surfactant Tween 20 to the

aqueous phase at 0.25% (v/v) did not affect the deposition of PSS on the droplet surface (figure 5.2 (b)), however higher concentrations of Tween 20 (0.5% and 1%) were found to create droplets without any PSS deposition.

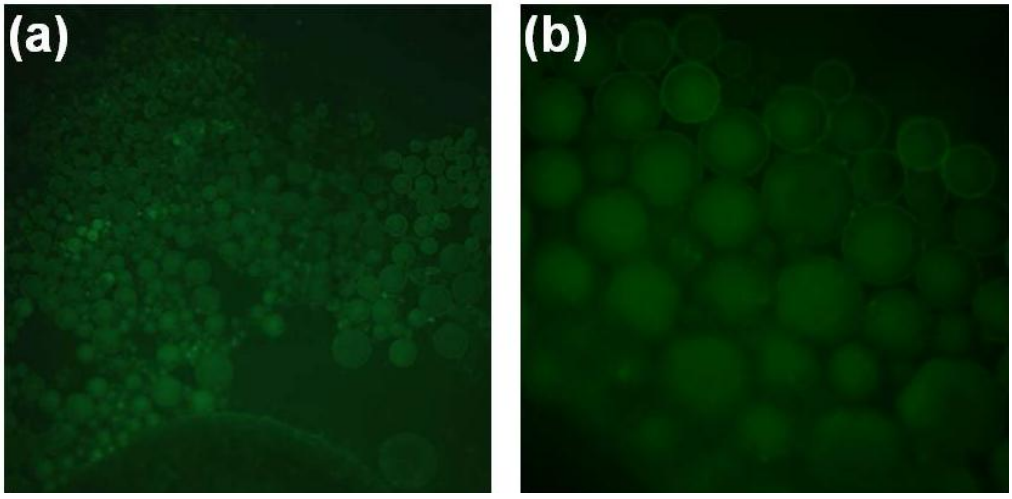

Figure 5.2. The deposition of PSS-FITC on the surface of BSA droplets could be observed without (a) and with surfactant Tween 20 (b).

It was difficult to carry out the further deposition of PEI on PSS-FITC coated BSA droplets in the conventional RP-LbL microtube technique due to their instability and coalescence. At last, to confirm that sequential Layer-by-Layer deposition of PSS and PEI in 1-undecanol, polystyrene microparticles were chosen. The final set of preliminary experiments was carried out by RP-LbL deposition on polystyrene particles (≅ 20 µm) in 1-undecanol wherein 4 alternate layers of each PSS-FITC and PEI-TRITC were coated. A linear increase in the fluorescence intensity was observed, as a new layer of polyelectrolyte was added on the microparticle surface. The increase in the fluorescence intensity after addition of each layer of PSS-FITC can be observed in figure 5.3. The decrease in the levels of fluorescence intensity after adding even numbered layer of PEI-TRITC could be contributed to the shielding of the fluorescence emitted by PSS-FITC. The similar decrease have also been reported by previous groups (Sukhurokov et al., 1998) for aqueous LbL on polystyrene particles

for a polymer pair of PAH and PSS. The decrease in the fluorescence intensities after adding PEI-TRITC also indicates the deposition of PEI layer on the particle surface.

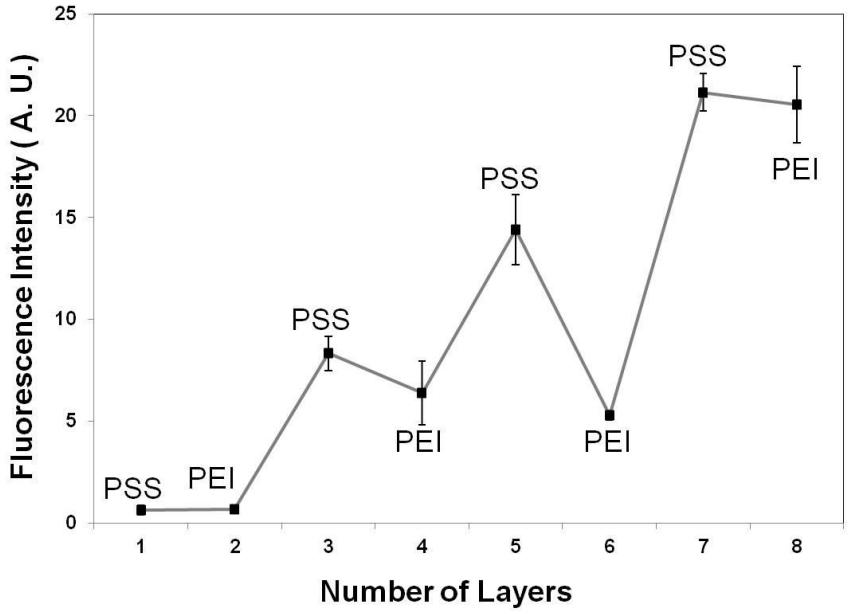

Figure 5.3. The RP-LbL deposition of PSS and PEI on the polystyrene microparticles for 4 layers each in 1-undecanol. The linear increase in the fluorescence intensity confirms the deposition of 8 layers.

5.3.2 Device Design and Fabrication for RP-LbL Deposition

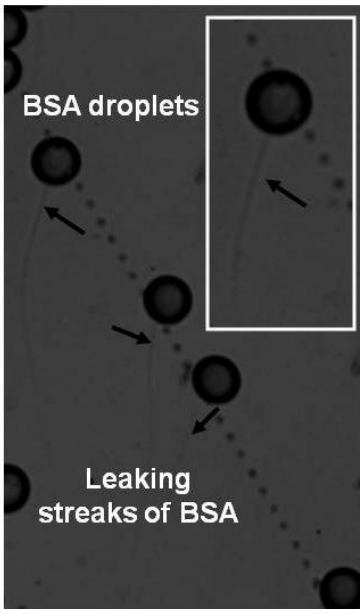

Figure 5.4. Experiments to roll the BSA microdroplets along the micropillars in PSS-FITC dissolved in 1-undecanol stream did not exhibit rolling of droplets. Arrows are showing the leaking streaks of BSA from the ruptured microdroplets.

To perform Layer-by-Layer deposition of polyelectrolytes on the BSA microdroplets in microdevice, previously described "Pinball microfluidic" chips with micro-pillars were used (Chapter 4 of this thesis). The surface of PDMS was kept hydrophobic by overnight heat treatment to improve the wettability with 1-undecanol.The BSA droplets generated at the T-junction were not able to roll along the micropillars, and instead were trapped in between the micropillars. This led to the damage of the capsule wall and leaking of BSA from the capsules as can be seen in figure 5.4 by the streaks of BSA. Debris from such empty capsules further blocked the flow in the microchannel, and paralysed the operation of the device. This could be attributed to the basic difference in the nature of oil microdroplets and aqueous phase BSA microdroplets. The aqueous microdroplets of BSA exhibit rigidity in contrast to the oil droplets which tend to be more conformable to the micropillar structures. In order to circumvent the above problems, a novel microfluidic design was realised which will be explained further.

Scheme 5.1 represents a schematic overview of the proposed device. The device has three prominent features:

(1) A t-junction for on-chip generation of microdroplets of BSA by sheering the stream by continuous phase of PSS-FITC dissolved in 1-undecanol.

(2) Placed in parallel manner, three microchannels for the transport and incubation of BSA microdroplets in the polyelectrolyte. Each channel has a width of 100 µm and approximate length of 8 cm for deposition of 2 layers of polyelectrolytes.

(3) Microstructures at the conjunction of two adjacent microchannels for offering high fluidic resistance to the capsules (Scheme 5.1 B) and deflecting them into adjacent

liquid stream in the next microchannel. For depositing 2 layers of (PSS/PEI), such structures were present for three times.

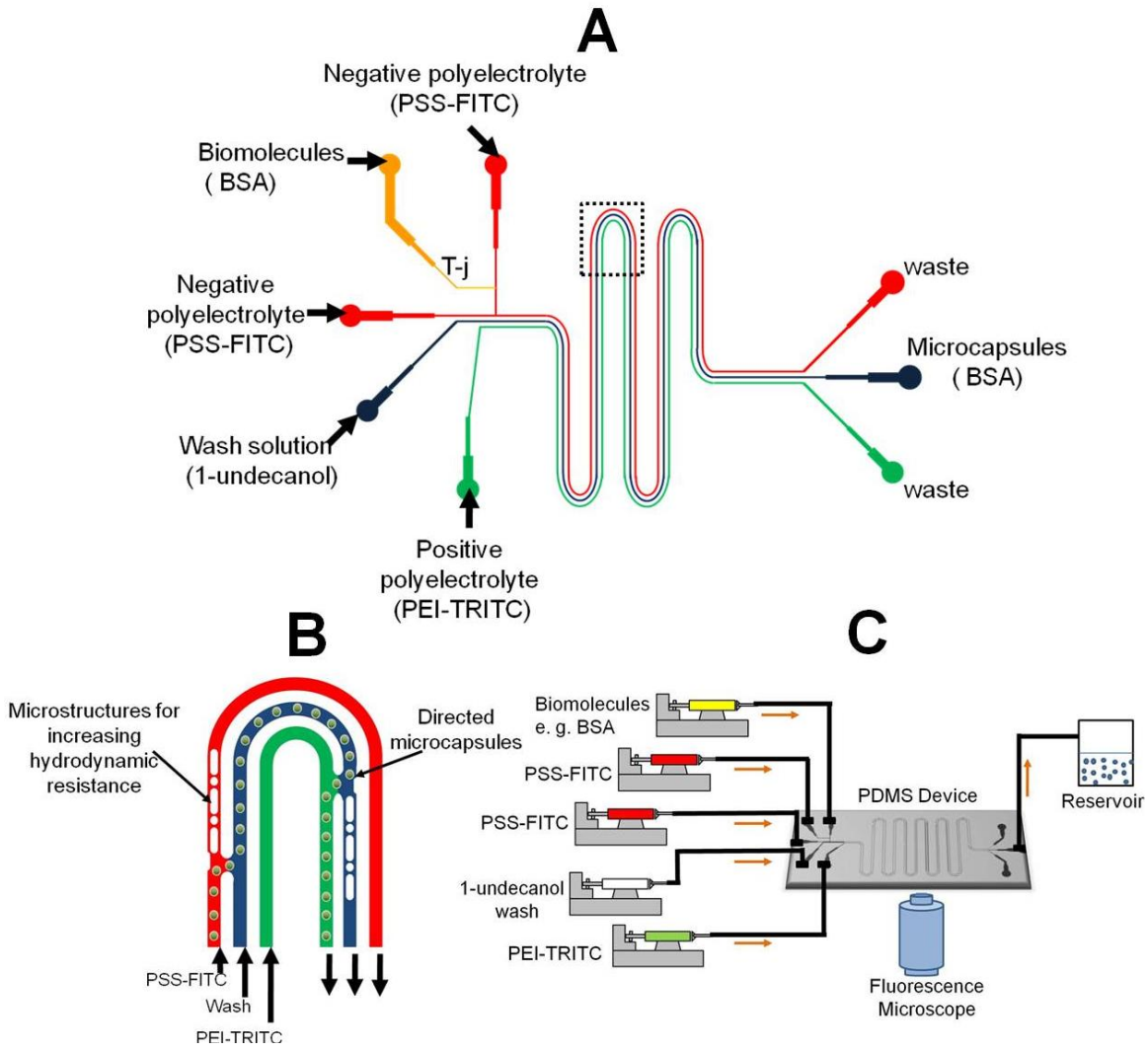

Scheme 5.1. (A) The schematic of the device consisting of a T-junction (T-j) for producing discrete droplets and connected to three parallel microchannels which are arranged in a serpentine manner. (B) Showing zoomed-in schematic view of the device with capsules being assisted to divert into adjacent channel due to less hydrodynamic resistance. (C) Depicting the experimental setup for generating Layer-by-Layer polyelectrolyte capsules encapsulating biomolecules using RP-LbL method.

The device was interfaced with five syringe pumps and was mounted on the microscope for continuous observation. The total number of PE layers deposited on the droplet surface is decided by the design of the microdevice, and does not depend on

the syringe pumps. This will greatly help in reducing the interfacial complexity (e.g. number of syringe pumps etc) for depositing higher number of layers, which is similar as in case of the "Pinball microfluidic" technique explained in the previous chapter 4. Additionally the new design offers another advantage over the "Pinball microfluidic" design. The width of the microchannel was reduced from 3 mm to 300 µm, by a factor of 10. This is expected to save the reagents considerably, such as polyelectrolyte solutions dissolved in 1-undecanol.

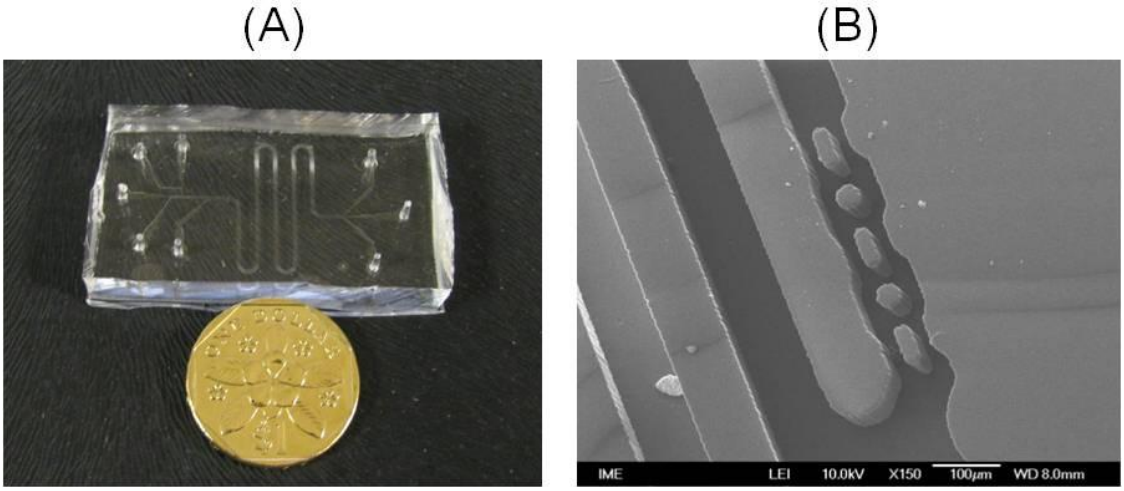

Figure 5.5. (A) Microfluidic device fabricated in PDMS for deposition of 2 LbL layers. (B) Showing the scanning electron microscopy image of PDMS device with the microstructures for diverting capsules into adjacent stream (Scale bar = 100 µm).

The microfluidic device for depositing 2 LbL layers was prototyped in PDMS which can be seen in the Figure 5.5 (A). Scanning electron microscopy (SEM) imaging was performed to observe the microstructures creating high resistance to flow as can be seen in figure 5.5 (B). The two micropillars with the diameter of 45 µm and three rectangular shaped smooth edged micropillars with the width 30 µm can be seen in the microchannel. The choice of these structures was intuitive and was inspired from Zimmermann et al. (Zimmermann et al., 2006) where the authors used the microstructures of different shapes to pump liquid by capillary action.

5.3.3 Working of the Microfluidic Device

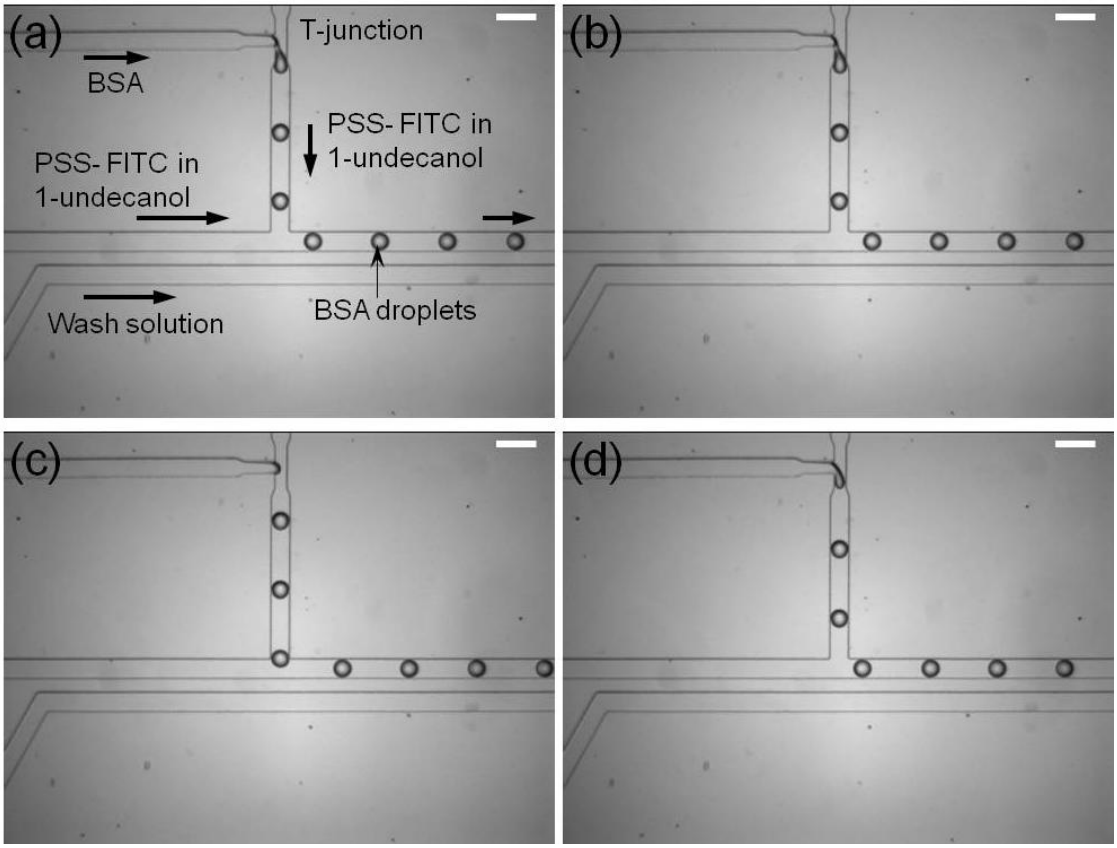

Figure 5.6. Frames (a)-(b) showing generation of microdroplets at the T-junction. The PSS-FITC in 1-undecanol (continuous phase) sheering the BSA (discontinuous stream) stream into microdroplets which were directed in the stream of PSS-FITC (Scale bar = 200 µm).

The microdevice was injected with PSS-FITC in 1-undecanol, wash solution consisting of 1-undecanol and PEI-TRITC in 1-undecanol at the flow rates of 0.01 ml/hr, 0.07 ml/hr and 0.06 ml/hr respectively, which were empirically determined by varying flow rates until the stability of flows was achieved. The droplets were generated at the T-junction at the flow rates of 0.015 ml/hr for discontinuous phase and 0.06 ml/hr for continuous phase (Figure 5.6). The 1-undecanol solution had 0.5 % (v/v) of Span 80, which does not allow the non-specific adsorption of the BSA molecules on the microchannel walls. After crossing the T-junction, the droplets travelled downstream in the stream of PSS-FITC in the microchannel. The total

residence time of droplets in the PSS-FITC was noted to be approximately 20-22 seconds. The PSS-FITC coated BSA microcapsules changed their direction at the point of high resistance deflection structures; (Figure 5.7) and were transferred into the washing stream. The interaction of capsules with wash solution (1-undecanol) helps to remove the unabsorbed PSS-FITC from the surface of the BSA microcapsule. The microstructures did not damage the capsule wall and demonstrated the successful manipulation of droplets into the adjacent stream.

Subsequently after the washing step in 1-undecanol, capsules moved to PEI-TRITC stream with the help from high resistance microstructures where the deposition of the second layer was achieved. Finally, the capsules were diverted into the washing solution and were successfully collected outside the microdevice. The total residence time for the capsules within the microdevice is noted to be about 90 seconds.

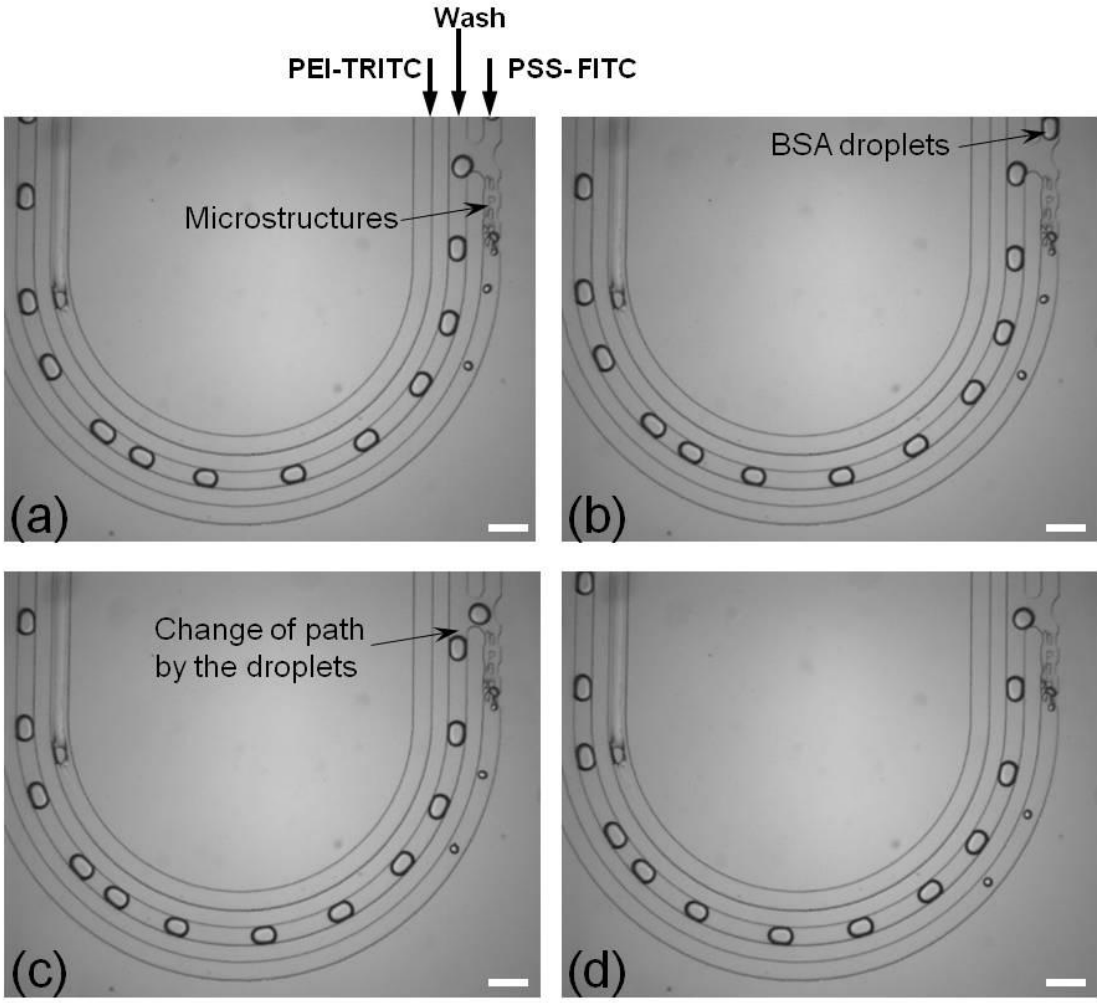

Figure 5.7. (a)-(b) shows four sequential frames of droplet manipulation by the microstructures placed in the microchannel for PSS-FITC to deflect the capsules into adjacent washing stream (Scale bar = 200 µm).

The movement of the droplets/capsule from one stream to the adjacent stream depends on the hydrodynamic resistance experienced by it within the microchannel at that instance. Squeezing of the droplets through microstructures has also been observed in some instances, especially for smaller droplets. It also needs to be reported here that device becomes unstable at higher droplet generation frequencies. This is probably due to the excessive presence of microdroplets within the microchannel which increase the resistance to subsequent droplets. Also, in few of the cases overflowing of the PSS-FITC stream into the washing stream was observed, which is undesirable. All of the

abovementioned issues need to be resolved for achieving higher number of PEM in the future. A hydrodynamic resistance based design approach can be taken while designing future generation of the devices.

5.3.4 Observation of Layer-by-Layer (PSS/PEI) Coated BSA Capsules

The concentration 50 mg/ml of BSA was used for making 2-layered capsules.

The capsules were collected on the glass slide and observed under the microscope. The collected capsules can be observed in the Figure 5.8 which were found to be non-coalescing and stable. The diameter of the capsules was found to be ~95 μm. The bright field and fluorescence images of the capsules show smooth surface of the capsules encapsulating BSA satisfactorily.

By considering the diameter of 95 μm for each capsule, the amount of BSA encapsulated within each capsule can be calculated to be 13.92 pg. Thus, by RP-LbL technique of direct encapsulation of substances using a microfluidic technique of accurate control on size of the capsule the total amount of substance encapsulated within each capsule could be precisely controlled. This technique could also be extended to other protein molecules for protein delivery.

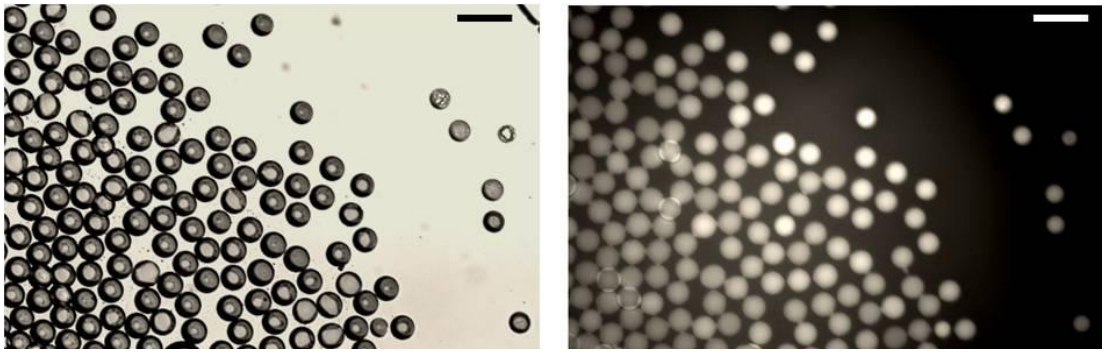

Figure 5.8. Bright field and fluorescence images of the (PSS/PEI) capsules observed under the microscope at 4X (Scale bar = 200 μm).

The same capsules on the glass slide showed wrinkles on their surface (Figure 5.9) after 2 hours which was observed to increase with the time. These wrinkles on the capsule surface could be possibly attributed to the mechanical instability of the capsular wall induced due to gradual evaporation of water inside the capsule.

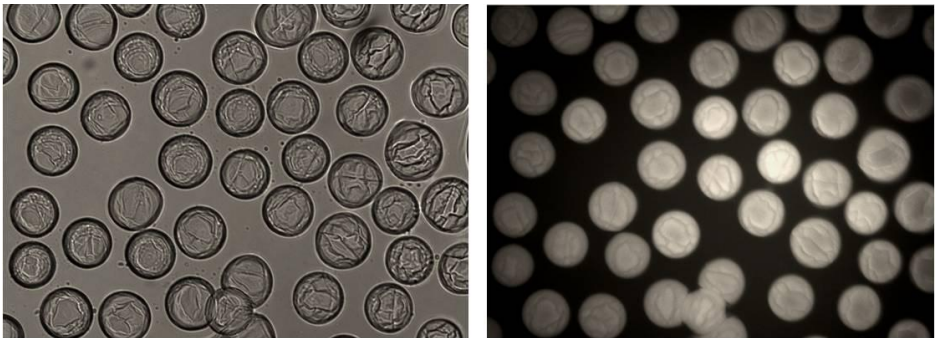

Figure 5.9. The microcapsules observed at 20X under the microscope after 2 hours. The wrinkled nature of capsules could be observed.

The bovine serum albumin is a typically amphiphilic molecule having hydrophilic and hydrophobic domains with fatty acids binding sites. The assembly of BSA molecules occurs during the emulsification in the device within hydrophobic 1-undecanol phase. These hydrophobic domains of BSA should be interacting with PSS to form polyelectrolyte complex. The deposition of PEI on the PSS molecules should be occurring as per standard RP-LbL principles.

The 2-layered capsules fabricated by RP-LbL technique have been reported by Beyer et al. (Beyer et al., 2012) to have thickness of 9.8 nm. The possible reason for the wrinkles on the surface of the capsules could be the fact that the size of the microcapsules varies in the ranges of tens of micrometer, in comparison with its thickness which is about a ten of nanometres, thus resulting in the development of

structural instability in the capsules. Nonetheless, it gives the visual representation of layer-by-layer membrane of the RP-LbL microcapsules.

5.4 Conclusion

This chapter demonstrated a microfluidic encapsulation approach to directly encapsulate template of water droplets containing biomolecules using Reverse Phase Layer-by-Layer (RP-LbL) technique. The polymers and a continuous phase for dissolving polymers were chosen to be PSS/PEI and 1-undecanol respectively. A novel generic design based on the high resistance microstructures was proposed to deposit 2 layers of (PSS/PEI) on the aqueous based BSA droplets. The device was prototyped in the PDMS by simple soft lithography. The preliminary experiments demonstrated the working of the device. The proof-of-concept experiments were conducted for depositing polymers PSS and PEI on the droplet surface to form 2 layered (PSS/PEI) microcapsules. The total duration for deposition of capsules was found to be 90 seconds approximately. The capsules were collected outside the microdevice and observed under bright field and fluorescence microscopy. The fluorescence from the capsule surface confirmed the deposition of polymer layers. The devices for depositing 4, 6 and 8 layers of polyelectrolytes will be explored in the future work. This work is the first demonstration of depositing LbL layers on the water droplets.

Chapter 6 - Conclusion and Future Works

Chapter 6

Conclusion and Future Works

6.1 Conclusion

In this thesis, multiphase microfluidic techniques for encapsulation of different template materials were presented for fabrication of polymeric micro-containers. The microfluidic techniques demonstrated in the previous three chapters were able to encapsulate the microdroplets of different carrier liquids such as hydrogel (polyethylene glycol), organic phase (mineral oil), and aqueous phase (water) for fabrication of micro-containers. In all three chapters, the droplets were generated at the T-junction and were manipulated/ handled downstream according to the type of micro-container. For droplet manipulation, only passive techniques were employed which rely on hydrodynamic forces, and not active techniques. In the first work, after generating microdroplets at the T-junction, they were crosslinked by ultraviolet light to form hydrogel microbeads. In the subsequent work, the complexity of droplet manipulation was augmented because multilayered structure of LbL microcapsules. The encapsulation of droplets of organic phase as a carrier liquid was achieved in this chapter by generating droplets at the T-junction; followed by guiding them through laminar streams in a single microchannel by rows of micropillars termed ‘microfluidic pinball’. In the final work, the microdroplets were generated at the T-junction, and were transferred through laminar flow in three parallel channels (instead of one as in the previous case) by high- resistance microstructures so as to encapsulate aqueous droplets.

Firstly, a microfluidic encapsulation technique for fabrication of polymeric micro-containers prepared from the hydrogel material was presented. A microfluidic device was fabricated in PDMS, and shown to be capable of producing highly monodisperse and structurally stable glucose sensing microbeads. The PEG hydrogel microbeads encapsulated physically entrapped FITC-dextran and TRITC-ConA biomacromolecules which work on the principle of Förster Resonance Energy Transfer (FRET). The sensing microbeads had an average size of 72 µm and successfully showed linearly proportional increase in the fluorescence intensity against the glucose concentration within physiological glucose range (1-10 mM).

Secondly, microfluidic encapsulation technique for fabrication of polymeric micro-containers with the organic phase template coated with six layers of LbL polymers was demonstrated. The novel approach which utilizes rows of micropillars arranged in a zigzag fashion to guide oil microdroplets through laminar streams of polymer and washing solution was termed 'microfluidic pinball'. Using this approach, LbL polyelectrolyte microcapsules of average size 45 µm were generated. The deposition of 3 bi-layers of polyelectrolytes PAA/PVPON was achieved in less than 3 minutes which was further confirmed by fluorescence microscopy and thickness of each PE layer was determined to be ~2.8 nm by AFM imaging.

Lastly, a microfluidic encapsulation approach to directly encapsulate template of water droplets containing biomolecules was presented based on Reverse Phase Layer-by-Layer (RP-LbL) principles. The continuous phase for dissolving polymers was selected to be 1-undecanol and polymers were chosen to be PSS and PEI. A novel generic design based on the high resistance microstructures was proposed and

prototyped in PDMS by simple soft lithography. The proof-of-concept experiments demonstrated deposition of PSS/PEI on the aqueous based BSA droplets. The total duration of deposition of polymers was found to be 90 seconds approximately. The capsules were successfully collected outside the microdevice and observed under bright field and fluorescence microscopy.

The proposed microfluidic encapsulation techniques were novel. In the third chapter, microfluidic encapsulation of a glucose assay based on Förster resonance energy transfer was demonstrated for the first time in the literature. In the forth chapter, the Layer-by-Layer deposition of six layers of polymers was demonstrated for the first time in the microfluidic devices. To the best of our knowledge, direct Layer-by-Layer polymer deposition on water droplets is the first demonstration in the microfluidic as well as in the conventional systems.

6.2 Future Works

The following future works could be carried out in continuation of the encapsulation techniques demonstrated in chapter 3, 4 and 5 respectively.

6.2.1 Encapsulation of Hydrogel Beads

- The hydrogel based microbeads proposed in the chapter 3 of this thesis can be used to create glucose map in the cellular microenvironments. With the slight modification of composition of the encapsulated material, these PEG-DA beads can be used to sense pH of the cellular microenvironment. The molecules of FITC exhibit the fluorescence based on the pH of the solution. The FITC

molecules acquire cationic, anionic or neutral form based on the pH of the surrounding solution. This results in the different intensity levels of FITC molecules than in its neutral form. This phenomenon can be used to sense the pH within the surroundings of FITC molecule. The similar properties of pH detection are retained by FITC even after conjugation with a macromolecule such as Dextran. Dextran-FITC can alone be encapsulated within the PEG beads to obtain pH sensing beads. These beads can be used along with the glucose sensing beads in the applications of studying micro-environment. The microbeads could be used in cell culture systems to sense the localized glucose concentration in the cell environment.

- The surface modification of these beads could enhance their functionality and thus requires a definitive focus in the future. The current size of the glucose sensing beads can be further reduced (approximately 20-30 μm) and can be post-processed with LbL technique to deposit LbL layers on the surface of the microbead. This will help in screening out the non-specific response from proteins (albumins, enzymes etc.) present in the cell culture media. Other surface modifications using biocompatible polymers such as chitosan can be explored in the near future works.
- The material PEG-DA has been known for its biocompatibility. Such PEG-DA glucose sensing beads can be hypodermally implanted into the body to study in-vivo glucose sensing ability of the PEG-DA beads.

6.2.2 Encapsulation of Oil Microdroplets

- The technique of pinball microfluidics for generating LbL capsules can be extended in future works to fabricate different types of LbL polymeric

capsules. The 'microfluidic pinball' technique had a focus on LbL deposition based on hydrogen bonding between the two polyelectrolytes, PAA and PVPON, in chapter 4. It can be extended towards achieving LbL deposition of electrostatic based polyelectrolytes such as the widely studied PSS/PAH system. In this case polyelectrolytes (PSS/PAH) can be dissolved in the washing solution of sodium chloride. Three solutions of PSS, washing solution and PAH can be injected into the chip to generate $(PSS/PAH)_3$ microcapsules.

- The proposed microfluidic method can be used as a platform to create oil core capules required for drug delivery. The droplets of mineral oil used as the core of PE microcapsule can either be replaced with suitable type of oil, for example canola oil, or can be even loaded with lipophilic substances. The pharmaceutical drugs are usually lipophilic in nature and can be encapsulated using the proposed technique. The encapsulation of lipophilic molecules such as cancer drugs like paclitaxel (He et al., 2011) or Vitamin A within oil microdroplets coated with PEM could generate great interest for fabricating drug loaded microcapsules.
- The droplet guiding technique proposed in the chapter 4 could be used for the applications in droplet microfluidics other than that of LbL microcapsules. By using micropillars oriented in a specific manner, generated droplets can be routed, sorted, filtered and incubated passively in microfluidic environment. The filtering and sorting of droplets can be modulated by varying the distance/gap between the micropillars in order to generate a threshold limit to filter out the droplets with undesirable size e. g. satellite droplets. Droplets can also be confined within the circular traps of micropillars for incubation. All of

the above techniques of droplet routing, sorting and incubation are useful for microfluidic cell encapsulation; which can be explored in the future works.

6.2.3 Encapsulation of Water Microdroplets

- The current device can deposit only two layers of (PSS/PEI). The devices for depositing 4 and 6 layers of polyelectrolytes on the water droplets can be explored in the future works.
- The hydrodynamic resistance structures proposed in the chapter 5 could be used in the applications where droplet routing or cell/beads routing required.

References

References

Abbott, N. L.; Sivakumar, S.; Gupta, J. K.; Caruso, F., Monodisperse emulsions through templating polyelectrolyte multilayer capsules. *Chemistry of Materials* **2008,** 20, (6), 2063-2065.

Abou-Hassan, A.; Sandre, O.; Cabuil, V., Microfluidics in inorganic chemistry. *Angewandte Chemie - International Edition* **2010,** 49, (36), 6268-6286.

Ahmed, R.; Jones, T. B., Dispensing picoliter droplets on substrates using dielectrophoresis. *Journal of Electrostatics* **2006,** 64, (7-9), 543-549.

Ahn, K.; Agresti, J.; Chong, H.; Marquez, M.; Weitz, D. A., Electrocoalescence of drops synchronized by size-dependent flow in microfluidic channels. *Applied Physics Letters* **2006,** 88, (26).

Allison, A. C.; Gregoriadis, G., Liposomes as immunological adjuvants. *Nature* **1974,** 252, (5480), 252.

An, S. Y.; Bui, M. P. N.; Nam, Y. J.; Han, K. N.; Li, C. A.; Choo, J.; Lee, E. K.; Katoh, S.; Kumada, Y.; Seong, G. H., Preparation of monodisperse and size-controlled poly(ethylene glycol) hydrogel nanoparticles using liposome templates. *Journal of Colloid and Interface Science* **2009,** 331, (1), 98-103.

Anna, S. L.; Bontoux, N.; Stone, H. A., Formation of dispersions using "flow focusing" in microchannels. *Applied Physics Letters* **2003,** 82, (3), 364-366.

Ballerstadt, R.; Schultz, J. S., Competitive-binding assay method based on fluorescence quenching of ligands held in close proximity by a multivalent receptor. *Analytica Chimica Acta* **1997,** 345, (1-3), 203-212.

Bangham, A. D.; Hill, M. W.; Miller, N. G. A., *Methods in Membrane Biology* **1974**, 1-68.

Banville, C.; Vuillemard, J. C.; Lacroix, C., Comparison of different methods for fortifying Cheddar cheese with vitamin D. *International Dairy Journal* **2000,** 10, (5-6), 375-382.

Barnadas-Rodríguez, R.; Sabés, M., Factors involved in the production of liposomes with a high-pressure homogenizer. *International Journal of Pharmaceutics* **2001,** 213, (1-2), 175-186.

Baruch, L.; Machluf, M., Alginate-chitosan complex coacervation for cell encapsulation: Effect on mechanical properties and on long-term viability. *Biopolymers* **2006,** 82, (6), 570-579.

Becker, H.; Gärtner, C., Polymer microfabrication technologies for microfluidic systems. *Analytical and Bioanalytical Chemistry* **2008,** 390, (1), 89-111.

Becker, H.; Locascio, L. E., Polymer microfluidic devices. *Talanta* **2002,** 56, (2), 267-287.

Bellamkonda, R.; Ranieri, J. P.; Bouche, N.; Aebischer, P., Hydrogel-based three-dimensional matrix for neural cells. *Journal of Biomedical Materials Research* **1995,** 29, (5), 663-671.

Berger, J.; Reist, M.; Mayer, J. M.; Felt, O.; Gurny, R., Structure and interactions in chitosan hydrogels formed by complexation or aggregation for biomedical applications. *European Journal of Pharmaceutics and Biopharmaceutics* **2004,** 57, (1), 35-52.

Beyer, S.; Bai, J.; Blocki, A. M.; Kantak, C.; Xue, Q.; Raghunath, M.; Trau, D., Assembly of biomacromolecule loaded polyelectrolyte multilayer capsules by using water soluble sacrificial templates. *Soft Matter* **2012**a, 8, (9), 2760-2768.

Beyer, S.; Bai, J.; Trau, D., Assembly of Polymer Multilayers from Organic Solvents for Biomolecule Encapsulation. In Decher, G.; Schlenoff, J., Eds. Wiley Publishers: **2012**b.

Beyer, S.; Mak, W. C.; Trau, D., Reverse-phase LbL-encapsulation of highly water soluble materials by layer-by-layer polyelectrolyte self-assembly. *Langmuir* **2007,** 23, (17), 8827-8832.

Bringer, M. R.; Gerdts, C. J.; Song, H.; Tice, J. D.; Ismagilov, R. F., Microfluidic systems for chemical kinetics that rely on chaotic mixing in droplets. *Philosophical Transactions of the Royal Society A: Mathematical, Physical and Engineering Sciences* **2004,** 362, (1818), 1087-1104.

Caruso, F.; Trau, D.; Möhwald, H.; Renneberg, R., Enzyme encapsulation in layer-by-layer engineered polymer multilayer capsules. *Langmuir* **2000,** 16, (4), 1485-1488.

Chaize, B.; Colletier, J. P.; Winterhalter, M.; Fournier, D., Encapsulation of Enzymes in Liposomes: High Encapsulation Efficiency and Control of Substrate Permeability. *Artificial Cells, Blood Substitutes, and Immobilization Biotechnology* **2004,** 32, (1), 67-75.

Chan, E. M.; Alivisatos, A. P.; Mathies, R. A., High-temperature microfluidic synthesis of CdSe nanocrystals in nanoliter droplets. *Journal of the American Chemical Society* **2005,** 127, (40), 13854-13861.

Chang, T. M. S., Semipermeable microcapsules. *Science* **1964,** 146, (3643), 524-525.

Cho, N. J.; Elazar, M.; Xiong, A.; Lee, W.; Chiao, E.; Baker, J.; Frank, C. W.; Glenn, J. S., Viral infection of human progenitor and liver-derived cells encapsulated in three-dimensional PEG-based hydrogel. *Biomedical Materials* **2009,** 4, (1).

Cho, S. K.; Moon, H.; Kim, C. J., Creating, transporting, cutting, and merging liquid droplets by electrowetting-based actuation for digital microfluidic circuits. *Journal of Microelectromechanical Systems* **2003,** 12, (1), 70-80.

Cho, S. K.; Zhao, Y.; Kim, C. J., Concentration and binary separation of micro particles for droplet-based digital microfluidics. *Lab on a Chip - Miniaturisation for Chemistry and Biology* **2007,** 7, (4), 490-498.

Choi, C. H.; Jung, J. H.; Hwang, T. S.; Leezz, C. S., In situ microfluidic synthesis of monodisperse PEG microspheres. *Macromolecular Research* **2009,** 17, (3), 163-167.

Choi, C. H.; Jung, J. H.; Rhee, Y. W.; Kim, D. P.; Shim, S. E.; Lee, C. S., Generation of monodisperse alginate microbeads and in situ encapsulation of cell in microfluidic device. *Biomedical Microdevices* **2007,** 9, (6), 855-862.

Choi, D.; Jang, E.; Park, J.; Koh, W. G., Development of microfluidic devices incorporating non-spherical hydrogel microparticles for protein-based bioassay. *Microfluidics and Nanofluidics* **2008,** 5, (5), 703-710.

Christopher, G. F.; Anna, S. L., Microfluidic methods for generating continuous droplet streams. *Journal of Physics D: Applied Physics* **2007,** 40, (19), R319-R336.

Chung, B. G.; Lee, K. H.; Khademhosseini, A.; Lee, S. H., Microfluidic fabrication of microengineered hydrogels and their application in tissue engineering. *Lab on a Chip - Miniaturisation for Chemistry and Biology* **2012,** 12, (1), 45-59.

Crespo-Biel, O.; Dordi, B.; Reinhoudt, D. N.; Huskens, J., Supramolecular layer-by-layer assembly: Alternating adsorptions of guest- and host-functionalized molecules and particles using multivalent supramolecular interactions. *Journal of the American Chemical Society* **2005,** 127, (20), 7594-7600.

De Cock, L. J.; De Koker, S.; De Geest, B. G.; Grooten, J.; Vervaet, C.; Remon, J. P.; Sukhorukov, G. B.; Antipina, M. N., Polymeric Multilayer Capsules in Drug Delivery. *Angewandte Chemie - International Edition* **2010**, 49, (39), 6954-6973.

De Geest, B. G.; Sukhorukov, G. B.; Möhwald, H., The pros and cons of polyelectrolyte capsules in drug delivery. *Expert Opinion on Drug Delivery* **2009,** 6, (6), 613-624.

De Geest, B. G.; Van Camp, W.; Du Prez, F. E.; De Smedt, S. C.; Demeester, J.; Hennink, W. E., Degradable multilayer films and hollow capsules via a 'click' strategy. *Macromolecular Rapid Communications* **2008,** 29, (12-13), 1111-1118.

De Koker, S.; De Cock, L. J.; Rivera-Gil, P.; Parak, W. J.; Auzly Velty, R.; Vervaet, C.; Remon, J. P.; Grooten, J.; De Geest, B. G., Polymeric multilayer capsules delivering biotherapeutics. *Advanced Drug Delivery Reviews* **2011,** 63, (9), 748-761.

Decher, G., Fuzzy nanoassemblies: Toward layered polymeric multicomposites. *Science* **1997,** 277, (5330), 1232-1237.

Decher, G.; Hong, J. D.; Schmitt, J., Buildup of ultrathin multilayer films by a self-assembly process: III. Consecutively alternating adsorption of anionic and cationic polyelectrolytes on charged surfaces. *Thin Solid Films* **1992,** 210-211, (PART 2), 831-835.

DeMello, A. J., Control and detection of chemical reactions in microfluidic systems. *Nature* **2006,** 442, (7101), 394-402.

Dendukuri, D.; Gu, S. S.; Pregibon, D. C.; Hatton, T. A.; Doyle, P. S., Stop-flow lithography in a microfluidic device. *Lab on a Chip - Miniaturisation for Chemistry and Biology* **2007,** 7, (7), 818-828.

Dendukuri, D.; Pregibon, D. C.; Collins, J.; Hatton, T. A.; Doyle, P. S., Continuous-flow lithography for high-throughput microparticle synthesis. *Nature Materials* **2006,** 5, (5), 365-369.

Diaspro, A.; Silvano, D.; Krol, S.; Cavalleri, O.; Gliozzi, A., Single living cell encapsulation in nano-organized polyelectrolyte shells. *Langmuir* **2002,** 18, (13), 5047-5050.

Dong, W. F.; Liu, S.; Wan, L.; Mao, G.; Kurth, D. G.; Möhwald, H., Controlled permeability in polyelectrolyte films via solvent treatment. *Chemistry of Materials* **2005,** 17, (20), 4992-4999.

Drury, J. L.; Mooney, D. J., Hydrogels for tissue engineering: Scaffold design variables and applications. *Biomaterials* **2003,** 24, (24), 4337-4351.

Duffy, D. C.; McDonald, J. C.; Schueller, O. J. A.; Whitesides, G. M., Rapid prototyping of microfluidic systems in poly(dimethylsiloxane). *Analytical Chemistry* **1998,** 70, (23), 4974-4984.

Edd, J. F.; Di Carlo, D.; Humphry, K. J.; Köster, S.; Irimia, D.; Weitz, D. A.; Toner, M., Controlled encapsulation of single-cells into monodisperse picolitre drops. *Lab on a Chip - Miniaturisation for Chemistry and Biology* **2008,** 8, (8), 1262-1264.

El-Ali, J.; Sorger, P. K.; Jensen, K. F., Cells on chips. *Nature* **2006,** 442, (7101), 403-411.

Elizarov, A. M., Microreactors for radiopharmaceutical synthesis. *Lab on a Chip - Miniaturisation for Chemistry and Biology* **2009,** 9, (10), 1326-1333.

Engl, W.; Backov, R.; Panizza, P., Controlled production of emulsions and particles by milli- and microfluidic techniques. *Current Opinion in Colloid and Interface Science* **2008,** 13, (4), 206-216.

Fäldt, P.; Bergenståhl, B.; Claesson, P. M., Stabilization by chitosan of soybean oil emulsions coated with phospholipid and glycocholic acid. *Colloids and Surfaces A: Physicochemical and Engineering Aspects* **1993,** 71, (2), 187-195.

Feng, Z.; Wang, Z.; Gao, C.; Shen, J., Direct covalent assembly to fabricate microcapsules with ultrathin walls and high mechanical strength. *Advanced Materials* **2007,** 19, (21), 3687-3691.

Fenske, D. B.; Cullis, P. R., Liposomal nanomedicines. *Expert Opinion on Drug Delivery* **2008,** 5, (1), 25-44.

Fung, Y. C., Stochastic flow in capillary blood vessels. *Microvascular Research* **1973,** 5, (1), 34-48.

Garstecki, P.; Fuerstman, M. J.; Stone, H. A.; Whitesides, G. M., Formation of droplets and bubbles in a microfluidic T-junction - Scaling and mechanism of break-up. *Lab on a Chip - Miniaturisation for Chemistry and Biology* **2006,** 6, (3), 437-446.

Garti, N.; Bisperink, C., Double emulsions: Progress and applications. *Current Opinion in colloid and interface science* **1998,** 3, (6), 657-667.

Geckil, H.; Xu, F.; Zhang, X.; Moon, S.; Demirci, U., Engineering hydrogels as extracellular matrix mimics. *Nanomedicine* 5, (3), 469-484.

Georgieva, R.; Moya, S.; Hin, M.; Mitlöhner, R.; Donath, E.; Kiesewetter, H.; Möhwald, H.; BÃ¤umler, H., Permeation of macromolecules into polyelectrolyte microcapsules. *Biomacromolecules* **2002,** 3, (3), 517-524.

Ghan, R.; Shutava, T.; Patel, A.; John, V. T.; Lvov, Y., Enzyme-catalyzed polymerization of phenols within polyelectrolyte microcapsules. *Macromolecules* **2004,** 37, (12), 4519-4524.

Grigoriev, D. O.; Bukreeva, T.; Möhwald, H.; Shchukin, D. G., New method for fabrication of loaded micro- and nanocontainers: Emulsion encapsulation by polyelectrolyte layer-by-layer deposition on the liquid core. *Langmuir* **2008,** 24, (3), 999-1004.

Guzey, D.; McClements, D. J., Formation, stability and properties of multilayer emulsions for application in the food industry. *Advances in Colloid and Interface Science* **2006,** 128-130, 227-248.

Hartman, R. L.; Jensen, K. F., Microchemical systems for continuous-flow synthesis. *Lab on a Chip - Miniaturisation for Chemistry and Biology* **2009,** 9, (17), 2495-2507.

He, T.; Liang, Q.; Zhang, K.; Mu, X.; Luo, T.; Wang, Y.; Luo, G., A modified microfluidic chip for fabrication of paclitaxel-loaded poly(l-lactic acid) microspheres. *Microfluidics and Nanofluidics* **2011,** 10, (6), 1289-1298.

Helgeson, M. E.; Chapin, S. C.; Doyle, P. S., Hydrogel microparticles from lithographic processes: Novel materials for fundamental and applied colloid science. *Current Opinion in Colloid and Interface Science* **2011** 16, (2), 106-117.

Henrik, B., *Theoretical Microfluidics*. 1 ed.; Oxford University Press: **2008**.

Hope, M. J.; Bally, M. B.; Webb, G.; Cullis, P. R., Production of large unilamellar vesicles by a rapid extrusion procedure. Characterization of size distribution, trapped volume and ability to maintain a membrane potential. *Biochimica et Biophysica Acta - Biomembranes* **1985,** 812, (1), 55-65.

Huebner, A.; Sharma, S.; Srisa-Art, M.; Hollfelder, F.; Edel, J. B.; DeMello, A. J., Microdroplets: A sea of applications? *Lab on a Chip - Miniaturisation for Chemistry and Biology* **2008,** 8, (8), 1244-1254.

Huh, D.; Bahng, J. H.; Ling, Y.; Wei, H. H.; Kripfgans, O. D.; Fowlkes, J. B.; Grotberg, J. B.; Takayama, S., Gravity-driven microfluidic particle sorting device with hydrodynamic separation amplification. *Analytical Chemistry* **2007,** 79, (4), 1369-1376.

Hung, L. H.; Choi, K. M.; Tseng, W. Y.; Tan, Y. C.; Shea, K. J.; Lee, A. P., Alternating droplet generation and controlled dynamic droplet fusion in microfluidic device for CdS nanoparticle synthesis. *Lab on a Chip - Miniaturisation for Chemistry and Biology* **2006,** 6, (2), 174-178.

Hwang, D. K.; Dendukuri, D.; Doyle, P. S., Microfluidic-based synthesis of non-spherical magnetic hydrogel microparticles. *Lab on a Chip - Miniaturisation for Chemistry and Biology* **2008,** 8, (10), 1640-1647.

Ibarz, G.; Dähne, L.; Donath, E.; Möhwald, H., Smart micro- and nanocontainers for storage, transport, and release. *Advanced Materials* **2001,** 13, (17), 1324-1327.

Janasek, D.; Franzke, J.; Manz, A., Scaling and the design of miniaturized chemical-analysis systems. *Nature* **2006,** 442, (7101), 374-380.

Jang, J. H.; Dendukuri, D.; Hatton, T. A.; Thomas, E. L.; Doyle, P. S., A route to three-dimensional structures in a microfluidic device: Stop-flow interference lithography. *Angewandte Chemie - International Edition* **2007,** 46, (47), 9027-9031.

Johnston, A. P. R.; Caruso, F., Exploiting the directionality of DNA: Controlled shrinkage of engineered oligonucleotide capsules. *Angewandte Chemie - International Edition* **2007,** 46, (15), 2677-2680.

Johnston, A. P. R.; Cortez, C.; Angelatos, A. S.; Caruso, F., Layer-by-layer engineered capsules and their applications. *Current Opinion in Colloid and Interface Science* **2006,** 11, (4), 203-209.

Jones, T. B., Liquid dielectrophoresis on the microscale. *Journal of Electrostatics* **2001,** 51-52, (1-4), 290-299.

Köhler, J. M.; Henkel, T.; Grodrian, A.; Kirner, T.; Roth, M.; Martin, K.; Metze, J., Digital reaction technology by micro segmented flow - components, concepts and applications. *Chemical Engineering Journal* **2004,** 101, (1-3), 201-216.

Köhler, K.; Sukhorukov, G. B., Heat treatment of polyelectrolyte multilayer capsules: A versatile method for encapsulation. *Advanced Functional Materials* **2007,** 17, (13), 2053-2061.

Kalshetti, P. P.; Rajendra, V. B.; Dixit, D. N.; Parekh, P. P., Hydrogels as a drug delivery system and applications: A review. *International Journal of Pharmacy and Pharmaceutical Sciences* **2012** 4, (1), 1-7.

Khan, S. A.; Günther, A.; Schmidt, M. A.; Jensen, K. F., Microfluidic synthesis of colloidal silica. *Langmuir* **2004,** 20, (20), 8604-8611.

Kida, T.; Mouri, M.; Akashi, M., Fabrication of hollow capsules composed of poly(methyl methacrylate) stereocomplex films. *Angewandte Chemie - International Edition* **2006,** 45, (45), 7534-7536.

Kobayashi, I.; Uemura, K.; Nakajima, M., Formulation of monodisperse emulsions using submicron-channel arrays. *Colloids and Surfaces A: Physicochemical and Engineering Aspects* **2007,** 296, (1-3), 285-289.

Kozlovskaya, V.; Kharlampieva, E.; Mansfield, M. L.; Sukhishvili, S. A., Poly(methacrylie acid) hydrogel films and capsules: Response to pH and ionic strength, and encapsulation of macromolecules. *Chemistry of Materials* **2006,** 18, (2), 328-336.

Kreft, O.; Georgieva, R.; Bäumler, H.; Steup, M.; Müller-Röber, B.; Sukhorukov, G. B.; Möhwald, H., Red blood cell templated polyelectrolyte capsules: A novel vehicle for the stable encapsulation of DNA and proteins. *Macromolecular Rapid Communications* **2006,** 27, (6), 435-440.

Ksinantova, L.; Koska, J.; Kvetnansky, R.; Marko, M.; Hamar, D.; Vigas, M., Effect of simulated microgravity on endocrine response to insulin-induced hypoglycemia in physically fit men. *Hormone and Metabolic Research* **2002,** 34, (3), 155-159.

Lee, J.; Moon, H.; Fowler, J.; Schoellhammer, T.; Kim, C. J., Electrowetting and electrowetting-on-dielectric for microscale liquid handling. *Sensors and Actuators, A: Physical* **2002,** 95, (2-3), 259-268.

Lee, J. N.; Park, C.; Whitesides, G. M., Solvent Compatibility of Poly(dimethylsiloxane)-Based Microfluidic Devices. *Analytical Chemistry* **2003,** 75, (23), 6544-6554.

Leng, J.; Salmon, J. B., Microfluidic crystallization. *Lab on a Chip - Miniaturisation for Chemistry and Biology* **2009,** 9, (1), 24-34.

Leporatti, S.; Voigt, A.; Mitlöhner, R.; Sukhorukov, G.; Donath, E.; Mhwald, H., Scanning force microscopy investigation of polyelectrolyte nano- and microcapsule wall texture. *Langmuir* **2000,** 16, (9), 4059-4063.

Li, L.; Boedicker, J. Q.; Ismagilov, R. F., Using a multijunction microfluidic device to inject substrate into an array of preformed plugs without cross-contamination: Comparing theory and experiments. *Analytical Chemistry* **2007,** 79, (7), 2756-2761.

Li, R. H., Materials for immunoisolated cell transplantation. *Advanced Drug Delivery Reviews* **1998,** 33, (1-2), 87-109.

Liau, A.; Kamik, R.; Majumdar, A.; Cate, J. H. D., Mixing crowded biological solutions in milliseconds. *Analytical Chemistry* **2005,** 77, (23), 7618-7625.

Link, D. R.; Anna, S. I.; Weitz, D. A.; Stone, H. A., Geometrically Mediated Breakup of Drops in Microfluidic Devices. *Physical Review Letters* **2004,** 92, (5), 545031-545034.

Liu, K.; Ding, H.; Chen, Y.; Zhao, X. Z., Droplet-based synthetic method using microflow focusing and droplet fusion. *Microfluidics and Nanofluidics* **2007,** 3, (2), 239-243.

Lorenz, R. M.; Edgar, J. S.; Jeffries, G. D. M.; Chiu, D. T., Microfluidic and optical systems for the on-demand generation and manipulation of single femtoliter-volume aqueous droplets. *Analytical Chemistry* **2006,** 78, (18), 6433-6439.

Luo, D.; Pullela, S. R.; Marquez, M.; Cheng, Z., Cell encapsules with tunable transport and mechanical properties. *Biomicrofluidics* **2007,** 1, (3).

Luo, Z. J.; King, R. H. M.; Lewin, J.; Thomas, P. K., Effects of nonenzymatic glycosylation of extracellular matrix components on cell survival and sensory neurite extension in cell culture. *Journal of Neurology* **2002,** 249, (4), 424-431.

Lvov, Y.; Antipov, A. A.; Mamedov, A.; Möhwald, H.; Sukhorukov, G. B., Urease Encapsulation in Nanoorganized Microshells. *Nano Letters* **2001,** 1, (3), 125-128.

Menetrier-Deremble, L.; Tabeling, P., Droplet breakup in microfluidic junctions of arbitrary angles. *Physical Review E - Statistical, Nonlinear, and Soft Matter Physics* **2006,** 74, (3).

Müller, M.; Heinen, S.; Oertel, U.; Lunkwitz, K., *Macromol. Symp.* **2001,** 164, 197-210.

Madou, M., *Fundamentals of Microfabrication,* Second Edition, CRC Press, **1997**.

Mak, W. C.; Bai, J.; Chang, X. Y.; Trau, D., Matrix-assisted colloidosome reverse-phase layer-by-layer encapsulating biomolecules in hydrogel microcapsules with extremely high efficiency and retention stability. *Langmuir* **2009,** 25, (2), 769-775.

Mak, W. C.; Cheung, K. Y.; Trau, D., Diffusion controlled and temperature stable microcapsule reaction compartments for high-throughput microcapsule-PCR. *Advanced Functional Materials* **2008,** 18, (19), 2930-2937.

Makamba, H.; Kim, J. H.; Lim, K.; Park, N.; Hahn, J. H., Surface modification of poly(dimethylsiloxane) microchannels. *Electrophoresis* **2003,** 24, (21), 3607-3619.

Mao, Z.; Ma, L.; Gao, C.; Shen, J., Preformed microcapsules for loading and sustained release of ciprofloxacin hydrochloride. *Journal of Controlled Release* **2005,** 104, (1), 193-202.

Mazutis, L.; Araghi, A. F.; Miller, O. J.; Baret, J. C.; Frenz, L.; Janoshazi, A.; Taly, V.; Miller, B. J.; Hutchison, J. B.; Link, D.; Griffiths, A. D.; Ryckelynck, M., Droplet-based microfluidic systems for high-throughput single DNA molecule isothermal amplification and analysis. *Analytical Chemistry* **2009,** 81, (12), 4813-4821.

McDonald, J. C.; Duffy, D. C.; Anderson, J. R.; Chiu, D. T.; Wu, H.; Schueller, O. J. A.; Whitesides, G. M., Fabrication of microfluidic systems in poly(dimethylsiloxane). *Electrophoresis* **2000,** 21, (1), 27-40.

McDonald, J. C.; Whitesides, G. M., Poly(dimethylsiloxane) as a material for fabricating microfluidic devices. *Accounts of Chemical Research* **2002,** 35, (7), 491-499.

Meadows, D.; Schultz, J. S., Fiber-optic biosensors based on fluorescence energy transfer. *Talanta* **1988,** 35, (2), 145-150.

Meadows, D. L.; Schultz, J. S., Design, manufacture and characterization of an optical fiber glucose affinity sensor based on an homogeneous fluorescence energy transfer assay system. *Analytica Chimica Acta* **1993,** 280, (1), 21-30.

Mellott, M. B.; Searcy, K.; Pishko, M. V., Release of protein from highly cross-linked hydrogels of poly(ethylene glycol) diacrylate fabricated by UV polymerization. *Biomaterials* **2001,** 22, (9), 929-941.

Morimoto, Y.; Tan, W. H.; Tsuda, Y.; Takeuchi, S., Monodisperse semi-permeable microcapsules for continuous observation of cells. *Lab on a Chip - Miniaturisation for Chemistry and Biology* **2009,** 9, (15), 2217-2223.

Nie, Z.; Li, W.; Seo, M.; Xu, S.; Kumacheva, E., Janus and ternary particles generated by microfluidic synthesis: Design, synthesis, and self-assembly. *Journal of the American Chemical Society* **2006,** 128, (29), 9408-9412.

Ohashi, T.; Kuyama, H.; Hanafusa, N.; Togawa, Y., A simple device using magnetic transportation for droplet-based PCR. *Biomedical Microdevices* **2007,** 9, (5), 695-702.

Okushima, S.; Nisisako, T.; Torii, T.; Higuchi, T., Controlled production of monodisperse double emulsions by two-step droplet breakup in microfluidic devices. *Langmuir* **2004,** 20, (23), 9905-9908.

Orive, G.; Hernández, R. M.; Gascón, A. R.; Calafiore, R.; Chang, T. M. S.; De Vos, P.; Hortelano, G.; Hunkeler, D.; Lacík, I.; Shapiro, A. M. J.; Pedraz, J. L., Cell encapsulation: Promise and progress. *Nature Medicine* **2003,** 9, (1), 104-107.

Paik, P.; Pamula, V. K.; Pollack, M. G.; Fair, R. B., Electrowetting-based droplet mixers for microfluidic systems. *Lab on a Chip - Miniaturisation for Chemistry and Biology* **2003,** 3, (1), 28-33.

Peng, K.; Ong, W.; Yobas, L.; Trau, D., *11th Intl. Conf. on TAS* **2007**.

Petrov, A. I.; Volodkin, D. V.; Sukhorukov, G. B., Protein-calcium carbonate coprecipitation: A tool for protein encapsulation. *Biotechnology Progress* **2005,** 21, (3), 918-925.

Polk, A.; Amsden, B.; De Yao, K.; Peng, T.; Goosen, M. F. A., Controlled release of albumin from chitosan-alginate microcapsules. *Journal of Pharmaceutical Sciences* **1994,** 83, (2), 178-185.

Price, A. D.; Zelikin, A. N.; Wang, Y.; Caruso, F., Triggered enzymatic degradation of DNA within selectively permeable polymer capsule microreactors. *Angewandte Chemie - International Edition* **2009,** 48, (2), 329-332.

Priest, C.; Herminghaus, S.; Seemann, R., Generation of monodisperse gel emulsions in a microfluidic device. *Applied Physics Letters* **2006,** 88, (2), 1-3.

Priest, C.; Quinn, A.; Postma, A.; Zelikin, A. N.; Ralston, J.; Caruso, F., Microfluidic polymer multilayer adsorption on liquid crystal droplets for microcapsule synthesis. *Lab on a Chip - Miniaturisation for Chemistry and Biology* **2008,** 8, (12), 2182-2187.

Prokop, A.; Hunkeler, D.; DiMari, S.; Haralson, M. A.; Wang, T. G., Water Soluble Polymers for Immunoisolation I: Complex Coacervation and Cytotoxicity. *Advances in Polymer Science* **1998**a**,** 136, X-51.

Prokop, A.; Hunkeler, D.; Powers, A. C.; Whitesell, R. R.; Wang, T. G., Water Soluble Polymers for Immunoisolation II: Evaluation of Multicomponent Microencapsulation Systems. *Advances in Polymer Science* **1998**b**,** 136, 52-73.

Psaltis, D.; Quake, S. R.; Yang, C., Developing optofluidic technology through the fusion of microfluidics and optics. *Nature* **2006,** 442, (7101), 381-386.

Rabanel, J. M.; Banquy, X.; Zouaoui, H.; Mokhtar, M.; Hildgen, P., Progress technology in microencapsulation methods for Cell therapy. *Biotechnology Progress* **2009,** 25, (4), 946-963.

Rosario, S. A.; Cha, G. S.; Meyerhoff, M. E.; Trojanowicz, M., Use of ionomer membranes to enhance the selectivity of electrode-based biosensors in flow-injection analysis. *Analytical Chemistry* **1990,** 62, (22), 2418-2424.

Rossier-Miranda, F. J.; Schroën, C. G. P. H.; Boom, R. M., Colloidosomes: Versatile microcapsules in perspective. *Colloids and Surfaces A: Physicochemical and Engineering Aspects* **2009,** 343, (1-3), 43-49.

Russell, R. J.; Pishko, M. V.; Gefrides, C. C.; McShane, M. J.; Cote, G. L., A fluorescence-based glucose biosensor using concanavalin A and dextran encapsulated in a poly(ethylene glycol) hydrogel. *Analytical Chemistry* **1999,** 71, (15), 3126-3132.

Schwartz, J. A.; Vykoukal, J. V.; Gascoyne, P. R. C., Droplet-based chemistry on a programmable micro-chip. *Lab on a Chip - Miniaturisation for Chemistry and Biology* **2004,** 4, (1), 11-17.

Seo, M.; Nie, Z.; Xu, S.; Mok, M.; Lewis, P. C.; Graham, R.; Kumacheva, E., Continuous microfluidic reactors for polymer particles. *Langmuir* **2005,** 21, (25), 11614-11622.

Shestopalov, I.; Tice, J. D.; Ismagilov, R. F., Multi-step synthesis of nanoparticles performed on millisecond time scale in a microfluidic droplet-based system. *Lab on a Chip - Miniaturisation for Chemistry and Biology* **2004,** 4, (4), 316-321.

Shintaku, H.; Kuwabara, T.; Kawano, S.; Suzuki, T.; Kanno, I.; Kotera, H., Micro cell encapsulation and its hydrogel-beads production using microfluidic device. *Microsystem Technologies* **2007,** 13, (8-10), 951-958.

Shui, L.; Pennathur, S.; Eijkel, J. C. T.; Van Den Berg, A., Multiphase flow in lab on chip devices: A real tool for the future? *Lab on a Chip - Miniaturisation for Chemistry and Biology* **2008,** 8, (7), 1010-1014.

Shutava, T.; Prouty, M.; Kommireddy, D.; Lvov, Y., pH responsive decomposable layer-by-layer nanofilms and capsules on the basis of tannic acid. *Macromolecules* **2005,** 38, (7), 2850-2858.

Sia, S. K.; Whitesides, G. M., Microfluidic devices fabricated in poly(dimethylsiloxane) for biological studies. *Electrophoresis* **2003,** 24, (21), 3563-3576.

Sivakumar, S.; Bansal, V.; Cortez, C.; Chong, S. F.; Zelikin, A. N.; Caruso, F., Degradable, surfactant-free, monodisperse polymer-encapsulated emulsions as anticancer drug carriers. *Advanced Materials* **2009,** 21, (18), 1820-1824.

Somasundaran, P.; Chen, T.; Sarkar, D., *Mater. Res. Innovations* **1999,** 81, 140.

Song, H.; Tice, J. D.; Ismagilov, R. F., A microfluidic system for controlling reaction networks in time. *Angewandte Chemie - International Edition* **2003,** 42, (7), 768-772.

Squires, T. M.; Quake, S. R., Microfluidics: Fluid physics at the nanoliter scale. *Reviews of Modern Physics* **2005,** 77, (3), 977-1026.

Srivastava, R.; Brown, J. Q.; Zhu, H.; McShane, M. J., Stable encapsulation of active enzyme by application of multilayer nanofilm coatings to alginate microspheres. *Macromolecular Bioscience* **2005,** 5, (8), 717-727.

Stone, H. A.; Stroock, A. D.; Ajdari, A., Engineering flows in small devices: Microfluidics toward a lab-on-a-chip. In *Annual Review of Fluid Mechanics*, **2004**; Vol. 36, pp 381-411.

Subotic, D.; Ferguson, J.; Warren, B. C. H., Polymer-polymer interactions and the influence of small molecules on the complexation reaction. *European Polymer Journal* **1989,** 25, (12), 1233-1237.

Such, G. K.; Quinn, J. F.; Quinn, A.; Tjipto, E.; Caruso, F., Assembly of ultrathin polymer multilayer films by click chemistry. *Journal of the American Chemical Society* **2006,** 128, (29), 9318-9319.

Sukhorukov, G. B.; Donath, E.; Lichtenfeld, H.; Knippel, E.; Knippel, M.; Budde, A.; Möhwald, H., Layer-by-layer self assembly of polyelectrolytes on colloidal particles. *Colloids and Surfaces A: Physicochemical and Engineering Aspects* **1998,** 137, (1-3), 253-266.

Sukhorukov, G. B.; Volodkin, D. V.; Günther, A. M.; Petrov, A. I.; Shenoy, D. B.; Möhwald, H., Porous calcium carbonate microparticles as templates for encapsulation of bioactive compounds. *Journal of Materials Chemistry* **2004,** 14, (14), 2073-2081.

Sung, Y. Y.; Rubner, M. F., Micropatterning of polymer thin films with pH-sensitive and cross-linkable hydrogen-bonded polyelectrolyte multilayers. *Journal of the American Chemical Society* **2002,** 124, (10), 2100-2101.

Tan, Y. C.; Fisher, J. S.; Lee, A. I.; Cristini, V.; Lee, A. P., Design of microfluidic channel geometries for the control of droplet volume, chemical concentration, and sorting. *Lab on a Chip - Miniaturisation for Chemistry and Biology* **2004,** 4, (4), 292-298.

Tanaka, H.; Matsumura, M.; Veliky, I. A., Diffusion characteristics of substrate in Ca-Alginate gel beads. *Biotechnology and Bioengineering* **1984,** 26, (1), 53-58.

Taylor, T. M.; Davidson, P. M.; Bruce, B. D.; Weiss, J., Liposomal nanocapsules in food science and agriculture. *Critical Reviews in Food Science and Nutrition* **2005,** 45, (7-8), 587-605.

Teh, S. Y.; Lin, R.; Hung, L. H.; Lee, A. P., Droplet microfluidics. *Lab on a Chip - Miniaturisation for Chemistry and Biology* **2008,** 8, (2), 198-220.

Temenoff, J. S.; Park, H.; Jabbari, E.; Conway, D. E.; Sheffield, T. L.; Ambrose, C. G.; Mikos, A. G., Thermally cross-linked oligo(poly(ethylene glycol) fumarate) hydrogels support osteogenic differentiation of encapsulated marrow stromal cells in vitro. *Biomacromolecules* **2004,** 5, (1), 5-10.

Teng, X. R.; Shchukin, D. G.; Möhwald, H., A novel drug carrier: Lipophilic drug-loaded polyglutamate/ polyelectrolyte nanocontainers. *Langmuir* **2008,** 24, (2), 383-389.

Theberge, A. B.; Courtois, F.; Schaerli, Y.; Fischlechner, M.; Abell, C.; Hollfelder, F.; Huck, W. T. S., Microdroplets in microfluidics: An evolving platform for discoveries in chemistry and biology. *Angewandte Chemie - International Edition* **2010,** 49, (34), 5846-5868.

Thorsen, T.; Roberts, R. W.; Arnold, F. H.; Quake, S. R., Dynamic pattern formation in a vesicle-generating microfluidic device. *Physical Review Letters* **2001,** 86, (18), 4163-4166.

Tong, W.; Gao, C., Multilayer microcapsules with tailored structures for bio-related applications. *Journal of Materials Chemistry* **2008,** 18, (32), 3799-3812.

Trau, D.; Yang, W.; Seydack, M.; Caruso, F.; Yu, N. T.; Renneberg, R., Nanoencapsulated microcrystalline particles for superamplified biochemical assays. *Analytical Chemistry* **2002,** 74, (21), 5480-5486.

Um, E.; Lee, D. S.; Pyo, H. B.; Park, J. K., Continuous generation of hydrogel beads and encapsulation of biological materials using a microfluidic droplet-merging channel. *Microfluidics and Nanofluidics* **2008,** 5, (4), 541-549.

Voigt, A.; Lichtenfeld, H.; Sukhorukov, G. B.; Zastrow, H.; Donath, E.; Bäumler, H.; Möhwald, H., Membrane filtration for microencapsulation and microcapsules fabrication by layer-by-layer polyelectrolyte adsorption. *Industrial and Engineering Chemistry Research* **1999,** 38, (10), 4037-4043.

Volodkin, D. V.; Larionova, N. I.; Sukhorukov, G. B., Protein encapsulation via porous CaCO3 microparticles templating. *Biomacromolecules* **2004,** 5, (5), 1962-1972.

Wang, J. T.; Wang, J.; Han, J. J., Fabrication of advanced particles and particle-based materials assisted by droplet-based microfluidics. *Small* **2011**,7, (13), 1728-1754.

Wang, L.; Flanagan, L. A.; Jeon, N. L.; Monuki, E.; Lee, A. P., Dielectrophoresis switching with vertical sidewall electrodes for microfluidic flow cytometry. *Lab on a Chip - Miniaturisation for Chemistry and Biology* **2007,** 7, (9), 1114-1120.

Wang, L.; Wang, Z.; Zhang, X.; Shen, J.; Chi, L.; Fuchs, H., A new approach for the fabrication of an alternating multilayer film of poly(4-vinylpyridine) and poly(acrylic acid) based on hydrogen bonding. *Macromolecular Rapid Communications* **1997,** 18, (6), 509-514.

Wang, Y.; Caruso, F., Mesoporous silica spheres as supports for enzyme immobilization and encapsulation. *Chemistry of Materials* **2005,** 17, (5), 953-961.

Wang, Y.; Caruso, F., Nanoporous protein particles through templating mesoporous silica spheres. *Advanced Materials* **2006,** 18, (6), 795-800.

Wells-Knecht, M. C.; Thorpe, S. R.; Baynes, J. W., Pathways of formation of glycoxidation products during glycation of collagen. *Biochemistry* **1995,** 34, (46), 15134-15141.

West, J. L.; Hubbell, J. A., Photopolymerized hydrogel materials for drug delivery applications. *Reactive Polymers* **1995,** 25, (2-3), 139-147.

Wheeler, J. J.; Palmer, L.; Ossanlou, M.; MacLachlan, I.; Graham, R. W.; Zhang, Y. P.; Hope, M. J.; Scherrer, P.; Cullis, P. R., Stabilized plasmid-lipid particles: Construction and characterization. *Gene Therapy* **1999,** 6, (2), 271-281.

Workman, V. L.; Dunnett, S. B.; Kille, P.; Palmer, D., Microfluidic chip-based synthesis of alginate microspheres for encapsulation of immortalized human cells. *Biomicrofluidics* **2007,** 1, (1).

Workman, V. L.; Dunnett, S. B.; Kille, P.; Palmer, D. D., On-chip alginate microencapsulation of functional cells. *Macromolecular Rapid Communications* **2008,** 29, (2), 165-170.

Yager, P.; Edwards, T.; Fu, E.; Helton, K.; Nelson, K.; Tam, M. R.; Weigl, B. H., Microfluidic diagnostic technologies for global public health. *Nature* **2006,** 442, (7101), 412-418.

Yang, C. G.; Xu, Z. R.; Wang, J. H., Manipulation of droplets in microfluidic systems. *TrAC - Trends in Analytical Chemistry* **2010**, 29, (2), 141-157.

Yobas, L.; Martens, S.; Ong, W. L.; Ranganathan, N., High-performance flow-focusing geometry for spontaneous generation of monodispersed droplets. *Lab on a Chip - Miniaturisation for Chemistry and Biology* **2006,** 6, (8), 1073-1079.

Yu, A.; Wang, Y.; Barlow, E.; Caruso, F., Mesoporous silica particles as templates for preparing enzyme-loaded biocompatible microcapsules. *Advanced Materials* **2005,** 17, (14), 1737-1741.

Zhang, H.; Tumarkin, E.; Peerani, R.; Nie, Z.; Sullan, R. M. A.; Walker, G. C.; Kumacheva, E., Microfluidic production of biopolymer microcapsules with controlled morphology. *Journal of the American Chemical Society* **2006,** 128, (37), 12205-12210.

Zhang, H.; Tumarkin, E.; Sullan, R. M. A.; Walker, G. C.; Kumacheva, E., Exploring microfluidic routes to microgels of biological polymers. *Macromolecular Rapid Communications* **2007,** 28, (5), 527-538.

Zhang, S.; Yobas, L.; Trau, D., *12th Intl. Conf. on TAS* **2008**.

Zhang, Y.; Yang, S.; Guan, Y.; Cao, W.; Xu, J., Fabrication of stable hollow capsules by covalent layer-by-layer self-assembly. *Macromolecules* **2003,** 36, (11), 4238-4240.

Zheng, B.; Roach, L. S.; Ismagilov, R. F., Screening of protein crystallization conditions on a microfluidic chip using nanoliter-size droplets. *Journal of the American Chemical Society* **2003,** 125, (37), 11170-11171.

Zheng, B.; Tice, J. D.; Ismagilov, R. F., Formation of droplets of alternating composition in microfluidic channels and applications to indexing of concentrations in droplet-based assays. *Analytical Chemistry* **2004,** 76, (17), 4977-4982.

Zhou, J.; Khodakov, D. A.; Ellis, A. V.; Voelcker, N. H., Surface modification for PDMS-based microfluidic devices. *Electrophoresis* **2012,** 33, (1), 89-104.

Zhou, L.; Huang, G.; Wang, S.; Wu, J.; Lee, W. G.; Chen, Y.; Xu, F.; Lu, T., Advances in cell-based biosensors using three-dimensional cell-encapsulating hydrogels. *Biotechnology Journal* **2011**, 6, (12), 1466-1476.

Zhuang, Y. X.; Hansen, O.; Knieling, T.; Wang, C.; Rombach, P.; Lang, W.; Benecke, W.; Kehlenbeck, M.; Koblitz, J., Vapor-phase self-assembled monolayers for anti-stiction applications in MEMS. *Journal of Microelectromechanical Systems* **2007,** 16, (6), 1451-1460.

Zimmermann, M.; Schmid, H.; Hunziker, P.; Delamarche, E., Capillary pumps for autonomous capillary systems. *Lab on a Chip - Miniaturisation for Chemistry and Biology* **2007,** 7, (1), 119-125.

Zuck, A.; Pavlukhina, S.; Sukhiskvill, S., Hydrogen-bonded layer-by-layer temperature triggered release films. *Langmuir* **2009,** 25, 14025.

APPENDIX A. Droplet size vs flow rate for PEG-DA micro-containers (with standard deviation)

Qd / Flow Rates Qc	0.002		0.004		0.008	
	Size (µm)	St. Dev.	Size (µm)	St. Dev.	Size (µm)	St. Dev.
0.02	96	1.185854	88.98913	3.471048	98.40441	1.486065
0.04	74.01563	1.566495	83.16	2.242905	81.73333	2.177754
0.06	68.66667	1.841365	61.83333	1.99632	71.4375	2.221595
0.08	53.42308	4.695282	56.91667	2.056196	56.63636	3.231976
0.1	48.5	1.915631	51.26786	1.827841	51.2	2.27088
0.2	43.09615	1.851933	44.12903	1.858394	45.275	1.934654
0.5	33.68182	1.538913	33.5	2.543374	38.15	2.998275
1	25.10294	2.613156	26.51087	1.979265	27.25	1.663503
2	No droplets		No droplets		20.14286	6.573893

APPENDIX B. Targeted blood glucose level ranges by International Diabetes Foundation

IDF recommended target blood glucose level ranges

Target Levels by Type	Before meals (pre prandial)	2 hours after (post prandial)
Non-diabetic	4.0 to 5.9 mmol/L	under 7.8 mmol/L*
Type 2 diabetes	4 to 7 mmol/L	under 8.5 mmol/L
Type 1 diabetes	4 to 7 mmol/L	under 9 mmol/L
Children w/ diabetes	4 to 8 mmol/L	under 10 mmol/L

Source: IDF International Diabetes Foundation (IDF)

The normal blood glucose level in humans is about 4 mM. The human body, when operating normally, restores the blood sugar level within a range of about 4.4 to 6.1 mM. Right shortly after eating the meal, blood glucose level could rise temporarily up to 7.8 mM.

APPENDIX C. A Comparision of surface properties of PDMS for microfluidic devices

Experiment	Continuous Phase	Surfactant	Surface properties	Surface treatment
Chapter 3	Hexadecane	Span 80	Hydrophobic	After bonding, PDMS devices were heat cured overnight for hydrophobic recovery.
Chapter 4	Water	Tween 20	Hydrophilic	Upstream plasma before starting the experiment to render surface hydrophilic.
Chapter 5	1-undecanol	Span 80	Hydrophobic	After bonding, PDMS devices were heat cured overnight for hydrophobic recovery.